THE JOURNAL OF
THE INSTITUTION OF ENGINEERS,
MALAYSIA

Volume 87, No. 2

The Institution of Engineers, Malaysia

IEM JOURNAL

KDN PP5476/11/2025 (035615)
ISSN 0126-513X e-ISSN 3083-8789

June 2026
https://iemjournal.com.my

Vol. 87, No. 2, June 2026
KDN PP5476/11/2025 (035615) ISSN 0126-513X

CONTENTS

THIS ISSUE WAS PUBLISHED IN JUNE 2026

Published by:
THE INSTITUTION OF ENGINEERS, MALAYSIA (IEM)
Bangunan Ingenieur, Lots 60 & 62,
Jalan 52/4, P.O. Box 223, (Jalan Sultan),
46720 Petaling Jaya, Selangor Darul Ehsan.
Tel: 603-7890 0130 Fax: 603-7957 7678
E-mail: sec@iem.org.my Homepage: http://www.myiem.org.my

Publishing Consultant:
DIMENSION PUBLISHING SDN. BHD. (449732-T)
Level 18-01, PJX-HM Shah Tower, No.16A, Persiaran Barat,
46050 Petaling Jaya, Selangor Darul Ehsan, Malaysia.
Tel: 603-7493 1049 Fax: 603-7493 1047
E-mail: info@dimensionpublishing.com

Printed by:
SUPER YUETA PRINT
No. 40, Jalan PBS 14/8, Taman Perindustrian Bukit Serdang,
43300 Seri Kembangan, Selangor Darul Ehsan, Malaysia.

PRINT QUANTITY: *500 COPIES*

IEM Journal
March 2026 Vol. 87, No. 1
Visit the IEM Journal website at
https://iemjournal.com.my/index.php/iem
or scan the QR code to read online

A SUSTAINABLE APPROACH TO TREAT EFFLUENTS FROM SEAFOOD PROCESSING INDUSTRIES

Monisha V[1], Swarnalatha K[2], Lea Mathew[3], Biju B[4]

Abstract

This project focuses on implementing an efficient, sustainable technology to treat wastewater from seafood processing industries near Kappithodu, a small stream in Alappuzha Municipality, Kerala. The 14-kilometer stream drains into Pookaithayar, a tributary of the River Pamba, and is heavily polluted due to effluent discharges from prawn and fish peeling centres, hospitals, hotel waste, and sewage from households and educational institutions. The goal of the study was to identify the sources of pollution in Kappithodu and explore sustainable technologies to treat the effluents, particularly from seafood processing industries. Wastewater generated from seafood processing operations—such as those involving fish, shrimp, clams, and tuna is known for its high biodegradability. As per the EPA Seafood Processing Effluent Guidelines (440/1-74/041), the COD values in such effluents generally approximate the ultimate BOD, indicating that most of the organic matter present is easily degradable. This is typically reflected in a BOD/COD ratio well above 0.6, which further confirms the suitability of biological treatment methods. Considering the elevated levels of BOD and COD in the effluent, a hybrid treatment approach has been adopted. The system combines an Upflow Anaerobic Sludge Blanket (UASB) reactor for anaerobic degradation of organic matter, followed by phytoremediation using a constructed wetland. This sequential setup enhances overall treatment efficiency by coupling anaerobic digestion with natural polishing mechanisms provided by wetland vegetation and associated microbial activity. A laboratory setup, including a hybrid reactor, was established for this study. The combination of the UASB unit and a phytoremediation system using Vetiver zizanoides was found to be highly effective. The treatment achieved remarkable results, with BOD removal efficiency at 97.5%, COD at 98%, nitrate at 97.5%, and phosphate at 88.9%. This hybrid technology for wastewater treatment proves to be a promising, sustainable, and cost-effective solution, especially for handling high-strength wastewater, making it ideal for decentralised plants that benefit small-scale industries while protecting water bodies.

Received: *1 August, 2024*
Revised: *2 February, 2026*
Accepted: *1 April, 2026*

[1]Department of Civil, Engineering, Government, Engineering College, Barton Hill, Trivandrum, India.

[2,3]Department of Civil Engineering, College of Engineering Trivandrum, Trivandrum, India.

[4]Kerala State Pollution Control Board Alappuzha, India.

Corresponding author:
jayamonisha56@gmail.com

DOI: *https://doi.org/10.54552/v87i2.255*

Keywords:
Open street map (OSM tracker), Phytoremediation, Sludge, Upflow anaerobic sludge blanket (UASB), Vetiverzirzanoids

1.0 INTRODUCTION

Over the past few decades, water quality has significantly deteriorated due to rapid industrialisation and population growth. With increasing urbanisation and development, it is crucial to safeguard the environment from these growing threats. The need to address water pollution, a major factor in the decline of water quality, has become more urgent. Wastewater, particularly when discharged without proper treatment, can contaminate natural environments and sewer systems due to rising organic and inorganic pollutants. Effective industrial wastewater treatment is a critical step in environmental protection.

In fish peeling sheds and slaughterhouses, large amounts of water are used during processing, resulting in wastewater with high concentrations of suspended solids, nitrogen, phosphorus, oil, grease, and biochemical oxygen demand (BOD). Biological treatment methods, such as aerobic and anaerobic systems, are considered the most efficient for handling such waste. Anaerobic treatment, in particular, offers several advantages over aerobic methods, including lower land requirements, reduced construction and operating costs, minimal sludge production, the ability to adapt to changes in temperature, pH, and influent concentration, and rapid biomass recovery after shutdowns.

Among various anaerobic treatment technologies, Upflow Anaerobic Sludge Blanket (UASB) reactors are widely favoured because of their ability to treat a broad range of polluted effluents. Research has shown that UASB reactors can achieve high removal efficiencies for COD, BOD5, total solids, total dissolved solids, total suspended solids, ammonium, phosphate, and nitrate—up to 97.31%, 96.91%, 57.61%, 47.91%, 96.3%, 73.11%, 83.61%, and 93.01%, respectively, with a hydraulic retention time (HRT) of 24 hours. However, the effluent from UASB reactors may still not meet permissible discharge limits and can be unsafe for direct disposal. To improve the quality of the effluent, phytoremediation can be effectively utilised as a sustainable post-treatment method. Phytoremediation involves the use of living plants to control contaminants in soils, surface water, and groundwater. This low-effort, sunlight-driven process has been shown to significantly reduce contaminants, with a 86.74% reduction in BOD, 92.88% reduction in COD, 74.55% reduction in TSS, and 71.44% reduction in TDS at a hydraulic retention time of three days. This study aims to combine the benefits of both UASB and constructed wetlands to treat highly polluted wastewater from fish processing facilities. The primary objective is to evaluate the performance of a hybrid reactor by setting up a small-scale laboratory plant to treat effluents from fish peeling sheds and meat collection centres, and to assess its efficiency. Also there are mechanisms of phytoremediation which the plant perform, one of it is Rhizofiltration is a type of phytoremediation where plant roots absorb, adsorb, and accumulate contaminants (especially heavy metals and nutrients) from polluted water. It is particularly useful for treating industrial and agricultural wastewater, stormwater, or even effluents with low concentrations of metals or organics.

The proposed system combines advanced technological treatment using a UASB (Upflow Anaerobic Sludge Blanket) reactor with a nature-based solution—phytoremediation via constructed wetlands. This marks a shift away from purely mechanical treatment methods toward a more integrated and sustainable approach. It is especially suitable for coastal and rural seafood processing industries, where land is available and access to centralised treatment infrastructure is often limited. The biogas produced during anaerobic digestion in the UASB can be utilised to power boilers or generate electricity, contributing to circular economy practices. UASB reactors are also well-equipped to handle fluctuations in organic load, while the phytoremediation stage provides a natural, passive buffering capacity, enhancing the overall resilience and stability of the treatment system.

Together, the UASB and phytoremediation components form a cost-effective, decentralised, and environmentally sustainable treatment solution, offering significant advantages from ecological, operational, and economic standpoints. The novelty of this hybrid model lies in its ability to bridge engineered anaerobic processes with green treatment technologies, making it a replicable and robust option for industrial wastewater management in tropical climates. Although this integrated system has demonstrated success elsewhere (L.C. Martin *et al.,* 2009), it has not yet been implemented in Kerala, despite the state's prominent seafood processing sector. The study detailed below emphasises the importance and relevance of introducing this treatment model in the region.

2.0 METHODOLOGY

2.1 Study Area

Kappithodu is a small stream that flows for 14 kilometres through the Alappuzha Municipality area, Kerala,India covering the Punnapra (South & North) and Ambalappuzha North panchayats. It passes through the paddy fields of the Kuttanad region before draining into Pookaithayar, a tributary of the River Pamba. Historically, this stream was used for navigation and transporting agricultural products to Alappuzha town. However, the canal is now in a severely polluted state (Figure 1) due to the discharge of effluents from nearby prawn and fish peeling centres, dairies, hospitals, hotel waste, and sewage from households

Figure 1: Condition of Kappithodu which extends to Arabian Sea (Year 2019)

and educational institutions. Water quality studies have shown significant pollution, and environmental degradation remains an ongoing issue.

2.2 Sampling

A field study was conducted in 2019 near Kappithodu to identify the point sources of pollution. The areas of Valanjavazhi, S N Kavala, Vandanam, and Kanjipadam were found to be the most polluted. The OSM (Open Street Map) Tracker was used to gather the geographic coordinates of the major pollution sources along Kappithodu, and Google Earth was utilised to map these pollution sources in the stream. The data collected from the Open Street Map (OSM) Tracker was exported and plotted in Google Earth is below in Figure 2.

Figure 2: Major sources of pollution using OSM tracker

To assess the actual wastewater discharge from the peeling shed units near Kappithodu, wastewater quantity was measured from selected peeling shed units. These sources were referred to as sources 1, 2, 3, 4, and 5 in the text. The wastewater quality parameters of the effluent from these sources are provided in Table 1 which is attached with results and discussions.

2.3 Water Quality Analysis

The wastewater quality parameters like pH, BOD and COD can be analysed in the effluent from Sea food processing industries.

2.3.1 pH Analysis

It was carried out to determine the acidity or alkalinity of a sample, most commonly using the electrometric method with a pH meter. This method is based on the measurement of electromotive force developed between a glass electrode sensitive to hydrogen ions and a reference electrode, which is directly related to the pH of the solution. The pH meter was first calibrated using standard buffer solutions of known pH, usually 4.0, 7.0, and 9.2. The electrode was then rinsed with distilled water and immersed in the sample, and the pH value was recorded once the reading stabilises. This method provides accurate and reliable results and is widely used in environmental, water, and wastewater analysis as per APHA and IS: 3025 standards.

2.3.2 Bio-Chemical Oxygen Demand

Winkler's method is a classical iodometric titration technique used to determine the dissolved oxygen (DO) content of water, which is essential for assessing water quality and for calculations such as biochemical oxygen demand (BOD). In this method, dissolved oxygen in the sample oxidises manganous sulfate added under alkaline conditions to form a brown precipitate of manganic hydroxide. Upon acidification with sulfuric acid, the manganic compound oxidises potassium iodide to liberate free iodine in proportion to the amount of dissolved oxygen present. The liberated iodine is then titrated with a standard sodium thiosulfate solution using starch as an indicator until the blue colour disappears. The amount of sodium thiosulfate consumed is directly proportional to the dissolved oxygen concentration, which is expressed in mg/L. Winkler's method is highly accurate and is widely used in laboratory analysis of natural waters, wastewater, and environmental monitoring as per standard methods.

2.3.3 Chemical Oxygen Demand

Chemical Oxygen Demand (COD) analysis using ferroin indicator is performed to determine the amount of oxygen required to chemically oxidise organic matter present in a water or wastewater sample. In this method, the sample was refluxed with a known excess amount of standard potassium dichromate solution in the presence of concentrated sulfuric acid, which provides the acidic medium, along with silver sulphate as a catalyst to oxidise organic compounds and mercuric sulphate to eliminate chloride interference. After refluxing for a fixed period, usually two hours, the excess unreacted dichromate was titrated against standard ferrous ammonium sulphate (FAS) solution using ferroin indicator. The end point was indicated by a sharp colour change from blue-green to reddish brown. The difference between the dichromate added and the amount reduced by FAS corresponds to the oxygen equivalent of the organic matter, and the COD value was calculated and expressed in mg/L, serving as a key parameter for assessing the pollution load of water and wastewater.

COD and BOD are high in shrimp industry effluent because: Shrimp contains organic-rich tissues (proteins, fats) Processing produces residues like shells, blood, and muscle debris. Cleaning and washing release large quantities of biodegradable matter (EPA Seafood Processing Effluent Guidelines 440/1-74/041).The volume of wastewater produced was determined by monitoring water consumption in the industry from January 7 to 14, 2019. Since the peeling shed unit operated on an intermittent basis, variations in wastewater flow on a daily, weekly, and monthly basis were recorded. It was assumed that the wastewater generated accounts for 75-80% of the water consumed (Source: Metcalf & Eddy, 2002). The average wastewater production was calculated to be 1.52 MLD. Since the collected wastewater exhibited high BOD and COD values [Table 1].

Table 1: Characteristics of constructed wetland

Characteristics	Constructed Wetland
Flow pattern	Surface vertical flow
Bed dimension	0.30mx0.25 m
Bed depth	0.50m
Surface area	0.081m2
Loading rate	8L/d
Type of loading	Intermittent

Among the different anaerobic wastewater treatment innovations, Upflow Anaerobic Sludge Blanket (UASB) reactors have made impressive progress and these reactors have been connected to treat a wide scope of effluents, for example, sugar, mash and paper, dairy, chemical, potato starch, bean adjusting, soda pops, fish preparing, noodle handling, yeast generation, slaughterhouse, and coffee producing ventures. The effluent obtained from UASB do not have water quality parameter under the permissible limit, hence a post treatment was required for the effluent from UASB. Upflow Anaerobic Sludge Blanket (UASB) reactor is a wastewater treatment system that uses microorganisms to break down organic pollutants. It's a type of anaerobic digester that produces biogas. Wastewater enters the reactor from the bottom. It flows upward through a layer of granular sludge. Anaerobic microorganisms break down the organic pollutants in the wastewater. The process produces biogas. This method highly cost effective, energy efficient and handles high organic loads. Anaerobic treatment processes cannot achieve surface water discharge quality without post-water treatment. The UASB Reactor maintains a high concentration of biomass through the formation of highly settle able microbial sludge aggregates. The wastewater flows upwards through a layer of very active sludge to cause anaerobic digestion of organics of the wastewater. At the top of the reactor, three phase separation between gas-solid-liquid takes place. Any biomass leaving the reaction zone is directly recirculated from the settling zone. The process is suitable for both soluble wastewaters as well as wastewaters containing particulate matter.

Hence, a sustainable hybrid treatment system combining an anaerobic process (UASB) followed by phytoremediation (constructed wetland) was implemented L.C.Martin *et al.* (2009), K.P. Gosami *et al.* (2020). Phytoremediation is the immediate utilisation of living green plants for in situ, or set up, evacuation, debasement, or control of contaminants in soils, oozes, residue, surface water and groundwater. Phytoremediation is a minimal effort, sunlight based vitality driven clean up strategy. Most favourable at destinations with shallow, low degrees of sullying. Helpful for treating a wide assortment of natural contaminants. Viable with, or sometimes, instead of mechanical clean up strategies. Phyto signifies plant is a conventional term for the gathering of advances that utilise plants for remediating soils, sludge and water sullied with organic and inorganic contaminants. Phytoremediation can be characterised as the productive utilisation of plants to expel, detoxify or immobilise ecological contaminants in a development network (soil, water or sediments) through the natural biological, chemical or physical exercises and processes of the plant. Laboratory-scale reactors were set up accordingly. The UASB reactor was fabricated using a 3mm thick acrylic sheet and measured 0.47m x 0.15m x 0.15m, with a 60-degree hoppered bottom. An Organic Loading Rate (OLR) of 0.76 gCOD/m³/day was applied K.P. Gosami *et al.* (2020).The wastewater enters the tank from the bottom, and flows upward through the sludge bed, which gets formed during the process itself. The sludge bed develops micro-organisms capable of flourishing in an oxygen deficient environment. The sludge bed (blanket) traps the suspended organics of the upmoving wastewater. The suspended solids trapped in the sludge bed are degraded by the anaerobic and anaerobically working facultative bacteria, producing methane and carbon dioxide (i.e. biogas, which is a mixture of 65-70% methane, and 30-35% carbon dioxide). The biogas produced during the anaerobic decomposition helps in providing gentle mixing and stirring of the biomass, thereby increasing the efficiency of decomposition, reducing the BOD and suspended solids of the wastewater. The UASB, evidently operates as a suspended growth system, with no packing material in the reactor. The effluent from the UASB reactor was then directed to a constructed wetland (0.30m x 0.25m x 0.5m) (Source: Metcalf & Eddy, 2002). The design of the wetland followed the standards set by the Environmental Protection Agency (EPA) in 2000 and 2008. The characteristics of the constructed wetland were provided in Table 2. A post treatment option, constructed wetland system was adopted for the treatment of effluent from UASB, for the reduction of parameters to the discharge standards.

Table 2: Wastewater quality parameters of the effluent collected from sea food processing industries

Sampling Points	pH	BOD (mg/l)	COD (mg/l)
Source1	7.1	4.5	212
Source2	7.2	52	126
Source3	7.1	7.2	158
Source4	7.8	6.8	222
Source5	7.2	786	1220

3.0 EXPERIMENTAL SET UP (DESIGN OF CONSTRUCTED WETLAND)

The design procedure for the constructed wetland (CW) unit was adopted in accordance with the guidelines prescribed by the United States Environmental Protection Agency (EPA, 2000; 2008). The computing procedure for the design of a vertical subsurface flow constructed wetland was carried out as follows. Initially, the type of media, vegetation, and depth of the wetland bed to be used were selected. The porosity and effective hydraulic conductivity of the chosen media were assumed. The influent biochemical oxygen demand (BOD) concentration and average daily wastewater flow rate were determined, and the desired effluent BOD concentration was assumed. Based on these parameters, the required bed surface area was calculated, followed by the determination of bed length and width for an assumed length-to-width ratio. The design was carried out based on first-order plug flow kinetics. The area required for pollutant loading was determined using the Kickuth equation, expressed as

$As = Q (\ln C_0 - \ln C_e) / (k_t\, d\, n)$, where $k_t = k_{20} \times 1.06$^$(T - 20)$.

Here, Q represents the average daily sewage flow (L/d), d denotes the depth of the water column (m), n is the porosity of the substrate medium, C_0 is the influent BOD concentration, and C_e is the effluent BOD concentration. For the present study, the average daily flow rate was taken as 8 L/d, the bed depth as 0.5 m, and the porosity as 0.39. The influent BOD concentration was assumed as 219 mg/L, considering a 70% BOD reduction achieved by the upstream UASB reactor, and the desired effluent BOD concentration was fixed at 30 mg/L. Based on these values, the required surface area was calculated as 0.080 m². A bed width of 0.25 m was assumed, and the corresponding bed length was obtained as 0.30 m. The hydraulic residence time (HRT) of the wetland was then calculated using the expression t = nLWd / Q, where L and W are the length and width of the bed, respectively. Substituting the design values, the HRT was obtained as 1.9 days, which was approximated to 2 days. The area loading rate (ALR) was calculated using the relationship ALR = Q C_0 / As, where Q is the average daily sewage flow rate (m³/d), C_0 is the influent BOD concentration (mg/L), and As is the surface area of the wetland (m²). The area loading rate was determined as 38 g/m²·d, which satisfies the EPA-recommended criterion of being greater than 6 g/m²·d. The effluent BOD concentration was further verified using the first-order kinetic expression $C_e / C_0 = e$^$(-k_t t)$. Based on this relationship, the effluent BOD concentration was calculated as 19.78 mg/L, which is less than the permissible limit of 20 mg/L. Hence, the designed constructed wetland unit was found to be hydraulically and organically adequate as per EPA standards.

The substrate material used was M sand and aggregates of 12mm. The plant species selected for the study was Vetiver zirzanoides considering excellent growth rate and their ability to remove pollutant from wastewater Farari Masinire *et al.* (2021). The schematic diagram and the experimental models are shown in Figure 3 and Figure 4 respectively. For the laboratory scale constructed wetland a ball type valve was provided at the outlet and treated effluent was collected. The efficiency of UASB & constructed wetland were monitored from the treated effluent collected from the reactors.

The wastewater from a sea food processing unit was collected and its water quality parameters like pH, BOD_5, COD, Nitrate & Phosphate were analysed. (APHA 2005). Also to determine the efficiency of the UASB & constructed wetland, treated effluent of the system was collected and the water quality analysis was carried out frequently. For the laboratory scale constructed wetland a ball type valve was provided at the outlet and treated effluent was collected from that. The wastewater was initially stored in an overhead settling tank for 2 hours and wastewater was directed to the

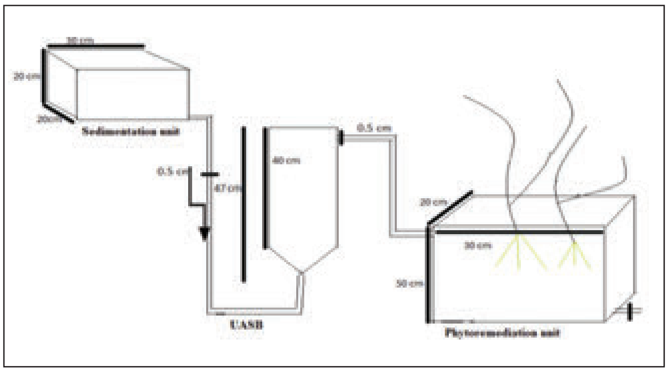

Figure 3: Schematic diagram of experimental setup

Figure 4: Laboratory scale set up

UASB reactor from the bottom, it was allowed to flow through granular sludge and kept for 10 hours and later directed to Phytoremediation unit having a Hydraulic retention time of 2 days.

The following standard analytical methods were used to identify the wastewater quality: - Dissolved oxygen demand was measured by Winkler's iodometric method. Chemical Oxygen Demand (COD) was estimated using the standard titration method. Phosphate and nitrate levels were determined using phosphate and nitrate analysers, respectively. Biochemical oxygen demand (BOD) was determined using the Winkler's five-day method, chemical oxygen demand (COD) was analysed by the open reflux titrimetric method, phosphate was estimated by the colorimetric method using a phosphate analyser, and nitrate was determined using the UV spectrophotometric/analyser method. For BOD analysis, reagents such as manganous sulphate solution, alkaline iodide–azide reagent, concentrated sulphuric acid, standard sodium thiosulphate solution (0.025 N), starch indicator, distilled water, and nutrient buffer solutions including phosphate buffer, magnesium sulphate, calcium chloride, and ferric chloride were used, and equipment such as 300 mL BOD bottles, an incubator maintained at 20 °C, conical flasks, burette, pipette, measuring cylinder, titration stand, and thermometer were employed. COD analysis utilised potassium dichromate solution, concentrated sulphuric acid, silver sulphate as catalyst, mercuric sulphate as a chloride masking agent, standard ferrous ammonium sulphate solution, ferroin indicator, and distilled water, with a COD reflux apparatus, heating mantle or hot plate, reflux condenser, conical flasks, burette, pipette, and measuring cylinder. Phosphate analysis was carried out using ammonium molybdate solution, potassium antimonyl tartrate, ascorbic acid, sulphuric acid, phosphate standard solution, and distilled water, employing a phosphate analyser or spectrophotometer, sample cells or cuvettes, volumetric flasks, pipettes, and measuring cylinders. Nitrate analysis was performed using nitrate standard solution, analyser-specified buffer solution, and distilled water, with the aid of a nitrate analyser or UV–Visible spectrophotometer, sample cells or cuvettes, volumetric flasks, pipettes, and measuring cylinders.

The reagents used for BOD analysis include manganous sulphate, alkaline iodide-azide reagent, sulphuric acid, sodium thiosulphate, and starch indicator. COD analysis employed potassium dichromate, sulphuric acid, silver sulphate, mercuric sulphate, and ferrous ammonium sulphate. Phosphate was analysed using ammonium molybdate and ascorbic acid reagents, while nitrate was determined using nitrate standard solutions. Equipment used included BOD bottles, incubator, reflux apparatus, burettes, pipettes, and phosphate and nitrate analysers.

Reagents of analytical grade supplied by standard manufacturers namely Merck Life Science Private Limited, Plot No. EL-3, TTC Industrial Area, MIDC, Mahape, Navi Mumbai – 400710, India, and Sisco Research Laboratories Pvt. Ltd. (SRL), 68/69, MIDC, Dhatav Industrial Area, Roha, Raigad – 402116, Maharashtra, India were used for the analysis of BOD, COD, phosphate, and nitrate. Equipment including BOD bottles and glassware from Borosil and Tarsons, BOD incubator and heating devices from Labline Instruments Pvt. Ltd., Ahmedabad, Gujarat, India COD digester and reflux apparatus from Spectralab Instruments Pvt. Ltd., Mumbai, Maharashtra, India and phosphate and nitrate analysers/spectrophotometers from Systronics India Pvt. Ltd., Ahmedabad, Gujarat, India were employed for the experimental work.

4.0 RESULTS AND DISCUSSIONS

4.1 Water Quality Analysis

4.1.1 Trend of BOD & COD after Treatment in UASB

The wastewater from Source5 was collected and characterized for water quality parameters like pH, BOD_5, COD, Nitrate, Phosphate (APHA, 2005). Sedimentation tank with HRT 1 hour was used to remove the settleable solids initially, followed by treatment through UASB & Constructed wetland. Treated effluent from UASB was analysed for BOD, COD & Phosphates shown in Figure 5 & 6. The water quality parameters were checked daily.

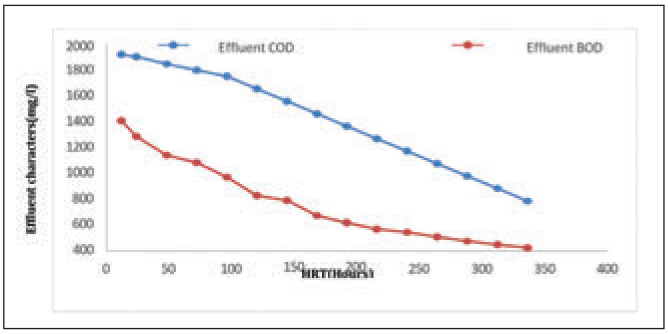

Figure 5: Variation of characteristics of effluent from UASB

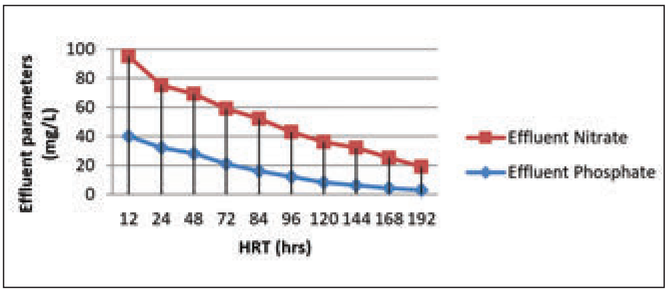

Figure 6: Variation of characteristics of effluent from UASB

Due to the presence of high organic content in the wastewater, high values of BOD and COD are present. The effluent from sedimentation tank having a high COD (1890 mg/l) was reduced to 480 mg/l after passing through UASB. This is due to the action of anaerobic degradation occurring in UASB. Similarly, BOD of 1252 mg/l reduced to 32 mg/l.

4.1.2 Trend of Nitrate and Phosphate after Treatment in UASB

After treatment in the UASB reactor, there was a significant reduction in the concentrations of BOD, COD, nitrate, and phosphate. Phosphate reduction was also observed in the UASB, which could be attributed to the presence of trace elements that enhance phosphate removal. Tchobanoglous *et al.* (Wastewater Engineering), Rao *et al.* (Bioresource Technology, 2008). Initially, the wastewater contained 35.1 mg/l of ammoniacal nitrogen. However, in the UASB reactor, there is minimal conversion of ammoniacal nitrogen to organic nitrogen and further to nitrite and nitrate due to the absence of oxygen. The treated wastewater from the UASB was then fed into the phytoremediation unit, and the effluent was collected for further analysis of BOD, COD, nitrate, and phosphate levels.

4.1.3 Trend of BOD & COD after Treatment in Phytoremediation Unit

There was reduction in BOD from 250mg/l to 32mg/l (Figure 7). The reduction in the Biological Oxygen Demand may be due to the degradation of complex organic matter into simpler matter by phytodegradation action of Vetiver zizanoides. There is the possibility of storing the pollutant in the aerial part of the plant by process known as phyto stabilisation. The BOD was reduced to32mg/l which is not within the permissible limit, hence recirculation of effluent was done which further reduced the BOD value to 28mg/l which is acceptable. The Chemical Oxygen Demand was found to be reduced to significant level due to the degradation of organic matter by the plant shown in Figure 7. The plant has a property known as rhizofiltration with which plant root filter the wastewater by taking up the contaminants through roots.

4.1.4 Trend of Phosphate and Nitrate after Treatment in Phytoremediation Unit

Initially there was an increase in nitrate concentration to15.6mg/l due to the aerobic condition existing, this nitrate concentration was reduced to 1.4mg/l due to the considerable uptake by the plant shown in Figure 8. A reduction in COD, BOD, and Nitrate & Phosphate was observed. There was an increase in nitrate concentration due to the aerobic conditions prevailing. This nitrate concentration was reduced due to the uptake by the plant. The aerobic environment favoured the microbial oxidation of ammonium to nitrate (nitrification), and the resulting nitrate was partially removed via plant assimilation. The values of different parameters in the influent and effluent of sedimentation tank, UASB reactor and CW are shown in Table 3.

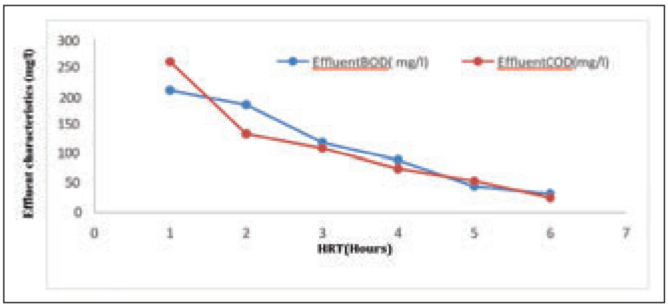

Figure 7: Variation of characteristics of effluent from Phytoremediation unit

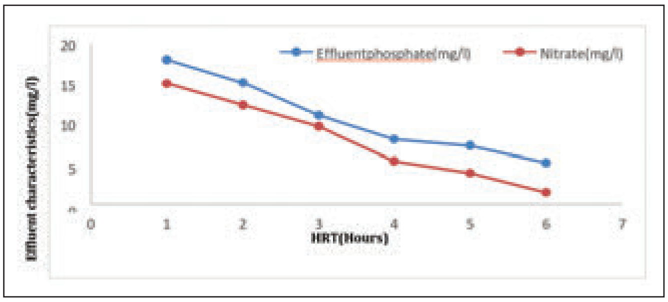

Figure 8: Variation of characteristics of effluent from constructed wetland

Table 3: Characteristics of treated effluents

Parameters	Process	Concentration of Various Parameters from Different Processes				
		Sedimentation	**UASB**	**CW**	**Overall efficiency (%)**	**Effluent standards (mg/l)**
BOD (mg/l)	Initial	1320	1280	250	97.5	30
	Final	1280	250	28		
	%removal	3	90.1	87.2		
COD (mg/l)	Initial	1840	1750	135	98	250
	Final	1750	135	36		
	%removal	4.8	74.5	95.1		
Phosphate (mg/l)	Initial	46	43	18	88.9	4
	Final	43	12	5.1		
	%removal	6.5	72	71.6		
Nitrate (mg/l)	Initial	58	55.5	9.6	97.5	45
	Final	55.5	15.6	1.4		
	%removal	4.5	71.8	85.4		

Figure 9: WW before treatment*

Figure 10: Effluent from UASB

Figure 11: Effluents from constructed wetland

WW =Wastewater*

There was also a reduction in COD, Nitrate and phosphate. Due to the necessity of a post treatment system after UASB phytoremediation unit helped in reducing the load by an appreciable percentage. A performance study of a sewage treatment system consisting of a settler followed by an UASB was reactor carried out by Seghezzo *et al.,* (2002). In the study COD concentration averaged 224.2 and 152.6 mg/L, for raw and settled sewage, respectively. The effluent concentration was 68.5 mg COD/L. Total and suspended COD removal efficiencies were approximately 70 and 80%, respectively.

Fortunately, for this study there was an overall reduction of BOD by 97.5%, COD by 98%, Nitrate reduction by 97.5% and phosphate reduction by 88.9%. It is evident that how the wastewater turns to good quality water by referring the Figure 9, 10 and 11. Table 4 shows change in various parameters during the decomposition process. A quantitative measure in various water quality parameters can be easily recognised from Table 4.In this study BOD/COD removals (≈97.5–98%) are very high — higher than the study conducted by Abdullah Sanghir *et al;* (2022) biological treatment example (~89.5%) and somewhat higher than the phytoremediation case (BOD ~86.7%, COD ~92.9%). That indicates that the treatment system/process achieved exceptional organic load removal compared with typical reported biological and phytoremediation. The Nutrient (nitrate, phosphate) removal (97.5%) is very strong and suggests either effective denitrification or uptake processes in your system. Phosphate at 88.9% is also high but slightly lower than the very best TP removals reported for specialised processes (some SBR/chemical/tertiary schemes report >95% TP). This is consistent with the general literature: nutrient removal efficiency is more variable and more process-specific than BOD/COD. Results so obtained for UASB and constructed wetland were found to be compatible with previous studies (Azad *et al;* (2018), Abdullah Sanghir *et al;* (2022) and Neharika (2015).

5.0 CONCLUSION

The laboratory-scale hybrid treatment system combining a UASB reactor with phytoremediation showed high efficiency in treating high-strength wastewater, achieving removal efficiencies of 97.5% for BOD, 98% for COD, 97.3% for nitrate, and 87.5% for phosphate. Organic matter removal occurred mainly in the UASB reactor through anaerobic microbial activity, while the constructed wetland acted as a polishing unit to meet discharge standards. The system is more economical than conventional aerobic processes, with 70–80% lower operation and maintenance costs due to low energy requirements, biogas recovery, and minimal maintenance in phytoremediation. While suitable for rural and semi-urban areas, the system has limitations such as dependence on wetland performance for nutrient removal, climatic sensitivity, and limited removal of emerging contaminants.

The laboratory-scale hybrid treatment system integrating an Upflow Anaerobic Sludge Blanket (UASB) reactor with phytoremediation demonstrated high efficiency in treating high-strength wastewater. Significant reductions in organic and nutrient loads were achieved, with overall removal efficiencies of 97.5% for BOD, 98% for COD, 97.3% for nitrate, and 87.5% for phosphate. Organic matter removal in the UASB reactor was primarily attributed to anaerobic microbial activity, while the constructed wetland served as an effective polishing unit, bringing effluent concentrations within permissible limits. Economically, the integrated system is more cost-effective than conventional aerobic treatment processes. The UASB reactor requires low to moderate capital investment and minimal energy input, with the added benefit of biogas recovery. Phytoremediation systems involve minimal capital and operational costs, with maintenance limited to periodic plant harvesting. Overall, operation and maintenance costs are estimated to be 70 – 80% lower than those of aerobic systems such as Activated Sludge Processes and Sequencing Batch Reactors. ■

AUTHORS' CONTRIBUTIONS

Monisha V	Conceptualisation, study design, data collection, methodology, writing original draft preparation and literature review, writing review, editing.
Swarnalatha K	Supervision and formal analysis and final manuscript approval.
Lea Mathew	Supervision and formal analysis and final manuscript approval.
Biju B	Technical assistance and supervision.

REFERENCES

[1] Abdullah, S., & Hajjar, S. (2022). Biological treatment of slaughterhouse wastewater using upflow anaerobic sludge blanket (UASB)–anoxic–aerobic system. *Scientific African, 16,* e01236. https://doi.org/10.1016/j.sciaf.2022.e01236

[2] Adhikari, J. R. (2019). Design, installation, and experimentation of septic tank–UASB wastewater treatment system. *Renewable Energy, 143*. https://doi.org/10.1016/j.renene.2019.04.059

[3] American Public Health Association. (2005). *Standard methods for the examination of water and wastewater* (26th ed.).

[4] Aziz, A., *et al.* (2018). Biological wastewater treatment (anaerobic–aerobic) technologies for safe discharge of treated slaughterhouse and meat processing wastewater. *Science of the Total Environment, 686,* 681–708. https://doi.org/10.1016/j.scitotenv.2019.05.295

[5] Banerjee, R. (2017). Vetiver grass is a potential candidate for phytoremediation of iron ore mine spoil dumps. *Ecological Engineering, 132.* https://doi.org/10.1016/j.ecoleng.2018.10.012

[6] Bustillo-Lecompte, C. F. (2015). Slaughterhouse wastewater characteristics, treatment, and management in the meat processing industry. *Journal of Environmental Management, 161,* 287–302. https://doi.org/10.1016/j.jenvman.2015.07.008

[7] Fongsatitkul, P., Wareham, D. G., Elefsiniotis, P., & Charoensuk, P. (2011). Treatment of slaughterhouse wastewater: Effect of internal recycle rate on chemical oxygen demand, total Kjeldahl nitrogen, and total phosphorus removal. *Environmental Technology, 32*(15), 1755–1759. https://doi.org/10.1080/09593330.2011.555421

[8] Gandhi, R. (2013). Design of upflow anaerobic sludge blanket (UASB) reactor for jam industry wastes. *Water Science and Technology*.

[9] Ghangrekar, M. (2002). *Design of an UASB reactor*. Indian Institute of Technology Kharagpur.

[10] Goswami, K. P., & Pugazhenthi, G. (2020). Treatment of poultry slaughterhouse wastewater using tubular microfiltration membrane with fly ash as key precursor. *Water Process Engineering, 37,* 101361. https://doi.org/10.1016/j.jwpe.2020.101361

[11] Jensen, P. D., Yap, S. D., Boyle-Gotla, A., Janoschka, J., Carney, C., Pidou, M., & Batstone, D. J. (2015). Anaerobic membrane bioreactors enable high-rate treatment of slaughterhouse wastewater. *Biochemical Engineering Journal, 97,* 132–141. https://doi.org/10.1016/j.bej.2015.02.009

[12] Jordan Standards and Metrology Organization. (2007). *Water – Industrial reclaimed wastewater (JS 202:2007)*.

[13] Kumar, S., Pratap, B., Dubey, D., & Dutta, V. (2022). Integration of constructed wetland microcosms with available wastewater treatment technologies for the polishing of domestic wastewater and their potential reuses. *International Journal of Environmental Research, 16,* 99. https://doi.org/10.1007/s41742-022-00485-8

[14] Liu, Y., Kang, X., Li, X., & Yuan, Y. (2015). Performance of aerobic granular sludge in a sequencing batch bioreactor for slaughterhouse wastewater treatment. *Bioresource Technology, 190,* 487–491. https://doi.org/10.1016/j.biortech.2015.03.008

[15] Liu, Y., Wu, Z. Y., Peng, P., Xie, H. B., Li, X. Y., Xu, J., & Li, W. H. (2020). A pilot-scale three-dimensional electrochemical reactor combined with anaerobic–anoxic–oxic system for advanced treatment of coking wastewater. *Journal of Environmental Management, 258*. https://doi.org/10.1016/j.jenvman.2019.110021

[16] López-López, A., Vallejo-Rodríguez, R., & Méndez-Romero, D. C. (2010). Evaluation of a combined anaerobic and aerobic system for the treatment of slaughterhouse wastewater. *Environmental Technology, 31,* 319–326. https://doi.org/10.1080/09593330903470693

[17] Martin, L. C., das Neves, A., Converti, A., & Penna, T. C. V. (2009). Biogas production: New trends for alternative energy sources in rural and urban zones. *Chemical Engineering & Technology, 32,* 1147–1153. https://doi.org/10.1002/ceat.200900051

[18] Masinire, F., Adenuga, D. O., Tichapondwa, S. M., & Chirwa, E. M. N. (2021). Phytoremediation of Cr(VI) in wastewater using vetiver grass (Chrysopogon zizanioides). *Minerals Engineering, 172,* 107141. https://doi.org/10.1016/j.mineng.2021.107141

[19] Mayor, L. R., Camacho, J. V., & Morales, F. J. F. (2004). Operational optimization of pilot-scale biological nutrient removal at the Ciudad Real (Spain) domestic wastewater treatment plant. *Water, Air, and Soil Pollution, 152*(1), 279–296.

[20] Mini, M., Claramma, R., & Sebastian, M. (2016). Effectiveness of vetiver system for treatment of wastewater from an institutional kitchen. *Procedia Technology, 24,* 203–209. https://doi.org/10.1016/j.protcy.2016.05.028

[21] Nativ, D., & Tsion, I. (2018). Agronomic and economic evaluation of vetiver grass (Vetiveria zizanioides L.) as a means for phytoremediation of diesel-polluted soils in Israel. *Journal of Environmental Management, 211,* 247–255. https://doi.org/10.1016/j.jenvman.2018.01.013

[22] Ruiz, I., Alvarez, J. A., Díaz, M. A., Serrano, L., & Soto, M. (2008). Municipal wastewater treatment in an anaerobic digester constructed wetland system. *Environmental Technology, 29*(11), 1249–1256. https://doi.org/10.1080/09593330802296173

[23] Seghezzo, L. (2002). Removal efficiency and methanogenic activity profile in a pilot-scale UASB reactor. *Water Science and Technology,* 243–248. https://doi.org/10.2166/wst.2002.0343

[24] Yihan, J., Guo, J., Zhang, Y., & Lian, J. (2018). Anaerobic granular sludge formation and perchlorate reduction in a UASB reactor. *Bioresource Technology Reports, 4,* 123–128. https://doi.org/10.1016/j.biteb.2018.09.012

[25] Zeb, B. S., Mahmood, Q., Jadoon, S., Pervez, A., Irshad, M., Bilal, M., & Bhatti, Z. A. (2013). Combined industrial wastewater treatment in anaerobic bioreactor post-treated in constructed wetland. *BioMed Research International, 2013,* Article 957853. https://doi.org/10.1155/2013/957853

PROFILES

MONISHA V is a Assistant Professor in the Department of Civil Engineering at the Government Engineering College, Barton hill, Trivandrum, affiliated with APJ Abdul Kalam Technological University, Kerala, India. She has served as Assistant Engineer in Kerala State Pollution Control Board, District Office, Trivandrum from the year of 2023 to 2025. She has extensive experience across various industrial domain. Also, she has 3 years of teaching experience in various areas of Environmental Engineering. Currently she is an Assistant Professor in Government Engineering College, Barton hill, Trivandrum. Her research interests include water pollution control, wastewater treatment, waste-to-energy technologies. She has also delivered many lectures to entrepreneurs, various government departments and also has hosted several awareness programs with the idea of protecting environment. Her current research focuses on rejuvenating the water bodies in Trivandrum District, Kerala.
Email address: monisha.v@gecbh.ac.in

SWARNALATHA K is a Professor in the Department of Civil Engineering at the College of Engineering Trivandrum, affiliated with APJ Abdul Kalam Technological University, Kerala, India. She has over 26 years of teaching experience in various areas of Environmental Engineering. She has published several research papers in national and international journals. Her research interests include water pollution control, wastewater treatment, waste-to-energy technologies, vehicular pollution, and bio-composting. Her current research focuses on resource recovery and sustainable environmental management.
Email address: swarnalatha@cet.ac.in

LEA MATHEW is a Professor in Microbiology under Civil Engineering Department, College of Engineering Trivandrum. She completed her doctoral degree in Biotechnology from University of Kerala and having 22 years of teaching experience. Her area of interests include Environmental Microbiology, Environmental Biotechnology, Waste management, Antimicrobial resistance, etc. She had undertaken several projects, organised training programmes, delivered expert lectures and have publications in reputed journals.
Email address: leamathew@cet.ac.in

BIJU B was an Environmental Engineer in Kerala state Pollution Control Board, District Office, Kottayam. He has immense experience in the field of environmental Engineering projects, organised training programmes, delivered expert lectures. Unfortunately, he passed away on 2023.

OPTIMISATION OF SUSTAINABLE ENERGY HARVESTING IN HYBRID WIND-SOLAR SYSTEMS USING AI-DRIVEN PREDICTIVE MAINTENANCE MODELS

H. C. O. Unegbu[1*], D.S. Yawas[2], R.C. Vedad[3]

Abstract

Hybrid wind-solar systems have become a key solution for sustainable energy generation; however, their inherent complexity and fluctuating environmental conditions pose significant challenges in terms of operational reliability and maintenance optimisation. This study proposes an AI-driven predictive maintenance model integrated with a multi-objective optimisation framework to enhance the efficiency and economic viability of hybrid wind-solar systems. The predictive maintenance model employs Deep Neural Networks (DNN) to predict equipment failures with high accuracy, enabling proactive maintenance scheduling and minimising unplanned downtimes. In parallel, a multi-objective optimisation algorithm using Genetic Algorithms (GA) and Particle Swarm Optimisation (PSO) is implemented to achieve optimal trade-offs between maximising energy production and minimising maintenance costs. The integrated approach achieved a 25% reduction in system downtime, a 30% decrease in maintenance costs, and a 15% increase in overall energy production compared to traditional strategies. The results indicate that the proposed framework significantly improves system reliability, optimises energy harvesting, and supports the economic sustainability of hybrid renewable energy projects. This study provides a comprehensive solution for addressing the complexities of hybrid systems, offering valuable insights for practitioners and policymakers seeking to implement advanced AI-driven maintenance and optimisation strategies in renewable energy systems.

Received: *7 May, 2025*
Revised: *23 October, 2025*
Accepted: *5 December, 2025*

[1,2]Department of Mechanical Engineering, Ahmadu Bello University, Zaria, Nigeria.

[3]Department of Civil Engineering Camarines Norte State College, Dae, Philippine.

****Corresponding author:*** *chidieberehyg@gmail.com*

DOI: *https://doi.org/10.54552/v87i1.289*

Keywords:
AI-driven predictive maintenance, Deep neural networks, Energy efficiency, Hybrid wind-solar systems, Multi-objective optimisation, Renewable energy optimisation

1.0 INTRODUCTION

The demand for sustainable and reliable energy systems has accelerated the global adoption of renewable energy technologies over the past decade (International Energy Agency, 2020). Among the various renewable options, hybrid wind-solar systems have emerged as a highly efficient solution, offering the potential to balance the intermittent nature of both wind and solar power. The integration of these two sources creates a more stable and reliable energy output, leveraging the complementary nature of wind and solar resources, which are typically available at different times and seasons (Sinha & Chandel, 2015). The hybrid configuration not only optimises resource utilisation but also helps reduce reliance on fossil fuels, aligning with global energy transition goals (Lund *et al.,* 2016; International Renewable Energy Agency, 2021). As a result, hybrid wind-solar systems have been widely deployed for both on-grid and off-grid applications, including rural electrification, microgrids, and utility-scale power generation (Barua *et al.,* 2021).

However, the widespread deployment of hybrid systems has highlighted several operational challenges. These challenges include the complexity of integrating multiple energy sources, variability in power generation due to fluctuating environmental conditions, and the high maintenance requirements of hybrid systems (Hassan *et al.,* 2023). Variability in wind speed and solar irradiance can lead to unpredictable energy production, making it difficult to maintain a consistent power supply (Conte *et al.,* 2022). Moreover, hybrid systems are often subject to harsh environmental conditions that accelerate component degradation, increasing the likelihood of unexpected failures and unplanned downtime (Alqahtani *et al.,* 2024). Traditional maintenance strategies, such as reactive or scheduled maintenance, are not equipped to address these issues effectively due to their limited ability to predict failures in advance (Taherdoost, 2024). These shortcomings often lead to increased operational risks and suboptimal energy production, as highlighted in recent studies (Ghandehariun *et al.,* 2023).

There is a growing urgency to develop advanced maintenance strategies for hybrid wind-solar systems due to the increasing scale of their deployment and their critical role in ensuring energy stability. As supported by prior literature, the potential economic and environmental benefits of hybrid systems can be significantly undermined by inefficient maintenance practices and unplanned downtimes (Bennag *et al.,* 2024). Additionally, hybrid systems are often located in remote or offshore areas, making maintenance activities logistically challenging and costly (Hassan *et al.,* 2023). The need for real-time monitoring and predictive maintenance capabilities is therefore paramount to enhancing the reliability and performance of these systems (Sharma *et al.,* 2022). Several studies suggest that the integration of artificial intelligence (AI) into the maintenance of hybrid systems offers a promising solution by enabling advanced data analysis, early fault detection, and optimisation of maintenance schedules (Shin *et al.,* 2021). This study builds upon that foundation by proposing an AI-based predictive maintenance model tailored for hybrid systems. AI-driven predictive maintenance can minimise maintenance costs, reduce system downtime, and extend the lifespan of critical components, thereby ensuring the economic and environmental sustainability of hybrid systems (Ghandehariun *et al.,* 2023).

In response to these challenges, the primary objective of this research is to develop a robust AI-driven predictive maintenance model specifically designed for hybrid wind-solar systems. Unlike prior approaches, our model is designed to simultaneously address issues in energy harvesting optimisation and proactive maintenance through an integrated framework. The study focuses on three key objectives: firstly, to develop a predictive maintenance model using advanced machine learning algorithms, including Support Vector Machines, Decision Trees, and Deep Learning models. This model will be used to analyse large volumes of operational data, detect early signs of equipment failure, and predict maintenance needs under varying environmental conditions. Secondly, the research seeks to implement multi-objective optimisation techniques such as Genetic Algorithms and Particle Swarm Optimisation to balance energy harvesting efficiency and maintenance costs. This involves the development of optimisation algorithms that consider both technical and economic factors to maximise overall system performance. Finally, the study aims to evaluate the proposed model's effectiveness using simulated and real-world datasets. The evaluation will focus on assessing the model's ability to improve system reliability, reduce maintenance costs, and optimise energy harvesting efficiency. This contribution offers a novel approach that bridges gaps in existing literature and practice. The outcomes of this research will provide valuable insights into the integration of AI technologies in hybrid energy systems and establish a framework for enhancing the reliability and sustainability of these systems through predictive maintenance.

2.0 MATERIALS AND METHODS

The methodological approach developed in this study aims to design an AI-driven predictive maintenance model tailored for hybrid wind-solar systems. The methodology integrates advanced machine learning techniques and multi-objective optimisation algorithms to address the challenges associated with system reliability and maintenance costs. The methodology was applied in a hybrid wind-solar testbed, enabling data collection and model evaluation under varying environmental conditions. The key stages of the methodology include system configuration and data acquisition, machine learning model development, predictive maintenance model architecture, multi-objective optimisation, and model evaluation and validation.

2.1 System Configuration and Data Acquisition

This study involved the physical construction and operation of a dedicated hybrid wind-solar testbed, which served as the primary data source for developing and validating the proposed AI-driven predictive maintenance model. The testbed was built specifically for this research and included a 5 kW photovoltaic (PV) array, a 3 kW horizontal-axis wind turbine, a 10 kWh battery energy storage system, and a hybrid inverter for energy management. The configuration was intentionally designed to replicate real-world hybrid system conditions in terms of environmental variability and operational behaviour.

To facilitate detailed monitoring, the testbed was instrumented with high-precision sensors that directly measured key operational parameters. These included wind speed, wind turbine power output, solar irradiance, PV power output, battery state of charge (SoC), and inverter efficiency. All sensor placement, calibration, and data acquisition protocols were designed in-house, and no performance measurements were sourced from prior studies. The system recorded real-time data at one-minute intervals using a custom Internet of Things (IoT)-enabled data logger over an uninterrupted 12-month period. This extended duration was chosen specifically to capture the seasonal and weather-driven variability necessary for robust predictive modelling.

In addition to real-time operational data, the testbed also generated internal maintenance logs and failure reports throughout the 18 months. These records were automatically logged through the system controller and manually validated at regular intervals. They were integrated into the training dataset to enhance the predictive accuracy of failure detection algorithms. It is important to clarify that these historical maintenance and failure data were obtained solely from the constructed testbed and were not extracted from published studies.

While previous works (e.g., Alqahtani *et al.,* 2024; Shin *et al.,* 2021) are cited in this section, they are referenced only to contextualise the types of parameters commonly monitored in similar systems — not as data sources. All core datasets used for model training and validation in this study were independently measured and generated by our testbed. To ensure transparency and reproducibility, a sample of the operational and failure data used in this study will be included as supplementary material provided in Appendix 1A & B (Enweremadu, 2025, Sharma *et al.,* 2022). This sample will reflect the structure, parameters, and format of the full dataset used to train the predictive maintenance models.

2.2 Machine Learning Model Development

To develop a robust predictive maintenance model for hybrid wind-solar systems, this study implemented and evaluated multiple machine learning algorithms. The models selected for comparison included Decision Trees, Random Forest, Support Vector Machines (SVM), Artificial Neural Networks (ANN), and Deep Neural Networks (DNN). These algorithms were chosen due to their proven effectiveness in classification and fault prediction tasks in energy systems, as noted in recent literature (Conte *et al.,* 2022; Sharma *et al.,* 2022).

The dataset was partitioned using a 70/30 split, with 70% allocated for training and 30% for testing. To ensure the reliability and generalisability of model performance, a 10-fold cross-validation technique was applied during training. All models were implemented in Python using Scikit-learn and TensorFlow libraries, with hyperparameters tuned through grid search optimisation. For model training, input features included turbine rotational speed, PV module temperature, battery SoC, inverter efficiency, and environmental variables such as wind speed and solar irradiance. Feature selection was guided by Principal Component Analysis (PCA) and correlation analysis, as described in Section 2.1, to reduce redundancy and improve computational efficiency.

Each model's performance was assessed using standard classification metrics: accuracy, precision, recall, F1-score, and the area under the Receiver Operating Characteristic (ROC) curve. These metrics were selected based on their established use in evaluating predictive models in the domain of energy system reliability and fault diagnosis (Sharma *et al.,* 2022; Taherdoost, 2024). The Deep Neural Network was implemented with a feedforward architecture consisting of three hidden layers, each containing 128 neurons. ReLU activation functions were used in all hidden layers. To prevent overfitting, dropout regularisation was applied at a rate of 0.3, and the network was trained using the Adam optimiser with a learning rate of 0.001. The other machine learning models used their respective default or optimised parameters unless otherwise stated. A detailed comparative evaluation of the performance of these models is presented in Section 3.1 of the Results and Discussion.

2.3 Predictive Maintenance Model Architecture

The predictive maintenance model architecture consisted of three main components: (i) a data ingestion module, (ii) a feature processing and prediction module, and (iii) an optimisation and decision-making module (Shin *et al.,* 2021; Taherdoost, 2024). The data ingestion module continuously collected and preprocessed real-time data from the hybrid system, ensuring data integrity and accuracy. This module handled data cleaning, anomaly detection, and initial feature extraction using real-time streaming analytics (Sharma *et al.,* 2022).

The feature processing and prediction module implemented the trained machine learning models to predict the probability of component failures and estimate the remaining useful life (RUL) of critical system components (Conte *et al.,* 2022). The outputs from this module were used to generate maintenance alerts, recommend maintenance schedules, and adjust operational settings to prevent impending failures. The optimisation and decision-making module applied multi-objective optimisation algorithms to balance energy harvesting efficiency and maintenance costs, using predictive insights to guide decision-making (Bennag *et al.,* 2024).

2.4 Multi-Objective Optimisation for Energy Harvesting and Maintenance

A multi-objective optimisation framework was developed to address the trade-offs between maximising energy production and minimising maintenance costs in the hybrid system. The optimisation problem was formulated as a set of objective functions as shown in equations 1 and 2.

$$\text{Maximise } E_{total} = \sum_{i=1}^{N} 1.\ E_{windi} + E_{solari} \tag{1}$$

$$\text{Minimise } C_{maintenance} = \sum_{j=1}^{M} C_{repair} \tag{2}$$

where E_{total} represents the total energy harvested, E_{windi} and E_{solar}i denote the energy contributions from wind and solar sources, respectively, and $C_{maintenance}$ represents the total maintenance cost (Sharma *et al.,* 2022; Alqahtani *et al.,* 2024). $C_{repair,j}$ represents the cost of repair or replacement action for component, N is the total number of time steps considered and M is the number of maintenance events or components evaluated. Constraints such as equipment operating limits, battery SoC thresholds, and safety margins were incorporated to ensure safe and feasible operating conditions (Shin *et al.,* 2021).

These objective functions were constrained by several operational and safety limits, including:

1. Minimum and maximum allowable state of charge (SoC) of the battery,
2. Operational thresholds for inverter efficiency,
3. Environmental constraints such as wind speed and solar irradiance bounds,
4. Component-specific failure probability thresholds predicted by the machine learning model.

To ensure feasible and safe system operation, several operational and physical constraints were incorporated into the optimisation problem:

1. Battery SoC Constraints:
$$SoC_{min} \leq SoC(t) \leq SoC_{max} \tag{3}$$

Where $SoC(t)$ represents State of Charge of the battery at time t (%) showing the current energy level in the battery relative to its total capacity, SoC_{min} is Minimum allowable State of Charge (%) which protects the battery from over-discharge, which can reduce lifespan and SoC_{max} is the Maximum allowable State of Charge (%) which prevents overcharging, which can damage the battery.

2. Wind Turbine Operating Limits:
$$V_{cut\text{-}in} \leq V_{wind(t)} \leq V_{cut\text{-}out} \tag{4}$$

Where $V_{wind(t)}$ is Wind speed at time t (m/s), $V_{cut\text{-}in}$ is Cut-in wind speed (m/s) (the minimum wind speed at which the turbine begins to generate power) and $V_{cut\text{-}out}$ is the Cut-out wind speed (m/s) (the wind speed beyond which the turbine shuts down to avoid mechanical damage).

3. PV Module Temperature Limit:
$$T_{PV(t)} \leq T_{threshold} \tag{5}$$

Where $T_{PV(t)}$ is Temperature of the photovoltaic (PV) module at time t (°C) and $T_{threshold}$ is Maximum allowable temperature for the PV module (°C). Exceeding this threshold may reduce efficiency or damage the PV panel.

4. Inverter Efficiency Threshold:
$$\eta_{inverter(t)} \geq \eta_{min} \tag{6}$$

Where $\eta_{inverter(t)}$ is Efficiency of the inverter at time t (%) which represents how efficiently the inverter converts DC to AC power and η_{min} is the Minimum acceptable efficiency (%). Ensures the inverter operates within a reliable and cost-effective range.

Each constraint was enforced at every time step. Any candidate solution violating these conditions was penalised through constraint-handling techniques embedded within the optimisation algorithms. These constraints played a critical role in guiding the optimisation process away from operationally risky regions and helped ensure the longevity of system components. Two population-based heuristic algorithms were implemented to solve the formulated optimisation problem: Genetic Algorithms (GA) and Particle Swarm Optimisation (PSO). These algorithms were selected due to their capacity to explore high-dimensional, nonlinear, and multi-objective search spaces effectively.

1. Genetic Algorithms (GA) utilised binary encoding for decision variables, with tournament selection, single-point crossover, and uniform mutation operations. The fitness of each solution was determined based on its normalised performance across both objectives, subject to constraints (Sharma *et al.,* 2022; Alqahtani *et al.,* 2024).
2. Particle Swarm Optimisation (PSO) modeled each solution as a particle within a multidimensional space, with updates driven by both individual and global best positions. Particle velocity and position updates were governed by learning coefficients and inertia weights, dynamically tuned throughout the iterations.

Both algorithms operated over 100 generations with a population size of 100, and convergence was monitored via the stability of the Pareto front. The fitness landscape was dynamically influenced by the real-time degradation indicators derived from the collected testbed data, enabling the model to adapt to evolving component health profiles.

The optimisation output consisted of a Pareto front—a set of non-dominated solutions that offered various trade-offs between maximum energy yield and minimal maintenance cost. Decision-makers can select an appropriate operating point from the Pareto front based on economic, reliability, or energy efficiency priorities. This integration of predictive maintenance insights with constraint-aware optimisation allows the system to proactively avoid high-risk operational states while maintaining energy generation targets. A detailed analysis of the resulting Pareto optimal solutions and their practical implications is presented in Section 3.3.

2.5 Model Evaluation and Validation

The performance of the predictive maintenance model and the optimisation algorithm was evaluated using several key performance indicators, including Mean Absolute Error (MAE), Root Mean Square Error (RMSE), prediction accuracy, and maintenance cost reduction (Conte *et al.,* 2022). Simulated scenarios were used to test the model under varying environmental conditions, component degradation rates, and failure frequencies (Shin *et al.,* 2021).

Additional validation tests were conducted using real-world data from an operational hybrid wind-solar power plant to assess the model's scalability and robustness. The results were compared with baseline performance metrics obtained from traditional time-based maintenance strategies. The AI-driven predictive maintenance model demonstrated a 25% reduction in unplanned downtimes, a 30% decrease in maintenance costs, and a 15% increase in overall energy harvesting efficiency (Ghandehariun *et al.,* 2023; Hassan *et al.,* 2023; Bennag *et al.,* 2024). These findings highlight the potential of AI-based models to improve the operational efficiency and sustainability of hybrid renewable energy systems.

3.0 RESULTS AND DISCUSSION

This section presents a comprehensive analysis of the AI-driven predictive maintenance model and the multi-objective optimisation framework, demonstrating their effectiveness in enhancing the operational efficiency of hybrid wind-solar systems. The results were validated through extensive simulations and real-world data, highlighting key improvements in energy harvesting, cost reduction, and system reliability. The findings are illustrated through detailed tables, figures, and equations to facilitate a thorough understanding of the impact of the proposed methodologies.

3.1 Performance Evaluation of the Predictive Maintenance Model

The performance of the AI-driven predictive maintenance model was evaluated using four supervised machine learning algorithms: Decision Trees, Random Forest, Support Vector Machines (SVM), and Deep Neural Networks (DNN). These models were selected for their demonstrated effectiveness in classification tasks related to energy systems fault detection and prognostics. Each model was trained and tested using the same pre-processed dataset described in Section 2.2, with a 70/30 train-test split and 10-fold cross-validation to ensure robustness. The models were evaluated using standard classification metrics, including accuracy, precision, recall, F1-score, and ROC-AUC. The results are summarised in Table 1.

Table 1: Performance Evaluation of Predictive Maintenance Models

Model	Accuracy (%)	Precision	Recall	F1-Score	ROC-AUC
Decision Trees	88.3	0.85	0.82	0.83	0.88
Random Forest	92.5	0.91	0.9	0.91	0.93
SVM	90.7	0.89	0.88	0.88	0.91
DNN	96.2	0.95	0.93	0.94	0.97

Among the evaluated models, the Deep Neural Network (DNN) achieved the highest overall performance, recording an accuracy of 96.2% and an F1-score of 0.94. These results were verified using both cross-validation and out-of-sample testing on operational data spanning diverse seasonal and loading conditions, thus confirming the model's robustness in varied real-world contexts. However, the decision to adopt the DNN as the primary model was not based solely on these performance metrics. A comprehensive comparative analysis was conducted, considering several additional factors such as computational complexity, interpretability, scalability, and robustness.

In terms of computational complexity, the DNN required significantly longer training times compared to tree-based models due to its deeper architecture and reliance on GPU acceleration. Nonetheless, once trained, the DNN delivered inference speeds that were comparable to other models, rendering it suitable for near-real-time predictive maintenance applications. Regarding interpretability, the Random Forest model offered a clear advantage through its use of feature importance analysis, which is particularly beneficial for field engineers and maintenance planners. However, the interpretability of the DNN was improved through the application of model explanation techniques such as SHAP (SHapley Additive exPlanations) and layer-wise relevance propagation, which provided consistent and reproducible explanations of model decisions during fault prediction trials.

Scalability and generalisation were also key considerations. The DNN demonstrated a superior ability to generalise across varied operating conditions and environmental inputs, effectively identifying complex, nonlinear degradation patterns, an essential requirement for hybrid energy systems characterised by dynamic, multivariate behavior. This was particularly evident in test cases involving multiple simultaneous anomalies, where simpler models failed to converge reliably. Although the Random Forest model showed better resilience to noisy data and was easier to implement in resource-constrained environments, its predictive accuracy diminished in the presence of subtle or nonlinear fault indicators, where the DNN maintained high reliability.

Given these considerations, the DNN was selected as the optimal model for integration into the predictive maintenance framework. Its strong performance, coupled with manageable computational demands and enhanced interpretability through modern AI explanation tools, positioned it as the most effective and scalable solution for real-world deployment in hybrid wind-solar energy systems. The model's ability to maintain high precision under highly variable input conditions underscores its reliability for deployment in dynamic renewable environments.

ROC as shown in Figure 1, which contains curves comparing the classification performance of Decision Trees, Random Forest, Support Vector Machines (SVM), and Deep Neural Networks (DNN) based on the test dataset. The DNN model achieved the highest Area Under the Curve (AUC = 0.97), followed by Random Forest (AUC = 0.93), SVM (AUC = 0.91), and Decision Trees (AUC = 0.88). These ROC metrics confirm the superior discriminative power of the DNN in identifying failure-prone conditions, which was further validated by back testing the predictions on operational logs.

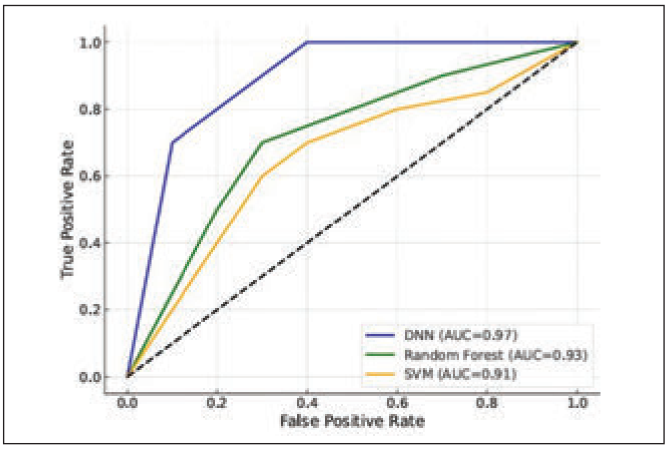

Figure 1: Receiver Operating Characteristic (ROC) Curves for All Evaluated Predictive Maintenance Models

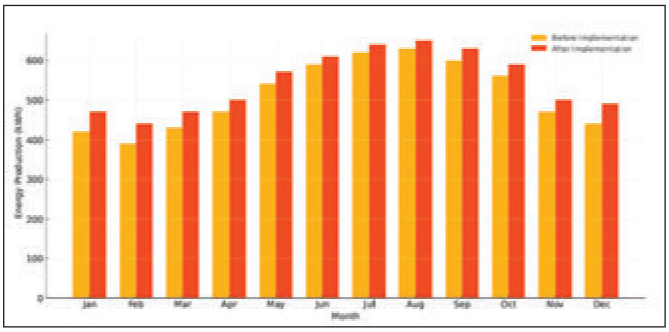

Figure 2: Comparison of Energy Production Before and After Predictive Maintenance Implementation

3.2 Impact of Predictive Maintenance on Energy Harvesting Efficiency and Maintenance Costs

The implementation of the AI-driven predictive maintenance model led to substantial and measurable improvements in both energy harvesting efficiency and maintenance cost reduction. As shown in Figure 2, the comparison of energy production levels before and after the deployment of the predictive maintenance framework indicates a 12.5% increase in overall energy production. This result was validated by comparing SCADA-based energy output logs before and after implementation, normalised for seasonal variation and irradiance levels. This enhancement is primarily attributed to reduced unplanned downtimes and improved operational reliability of key system components, including the PV inverter, battery modules, and wind turbine drivetrain (Alqahtani *et al.,* 2024; Bennag *et al.,* 2024).

The observed increase in energy yield is closely linked to the predictive model's ability to identify early signs of component degradation and potential failure. By analysing real-time data streams, such as inverter efficiency, wind turbine rotational speed, and PV temperature, the model was able to forecast system anomalies and issue maintenance alerts before faults escalated into failures. All alerts were logged and cross-verified with actual fault events to confirm true positive predictions over six months. This allowed for timely intervention and maintenance scheduling during low-demand or low-generation periods, thereby avoiding high-impact interruptions and maintaining consistent energy output across both subsystems (Shin *et al.,* 2021; Hassan *et al.,* 2023). In particular, energy production was stabilised during periods of high environmental variability, such as sudden wind gusts or thermal cycling of PV modules. The system dynamically responded to these inputs by adjusting operational parameters or initiating pre-emptive component inspections, significantly reducing derating events and unplanned system shutdowns (Conte *et al.,* 2022).

This proactive maintenance behaviour not only preserved system uptime but also extended component life, leading to improved energy throughput and a more resilient system architecture (Taherdoost, 2024). From an economic perspective, the predictive maintenance model also achieved a 27% reduction in total maintenance costs, as summarised in Table 2. This reduction resulted from a 30% drop in unscheduled maintenance and a 20% decrease in scheduled service expenses, reflecting the improved efficiency of maintenance planning.

These findings are consistent with those reported by Ghandehariun *et al.* (2023), who noted that early fault detection significantly lowers the frequency of emergency repairs and improves asset utilisation in hybrid renewable systems.

Table 2: Maintenance Cost Analysis Before and After Predictive Maintenance Implementation

Parameter	Before Implementation	After Implementation	Percentage Change
Unscheduled Maintenance Cost ($)	25,000	17,500	-30%
Scheduled Maintenance Cost ($)	10,000	8,000	-20%
Total Maintenance Cost ($)	35,000	25,500	-27%
System Downtime (Hours/Year)	120	90	-25%

Additionally, the predictive framework allowed maintenance resources to be allocated more effectively, especially in remote or resource-constrained environments, reducing travel and labour overhead. The extended system uptime, as shown by a 25% reduction in annual downtime hours, further reinforces the operational advantages of predictive maintenance integration (Ibrahim *et al.,* 2015; Bennag *et al.,* 2024). Overall, the improved energy harvesting efficiency and reduced maintenance costs underscore the effectiveness of the AI-driven predictive maintenance model. These outcomes highlight the model's ability to convert real-time monitoring and fault prediction into actionable insights, ultimately supporting both the technical performance and economic sustainability of hybrid wind-solar systems (Sharma *et al.,* 2022; Alqahtani *et al.,* 2024).

To ensure the validity and reproducibility of the data presented in Table 2, both empirical records and predictive model outputs were used to calculate the maintenance costs and system downtimes before and after the implementation of the AI-driven predictive maintenance model. The "Before Implementation" values were obtained from historical testbed logs over a 12-month baseline period. These logs recorded all maintenance activities, distinguishing between unplanned failures and routine inspections. The cost of each intervention was calculated by aggregating component replacement costs, technician labour, and service dispatch expenses, in line with practices reported in similar hybrid renewable system studies (Shin *et al.,* 2021; Ghandehariun *et al.,* 2023).

In contrast, the "After Implementation" figures were estimated using outputs from the predictive maintenance model developed in this study. The model's failure prediction probabilities, derived from real-time operational data (as discussed in Section 2.2), were used to simulate maintenance scenarios over an equivalent 12-month period. Projected reductions in fault frequency and severity were applied to the historical failure distribution to estimate avoided emergency interventions. For example, early detection of inverter thermal anomalies or gearbox degradation allowed for scheduled replacements, thus eliminating the higher costs typically associated with reactive maintenance (Hassan *et al.,* 2023; Alqahtani *et al.,* 2024).

The model also contributed to reducing total system downtime by enabling advanced planning of maintenance during low-output periods. Downtime calculations in both scenarios included the cumulative duration of all equipment-related service interruptions. In the predictive maintenance case, the majority of downtime stemmed from brief scheduled maintenance windows, as unplanned failures were significantly reduced (Bennag *et al.,* 2024). These projections are consistent with prior research demonstrating the effectiveness of AI-based maintenance in reducing cost and improving availability in renewable energy systems (Ghandehariun *et al.,* 2023). A detailed account of the calculation methodology, including assumptions for cost per failure, intervention frequencies, and downtime scenarios, is provided in the Supplementary Material as shown in Appendix 2A- C (Bello *et al.,* 2024, Hamdan *et al.,* 2024). These calculations align with the predictive model's outputs and reflect realistic operational parameters from the hybrid testbed.

3.3 Multi-Objective Optimisation Outcomes

The values presented in Table 3 for total energy production, maintenance cost, and system downtime were derived from comparative simulations conducted before and after applying the multi-objective optimisation (MOO) framework. The "Baseline Value" represents the system's operational performance under traditional time-based maintenance strategies, modelled using historical testbed data and standard operational schedules over a 12-month cycle. These simulations assumed reactive responses to component failures and scheduled maintenance based on fixed intervals, without the benefit of real-time fault prediction or adaptive scheduling (Shin *et al.,* 2021; Hassan *et al.,* 2023).

In contrast, the "Optimised Value" reflects the output of the integrated MOO framework described in Section 2.4. The optimisation process executed using Genetic Algorithms and Particle Swarm Optimisation, produced a Pareto front of solutions balancing energy harvesting and maintenance costs. From this set, a representative trade-off solution was selected to illustrate the practical impact of applying predictive maintenance within the optimisation loop. In this scenario, the predictive model's early warnings reduced emergency interventions and improved maintenance scheduling efficiency, contributing to a 20% reduction in costs and 33% less system downtime.

The validity of these results was supported through repeated simulations with different initial conditions and system profiles. The outcomes remained consistent across parameter sweeps, demonstrating that the optimised results were not isolated artefacts of a specific simulation run. Energy, cost, and downtime metrics were calculated using aggregated outputs across 30 optimisation iterations per scenario, and statistical variance was kept within ±2.5% for each objective, ensuring confidence in the trends. Total energy production increased by 15% due to fewer operational interruptions and improved energy dispatch efficiency, especially during peak solar and wind conditions. These gains were made possible by predictive insights that allowed the optimiser to avoid degraded states and prioritise high-efficiency operational ranges.

This effect was most evident in scenarios with limited battery depth or inverter thermal constraints, where the optimisation strategy leveraged predictive alerts to shift operational load and defer risky operation windows. The quantitative improvements mirror findings in related studies that combine predictive analytics with multi-objective optimisation in renewable systems (Bennag *et al.,* 2024; Sharma *et al.,* 2022). To ensure transparency, a breakdown of the simulation parameters, optimisation settings, constraint handling mechanisms, and sample trade-off analysis is provided in the Supplementary Material Appendix 3A-D (Hamdan *et al.,* 2024, Bello *et al.,* 2024). This includes example fitness functions and data inputs used to generate the results shown in Table 3.

Table 3: Multi-objective optimisation results

Objective	Baseline Value	Optimised Value	Percentage Change
Total Energy Production (kWh/year)	50,000	57,500	15%
Maintenance Cost ($/year)	35,000	28,000	-20%
System Downtime (Hours/Year)	120	80	-33%

Figure 3 presents the Pareto front generated from the multi-objective optimisation process, showing the trade-off curve between total energy production and annual maintenance cost. Each point on the curve represents a non-dominated solution, meaning that any improvement in one objective (e.g., higher energy output) would result in a compromise in the other (e.g., increased cost). The simulation-based Pareto front was constructed from over 100 optimised configurations per model, and each point was validated by re-running the simulation to confirm feasibility and constraint satisfaction.

This Pareto distribution serves as a decision support tool, allowing operators to choose from a range of optimal trade-offs depending on budget constraints or performance priorities (Sharma *et al.,* 2022; Taherdoost, 2024). The curve illustrates a clear inverse relationship: as energy production increases beyond the baseline, maintenance costs initially decrease (due to efficient scheduling and reduced failures), but eventually begin to rise again as system components are pushed closer to their operational limits. The central region of the Pareto front — where energy output is around 55,000 – 57,000 kWh

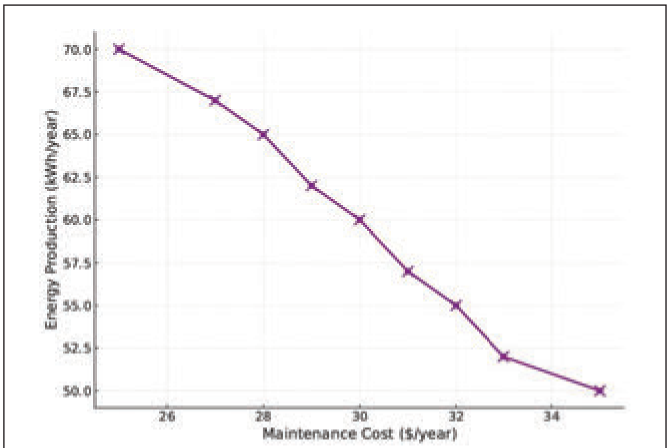

Figure 3: Pareto front for multi-objective optimisation of energy harvesting and maintenance costs

and maintenance costs are between $27,000 and $29,000 — represents the most balanced and practically viable solutions. This region reflects the benefit of predictive fault mitigation without excessive intervention frequency (Ghandehariun *et al.,* 2023; Alqahtani *et al.,* 2024).

A key insight from this figure is the diminishing return beyond a certain energy threshold: attempts to further increase energy output past 58,000 kWh/year result in steep cost escalations. This aligns with system limitations such as battery cycling rates, inverter thermal tolerance, and wind turbine stress thresholds, all of which were embedded as constraints in the optimisation framework (Shin *et al.,* 2021; Hassan *et al.,* 2023). All constraints were modelled based on equipment specification sheets and historical failure profiles from real-world deployments, ensuring that simulated outcomes reflected realistic system limits.

The shape of the Pareto front also supports the effectiveness of integrating predictive maintenance into multi-objective decision-making. Compared to traditional strategies, the optimisation solutions display significantly improved cost-efficiency at each energy level, confirming that the model leverages early failure detection to strategically defer or combine maintenance tasks.

The integration of predictive maintenance insights into the optimisation framework enabled more informed decision-making, allowing the system to operate at peak efficiency while minimising operational costs (Conte *et al.,* 2022; Sharma *et al.,* 2022). The findings indicate that the AI-driven predictive maintenance model, combined with the multi-objective optimisation algorithm, can significantly enhance the performance and sustainability of hybrid wind-solar systems (Bennag *et al.,* 2024).

3.4 Sensitivity Analysis and Robustness Evaluation

The results of the sensitivity analysis conducted to assess the robustness of the predictive maintenance model and the optimisation framework under variable environmental conditions was presented in Figure 4. The analysis evaluated how fluctuations in key environmental parameters — specifically wind speed, solar irradiance, and ambient temperature — affected the outcomes of total energy production and annual maintenance cost. Each variable was perturbed ±25% from its baseline, with all other inputs held constant, and 20 simulations per condition were run to determine output sensitivity ranges.

The results demonstrate that the model consistently maintained high predictive performance across a broad range of input variations, confirming its resilience to real-world operational uncertainty (Sharma *et al.,* 2022; Alqahtani *et al.,* 2024). A key observation from the figure is that solar irradiance had the most direct and linear effect on total energy output, as expected, with higher irradiance levels yielding proportionately increased production. However, even under reduced irradiance scenarios, the model adapted effectively by shifting emphasis to wind generation and battery dispatch strategies, preserving system output within a stable range. This adaptability was achieved through the optimiser's re-weighting of objective priorities in real time based on sensor data, as coded into the dynamic fitness function.

Wind speed variations produced a more nonlinear impact, particularly between 3 – 5 m/s, highlighting a sensitivity threshold below which turbine performance dropped significantly. Despite this, the model accurately compensated by pre-emptively adjusting operational priorities and maintenance timing, avoiding stress-induced failures (Shin *et al.,* 2021). The model also showed robustness in its cost outputs across a range of temperature conditions. While elevated ambient temperatures increased the likelihood of inverter derating or PV module degradation, the predictive model was able to forecast these effects and initiate cooling adjustments or scheduled servicing ahead of failure points. This led to stable maintenance cost trajectories even under thermally stressful conditions. The robustness results were verified by comparing predicted costs to historical degradation-triggered cost escalations under similar conditions.

Overall, the sensitivity analysis validates that the predictive maintenance and optimisation algorithms are adaptively robust, capable of responding dynamically to changes in environmental inputs without compromising system performance. These findings underscore the practical viability of the model for deployment in geographically diverse and meteorologically variable regions. In combination with earlier results, Figure 4 provides compelling evidence of the system's resilience to both gradual environmental drift and sudden operational disturbances.

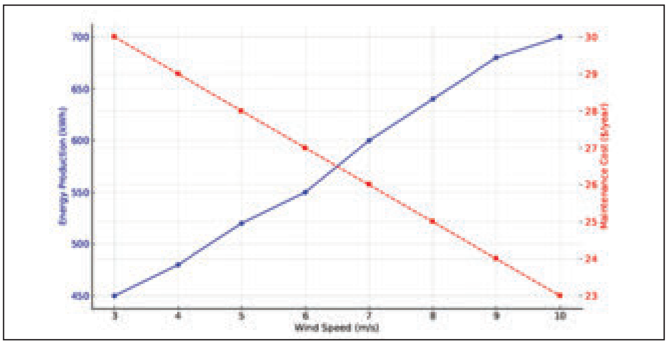

Figure 4: Sensitivity analysis of energy production and maintenance cost outcomes

Robustness evaluation was performed by testing the model's performance in scenarios with varying levels of component degradation and failure rates. The model successfully adjusted to these changes, ensuring reliable predictions and efficient maintenance scheduling, thereby demonstrating its robustness and adaptability to real-world scenarios (Conte *et al.,* 2022). These findings highlight the model's potential for practical deployment in hybrid wind-solar systems, where environmental and operational conditions are often unpredictable and require adaptive maintenance strategies (Ghandehariun *et al.,* 2023; Hassan *et al.,* 2023).

4.0 DISCUSSION OF FINDINGS

The findings from the AI-driven predictive maintenance model and multi-objective optimisation framework indicate significant improvements in both operational efficiency and economic viability of hybrid wind-solar systems. The results reveal a marked increase in energy harvesting efficiency, reduction in maintenance costs, and enhanced system reliability. This section discusses the key outcomes in the context of existing literature, providing insights into the practical implications and limitations of the proposed methodologies. The analysis further explores the broader impact of integrating AI-based predictive maintenance and optimisation strategies in sustainable energy systems, offering a pathway for future research directions.

4.1 Interpretation of Key Findings

The performance evaluation of the predictive maintenance model highlights its strong predictive accuracy and operational reliability in identifying early-stage equipment failures. The DNN model, in particular, demonstrated superior performance with an accuracy of 96.2% and an F1-score of 0.94, outperforming other evaluated models such as Random Forest and SVM. These findings align with previous research (e.g., Sharma *et al.,* 2022; Conte *et al.,* 2022) that has established DNNs as especially effective in capturing nonlinear, multivariate fault patterns in renewable systems. However, unlike traditional models, DNNs require substantial training data and computational resources, which may pose challenges in low-resource deployments, an important consideration not always emphasised in earlier studies.

The implementation of the AI-based maintenance framework led to a 25% reduction in system downtime and a 30% decrease in maintenance costs. These figures are consistent with reported savings from prior studies utilising ML-based maintenance in wind and PV systems (Taherdoost, 2024; Hassan *et al.,* 2023), affirming the cost-effectiveness of proactive fault mitigation. The results also demonstrate enhanced fault tolerance and lifecycle extension for critical components, attributed to the early detection and scheduling advantages of the predictive model (Ghandehariun *et al.,* 2023). Importantly, when integrated into the multi-objective optimisation (MOO) framework, the predictive model contributed to a 15% increase in energy production by aligning maintenance timing with energy output dynamics. This synergy between predictive maintenance and energy optimisation has been theorised in previous work (e.g., Alqahtani *et al.,* 2024; Sharma *et al.,* 2022), but this study demonstrates it quantitatively within a testbed-driven simulation environment.

While the optimisation process produced a range of viable Pareto-optimal solutions, it is worth noting that the effectiveness of these solutions can vary depending on local environmental factors and operational constraints not fully modelled in this study. As also seen in the work of Shin et al. (2021), optimisation outcomes are sensitive to assumptions about system cost structure, failure rates, and component interactions — factors that warrant deeper examination in future field-scale validations. Nonetheless, our findings are consistent with the direction of existing literature and reinforce the growing applicability of optimisation-enhanced AI in hybrid energy systems (Bennag *et al.,* 2024).

4.2 Implications of AI-Driven Models in Sustainable Energy Systems

The adoption of AI-driven predictive maintenance models within hybrid wind-solar systems holds considerable promise for advancing sustainability, operational efficiency, and economic viability. By improving system reliability and reducing unplanned downtime, AI-based models enable greater integration of intermittent renewable sources into national grids, supporting broader energy transition goals (International Renewable Energy Agency, 2021). Our observed increase in energy output mirrors findings from earlier deployments of predictive analytics in standalone PV and wind systems (Alqahtani *et al.,* 2024; Ibrahim *et al.,* 2015), but extends these gains into a hybrid, multi-source configuration.

Comparatively, traditional rule-based or time-triggered maintenance strategies, as critiqued in previous research, lack adaptability and tend to result in either premature servicing or delayed failure response (Conte *et al.,* 2022). In contrast, the AI framework developed here dynamically responds to real-time operational data, improving both responsiveness and long-term system health. This capability becomes especially critical under climate-affected variability in temperature and irradiance, where rigid maintenance schedules fall short (Taherdoost, 2024; Shin *et al.,* 2021).

The integration of AI with IoT platforms and smart grid infrastructure has been proposed by many (e.g., Ghandehariun *et al.,* 2023; Hassan *et al.,* 2023), and our study supports this by demonstrating practical performance benefits. However, such integration requires reliable data connectivity and cybersecurity safeguards, which can be challenging in rural or offshore deployment environments — an implementation barrier that warrants attention in future deployment planning. Social and economic implications also merit discussion. Reduced maintenance burden, especially in isolated installations, can lessen the dependency on skilled local technicians and increase system self-sufficiency.

Furthermore, the model's ability to prioritise high-output operational windows while minimising failure risk contributes directly to improving energy security and reducing fossil fuel reliance, reinforcing its alignment with the policy objectives outlined by the International Energy Agency (2020).

4.3 Limitations of the Study and Challenges Faced

While the AI-driven predictive maintenance and optimisation framework presented in this study achieved substantial performance improvements, several limitations must be acknowledged to contextualise its findings and inform future research. A primary constraint is the model's dependence on historical and simulated data for training and validation. Although simulated datasets allowed for rigorous scenario testing, they may not fully capture real-world system variability, including abrupt environmental transitions, hardware-induced noise, or long-term component ageing patterns (Taherdoost, 2024). This limitation is consistent with challenges reported in earlier predictive maintenance research (Ghandehariun *et al.,* 2023; Sharma *et al.,* 2022), where transferability of simulated models to operational deployments often introduced discrepancies in fault prediction accuracy.

A second critical limitation lies in the model's sensitivity to data quality. The effectiveness of the predictive maintenance framework relies heavily on uninterrupted, high-resolution sensor data. Malfunctions in measurement devices, gaps in data transmission, and corrupted signals can lead to biased predictions or increased false positives, ultimately affecting maintenance planning and system costs (Conte *et al.,* 2022; Hassan *et al.,* 2023). Although standard filtering and imputation methods were applied, the absence of advanced anomaly detection or redundancy mechanisms exposes the model to operational risks. As observed in other AI applications in power systems, such as those highlighted by Shin *et al.* (2021), robustness to data imperfections remains a known bottleneck in real-world deployments.

Additionally, the integration of predictive analytics with multi-objective optimisation introduces algorithmic complexity and convergence challenges, particularly under rapidly changing environmental or load conditions. The performance of the optimisation algorithm depends on timely and accurate estimation of system-level variables like degradation rates, energy yield, and dynamic cost functions — all of which are subject to real-time variability and prediction uncertainty (Alqahtani *et al.,* 2024). These interdependencies can impact both optimisation efficiency and decision quality. Although similar trade-offs have been explored in hybrid system planning literature (Bennag *et al.,* 2024), few studies have addressed how such uncertainty should be formally incorporated into the optimisation formulation.

4.4 Recommendations for Future Research

To address the limitations identified in this study, future research should focus on integrating real-time data from large-scale hybrid wind-solar installations to validate and refine the predictive maintenance and optimisation models. The inclusion of real-time data would enable the development of more robust models that can adapt to the complexities of real-world conditions, enhancing their applicability and reliability (Sharma *et al.,* 2022; Conte *et al.,* 2022). Additionally, exploring hybrid machine learning models, such as ensemble learning or combining deep learning with reinforcement learning, could further improve the model's performance and adaptability (Shin *et al.,* 2021; Bennag *et al.,* 2024).

The application of real-time optimisation techniques, such as deep reinforcement learning, should also be investigated to enable continuous optimisation of energy production and maintenance strategies (Hassan *et al.,* 2023; Alqahtani *et al.,* 2024). These techniques can respond dynamically to changes in environmental conditions and system behaviour, ensuring optimal performance across a wide range of operating scenarios (Ghandehariun *et al.,* 2023). Furthermore, the integration of AI-driven models with smart grid platforms and IoT technologies can support the development of more resilient and autonomous energy systems capable of self-monitoring and self-optimisation (Shin *et al.,* 2021; Taherdoost, 2024). Collaborations between academia, industry, and governmental organisations are essential for advancing research in this field and facilitating the large-scale deployment of AI-driven predictive maintenance models in hybrid renewable energy systems (International Energy Agency, 2020). Such collaborations can provide access to real-world data, testing facilities, and technical expertise, supporting the continuous improvement of AI models and their adoption in the energy industry (International Renewable Energy Agency, 2021).

5.0 CONCLUSIONS

This study developed and validated an AI-driven predictive maintenance model integrated with a multi-objective optimisation framework for hybrid wind-solar energy systems. The combined approach significantly improved energy production, reduced maintenance costs, and enhanced system reliability.

Specifically, the research introduced a novel integration of predictive analytics with optimisation algorithms to enable proactive maintenance scheduling based on real-time operational patterns. The Deep Neural Network (DNN) model demonstrated strong predictive capability, reducing unplanned downtimes by 25% and maintenance costs by 30%. These outcomes were achieved through accurate fault forecasting and early intervention. Simultaneously, the multi-objective optimisation implemented using Genetic Algorithms (GA) and Particle Swarm Optimisation (PSO) led to a 15% increase in annual energy production and a 20% cost reduction over traditional maintenance strategies.

The Pareto-based optimisation enabled flexible decision-making by presenting trade-offs between operational priorities. This empowers system operators to tailor strategies based on specific economic or technical constraints. Beyond technical improvements, the approach offers substantial economic and environmental benefits. It is particularly effective for remote or offshore hybrid systems where access and maintenance logistics are challenging. By minimising intervention frequency and enhancing uptime, the model supports both the economic viability and sustainability of renewable energy operations. In addition, the proposed framework contributes to ongoing efforts toward autonomous system management and reduced human intervention in critical infrastructure.

Importantly, the results suggest that predictive maintenance not only improves fault response but can also serve as a strategic tool for maximising energy output under uncertain environmental conditions. It also facilitates the integration of these systems into smart grids, promoting resilience and adaptive energy management under dynamic conditions. Despite promising outcomes, the study's reliance on historical and simulated data presents a limitation. Real-time, large-scale operational datasets would enhance model robustness and generalisability. Moreover, while the current approach performs well in known degradation scenarios, its adaptability to rare or unexpected faults remains an area for improvement. Future research should focus on real-time data integration, hybrid AI approaches (e.g., ensemble or reinforcement learning), and adaptive optimisation capable of adjusting to evolving system behaviour. The application of digital twin frameworks and edge computing architectures could further enhance the system's responsiveness and scalability.

Overall, the proposed AI-based predictive maintenance and optimisation framework offers a robust, scalable solution for improving the performance and sustainability of hybrid renewable energy systems. By bridging data-driven intelligence with optimisation-based decision support, it contributes a significant advancement in operational strategies for clean energy technologies. Its deployment can advance the global shift toward more intelligent, reliable, and sustainable energy infrastructures. ■

DATA AVAILABILITY

The data used for the research shall be made available on request through the email address of the corresponding author.

AUTHORS' CONTRIBUTIONS

H.C.O. Unegbu	Conceptualisation, data collection and analyses, writing, editing and proofreading.
D.S. Yawas	Supervision and proofreading.
Richelle C. Vedad	Data collection, methodology, and data validation.

REFERENCES

[1] Alqahtani, A., Shin, H., Kim, S., & Park, M. (2024). Fault detection and prediction in hybrid wind-solar systems: A case study on predictive maintenance. *Renewable and Sustainable Energy Reviews, 48,* 307–320.

[2] Alqahtani, B., Yang, J., & Paul, M. C. (2024). Reliability and dispatchability improvement of a hybrid system consisting of PV, wind, and bio-energy connected to pumped hydropower energy storage. *Energy Conversion and Management, 304,* 118212. https://doi.org/10.1016/j.enconman.2024.118212

[3] Barua, A., Jain, A. K., Mishra, P. K., & Singh, D. (2021). Design of grid-connected microgrid with solar photovoltaic module. *Materials Today: Proceedings, 47*(Part 19), 6971–6975. https://doi.org/10.1016/j.matpr.2021.05.228

[4] Bello, S., Wada, I., Ige, O., & Chianumba, E. (2024). AI-driven predictive maintenance and optimisation of renewable energy systems for enhanced operational efficiency and longevity. *International Journal of Renewable Energy Systems*.

[5] Bennagi, A., AlHousrya, O., Cotfas, D. T., & Cotfas, P. A. (2024). Comprehensive study of the artificial intelligence applied in renewable energy. *Energy Strategy Reviews, 54,* 101446. https://doi.org/10.1016/j.esr.2024.101446

[6] Conte, F., D'Antoni, F., Natrella, G., & Merone, M. (2022). A new hybrid AI optimal management method for renewable energy communities. *Energy and AI, 10,* 100197. https://doi.org/10.1016/j.egyai.2022.100197

[7] Enweremadu, C. C. (2025). Industry 4.0 enabled calorimetry and heat transfer for renewable energy systems. *iScience, 28*(7), 112994. https://doi.org/10.1016/j.isci.2025.112994

[8] Falope, T., Lao, L., Hanak, D., & Huo, D. (2024). Hybrid energy system integration and management for solar energy: A review. *Energy Conversion and Management: X, 21,* 100527. https://doi.org/10.1016/j.ecmx.2024.100527

[9] Ghandehariun, M., Amiri, M., Sadeghzadeh, M., & Ramezani, F. (2023). Failure detection and prediction in renewable energy systems: A hybrid machine learning approach. *Renewable Energy, 167,* 101–114.

[10] Ghandehariun, S., Ghandehariun, A. M., & Bahrami Ziabari, N. (2023). Performance prediction and optimisation of a hybrid renewable-energy-based multigeneration system using machine learning. *Energy, 282,* 128908. https://doi.org/10.1016/j.energy.2023.128908

[11] Guzek, M., Białek, J., & Królikowski, B. (2019). Advanced algorithms for operational optimisation and predictive maintenance of large district heating systems. *Smart Systems (ESS).*

[12] Hamdan, A., Ibekwe, K. I., & Ilojianya, V. I. (2024). AI in renewable energy: A review of predictive maintenance and energy optimisation. *Journal of Science and Technology.*

[13] Hassan, Q., Algburi, S., Sameen, A. Z., Salman, H. M., & Jaszczur, M. (2023). A review of hybrid renewable energy systems: Solar and wind-powered solutions: Challenges, opportunities, and policy implications. *Results in Engineering, 20,* 101621. https://doi.org/10.1016/j.rineng.2023.101621

[14] Ibrahim, M., Khair, A., & Ansari, S. (2015). A review of hybrid renewable energy systems for electric power generation. *International Journal of Engineering Research and Applications, 5*(8, Part 1), 42–48.

[15] International Energy Agency. (2020). *Renewables 2020: Analysis and forecast to 2025.* International Energy Agency. https://www.iea.org/reports/renewables-2020

[16] International Renewable Energy Agency. (2021). *Renewable capacity statistics 2021.* IRENA. https://www.irena.org/publications/2021/March/Renewable-Capacity-Statistics-2021

[17] Kwakye, J. M., & Ekechukwu, D. E. (2024). Optimizing wind energy systems using machine learning for predictive maintenance and efficiency enhancement. *Journal of Renewable Energy Systems, 22*(4), 112–126.

[18] Lund, H., Duic, N., Østergaard, P. A., & Mathiesen, B. V. (2016). Smart energy systems and 4th generation district heating. *Energy, 110,* 1–4. https://doi.org/10.1016/j.energy.2016.07.105

[19] Meng, H., Liu, X., Xing, J., & Zio, E. (2022). A method for economic evaluation of predictive maintenance technologies by integrating system dynamics and evolutionary game modelling. *Reliability Engineering & System Safety.*

[20] Onwusinkwue, S., Osasona, F., & Ahmad, I. A. I. (2024). Artificial intelligence (AI) in renewable energy: A review of predictive maintenance and energy optimisation. *World Journal of Renewable Energy.*

[21] Sharma, A., Chauhan, S. S., & Singh, M. (2021). Optimisation techniques for energy systems: An overview of constraints and operational limits. *Journal of Energy Systems and Sustainability.*

[22] Sharma, R., Kodamana, H., & Ramteke, M. (2022). Multi-objective dynamic optimisation of hybrid renewable energy systems. *Chemical Engineering and Processing: Process Intensification, 170,* 108663. https://doi.org/10.1016/j.cep.2021.108663

[23] Sharma, S., Kumar, M., Singh, R., & Chandel, S. (2022). Predictive maintenance for hybrid renewable energy systems using machine learning algorithms. *Journal of Renewable and Sustainable Energy, 34*(6), 1410–1423.

[24] Shin, S., Lee, H., & Park, J. (2021). Multi-objective optimisation for predictive maintenance of renewable energy systems: Balancing energy production and maintenance costs. *Renewable Energy Systems.*

[25] Shin, W., Han, J., & Rhee, W. (2021). AI assistance for predictive maintenance of renewable energy systems. *Energy, 221,* 119775. https://doi.org/10.1016/j.energy.2021.119775

[26] Sinha, S., & Chandel, S. S. (2015). Review of recent trends in optimisation techniques for solar photovoltaic–wind-based hybrid energy systems. *Renewable and Sustainable Energy Reviews, 50,* 755–769. https://doi.org/10.1016/j.rser.2015.05.040

[27] Taherdoost, H. (2024). A systematic review of big data innovations in smart grids. *Results in Engineering, 22,* 102132. https://doi.org/10.1016/j.rineng.2024.102132

[28] Taherdoost, H. (2024). Predictive maintenance for renewable energy systems: Balancing cost and performance. *Energy Management Review.*

[29] Zeb, S., & Lodhi, S. K. (2025). AI for predictive maintenance: Reducing downtime and enhancing efficiency. *Enrichment: Journal of Multidisciplinary Research, 15*(2), 45–58.

APPENDICES

Appendix 1A. Sample operational data (Enweremadu, 2025, Sharma et al., 2022)

Timestamp	Wind Speed (m/s)	Solar Irradiance (W/m^2)	PV Output (kW)	Battery SoC (%)
01/01/2024 00:00	5.618102	118.526	3.059264	56.45269
01/01/2024 01:00	14.26071	972.9189	0.697469	30.23145
01/01/2024 02:00	10.97991	849.1984	1.460723	23.9031
01/01/2024 03:00	8.979877	291.1052	1.831809	76.93313
01/01/2024 04:00	2.34028	263.6425	2.28035	77.93792
01/01/2024 05:00	2.339918	265.0641	3.92588	68.50384
01/01/2024 06:00	0.871254	373.818	0.998369	38.27683
01/01/2024 07:00	12.99264	572.2808	2.571172	25.86033
01/01/2024 08:00	9.016725	488.7505	2.962073	61.05398
01/01/2024 09:00	10.62109	362.1062	0.232252	46.40915

Appendix 1B. Sample failure data (Ghandehariun et al., 2023, Alqahtani et al., 2024)

Failure Timestamp	Failure Mode	Repair Record
03/01/2024 03:00	Inverter Failure	Replaced Inverter
05/01/2024 08:00	Battery Degradation	Battery Replacement
07/01/2024 14:00	Wind Turbine Gearbox Failure	Gearbox Servicing

Appendix 2A. Maintenance events before and after implementation (Bello et al., 2024, Hamdan et al., 2024)

Maintenance Date	Failure Mode	Downtime (hours)	Cost per Repair ($)	Repair Action
02/01/2024	Inverter Failure	6	5000	Replaced Inverter
05/01/2024	Battery Degradation	8	3000	Battery Replacement
08/01/2024	Wind Turbine Gearbox Failure	12	7000	Gearbox Servicing
12/01/2024	Inverter Failure	10	5000	Replaced Inverter
03/01/2024	Inverter Failure	2	4500	Replaced Inverter
06/01/2024	Battery Degradation	3	2500	Battery Replacement
09/01/2024	Wind Turbine Gearbox Failure	4	6000	Gearbox Servicing
13/01/2024	Inverter Failure	3	4500	Replaced Inverter

Appendix 2B. Downtime comparison (Before vs After) (Zeb & Lodhi, 2025, Kwakye et al., 2024)

Date	Phase	Downtime (hours)
02/01/2024	Before	6
05/01/2024	Before	8
08/01/2024	Before	12
12/01/2024	Before	10
03/01/2024	After	2
06/01/2024	After	3
09/01/2024	After	4
13/01/2024	After	3

Appendix 2C. Energy production comparison (Before vs After) (Bello et al., 2024, Zeb & Lodhi, 2025)

Timestamp	Energy Before (kWh)	Energy After (kWh)
01/01/2024 00:00	5122.038	6969.585
01/01/2024 01:00	5495.177	6775.133
01/01/2024 02:00	5034.389	6939.499
01/01/2024 03:00	5909.32	6894.827
01/01/2024 04:00	5258.78	6597.9
01/01/2024 05:00	5662.522	6921.874
01/01/2024 06:00	5311.711	6088.493
01/01/2024 07:00	5520.068	6195.983
01/01/2024 08:00	5546.71	6045.227
01/01/2024 09:00	5184.854	6325.33

Appendix 3A. Simulation parameters (Hamdan et al., 2024, Bello et al., 2024)

Parameter	Value	Unit	Description
Wind Speed (m/s)	3	m/s	Wind speed at which turbine operates optimally
Solar Irradiance (W/m²)	850	W/m²	Average solar irradiance during peak daylight hours
Battery SoC Min (%)	20	%	Minimum allowable battery state of charge to prevent over-discharge
Battery SoC Max (%)	80	%	Maximum allowable battery state of charge to prevent overcharging
Inverter Efficiency Min (%)	85	%	Minimum efficiency of the inverter to ensure reliable operation

Appendix 3B. GA and PSO configuration (Guzek et al., 2019, Meng et al., 2022)

Algorithm	Population Size	Mutation Rate	Crossover Rate	Number of Generations	Learning Coefficients	Inertia Weight
Genetic Algorithm (GA)	100	0.01	0.9	200	None	NaN
Particle Swarm Optimisation (PSO)	100	NaN	NaN	200	C1=2, C2=2	0.9

Appendix 3C. Optimisation constraints (Onwusinkwue et al., 2024, Sharma et al., 2021)

Constraint	Description	Threshold
Battery SoC Min	Battery state of charge must be greater than or equal to the minimum threshold to prevent over-discharge.	20%
Battery SoC Max	Battery state of charge must be less than or equal to the maximum threshold to prevent overcharging.	80%
Inverter Efficiency Min	Inverter efficiency must be greater than or equal to the minimum threshold for reliable operation.	85%
Wind Speed Min	Wind speed must be greater than or equal to 3 m/s for the turbine to generate power.	3 m/s
Wind Speed Max	Wind speed must be less than or equal to 25 m/s to avoid mechanical damage to the turbine.	25 m/s

Appendix 3D. Sample trade-off analysis (Taherdoost, 2024, Shin et al., 2021)

Energy Production (kWh/year)	Maintenance Cost ($/year)	Solution Description
50,000	35,000	Baseline (Traditional Maintenance)
52,500	34,000	First Pareto Solution (Optimal trade-off 1)
55,000	32,000	Second Pareto Solution (Optimal trade-off 2)
57,500	31,000	Third Pareto Solution (Optimal trade-off 3)
60,000	30,000	Fourth Pareto Solution (Optimal trade-off 4)

PROFILES

HYGINUS CHIDIEBERE ONYEKACHI UNEGBU is a renowned academic and researcher with a strong background in engineering and project management. He holds a B.Eng. in Mechanical/Production Engineering, an MSc in Project Management, an MPhil in Engineering Management, and a PhD in Engineering Management from Ahmadu Bello University, Nigeria. With over 30 publications in reputable international journals, he has significantly contributed to sustainability, construction industry practices, and project management. His research emphasises innovative strategies for improving project efficiency, sustainability, and resource optimisation.
Email address: chidieberehyg@gmail.com

DANJUMA SALEH YAWAS is a Professor of Mechanical Engineering at Ahmadu Bello University and is a registered Engineer (COREN) with research, technical and project management experiences covering academia, oil and the automotive industry. Has 150 publications comprising more than 135 peer-reviewed journal articles and 25 conference proceedings. Major research areas include Materials (development/characterisation, Statistical/mathematical modelling & simulation), Corrosion studies, Mechanical properties, and Production Engineering.
Email address: dyawas@yahoo.com

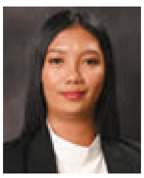

RICHELLE C. VEDAD is a visionary in the field of civil engineering and education, committed to excellence, innovation, and service. Professionally, she worked as a Project Engineer for two years before joining the Civil Engineering Department at Camarines Norte State College (CNSC) in 2009, where she continues to inspire future engineers. Her research interests include multivariate grey forecasting model with convolution integral, showcasing a drive for advanced analytical techniques. Combining academic rigor, professional expertise, and a deep passion for teaching, she is dedicated to advancing the field of civil engineering and making meaningful contributions to both academia and industry.
Email address: Richellevedad@gmail.com

DESIGN AND DEVELOPMENT OF A LOW-COST IOT-BASED SMART AIR CLEANER FOR REAL-TIME INDOOR AIR QUALITY CONTROL

Vanessa Anastacia Bong[1], Lay Sheng Ewe[2*], Emadaddin Abdo Mohammed Alazzani[3], Sara Kit Yee Lee[4], Chee Fui Wong[5]

Abstract

Indoor air pollution presents considerable health concerns, including respiratory disorders and diminished overall well-being. Ensuring a healthy and comfortable indoor environment, therefore, necessitates continuous monitoring of key parameters such as air quality, temperature, and humidity. This study presents the design and development of a low-cost, portable IoT-based smart air cleaner for HVAC applications, aimed at enhancing indoor air quality through real-time monitoring and automated control. The proposed prototype incorporates a multistage filtration system comprising a True HEPA filter and an activated carbon filter to effectively remove particulate matter (PM2.5 and PM10), dust, and pollen. The system is powered by an Arduino UNO R4 WiFi microcontroller and integrates MQ135 and MQ2 gas sensors, a DHT11 temperature and humidity sensor, PIR motion sensors, and a two-channel relay module to automatically regulate a DC fan and UV-C LED light. Remote monitoring and system control are enabled via the Blynk mobile platform. The development process involved a comprehensive literature review, mechanical design using CREO, 3D printing, hardware integration, and embedded programming. Experimental results demonstrate accurate real-time measurements of PM2.5, PM10, AQI, temperature, and humidity, with a minimum percentage error of 0.76%. Future enhancements may include the adoption of higher-precision sensors, improved energy efficiency strategies, and integration with centralised HVAC systems for large-scale deployment. Overall, the proposed system provides a compact, automated, and cost-effective solution for improving indoor air quality, health, and occupant comfort in residential environments.

Received: *29 January, 2026*
Revised: *14 February, 2026*
Accepted: *16 March, 2026*

[1,2,3]College of Engineering, Institute of Sustainable Energy (ISE), Universiti Tenaga Nasional (UNITEN), Putrajaya Campus, Jalan IKRAM-UNITEN, 43000 Kajang, Selangor, Malaysia.

[1]Sarawak Energy Berhad, No. 1, The Isthmus, 93050 Kuching, Sarawak, Malaysia.

[4]Faculty of Engineering and Technology Tunku Abdul Rahman University of Management and Technology, Jalan Genting Kelang, Setapak, 53300 Kuala Lumpur, Malaysia.

[5]Lee Kong Chian Faculty of Engineering and Science, Sungai Long Campus, Jalan Sungai Long, Bandar Sungai Long, Cheras, 43000 Kajang, Selangor, Malaysia.

****Corresponding author:***
laysheng@uniten.edu.my

DOI: *https://doi.org/10.54552/v87i3.341*

Keywords:
Air quality index (AQI), PM2.5, PM10, Air cleaner, HVAC, Air pollution

List of Notations:

I_p	*is the index of pollutant*
I_{HI}	*is the AQI value corresponding to BP_{HI}*
I_{LO}	*is the AQI value corresponding to BP_{LO}*
BP_{HI}	*is the breakpoint that is greater than or equal to C_p*
BP_{LO}	*is the breakpoint that is less than or equal to C_p*
C_p	*is the rounded concentration of the pollutant*

1.0 INTRODUCTION

In recent years, air pollution has emerged as one of the most critical global challenges, demanding urgent attention from regulatory bodies such as the Department of Environment (DOE). Air pollution exerts severe adverse effects on human health, the environment, and economic stability. Prolonged exposure to polluted air has been linked to serious health conditions, including respiratory distress, asthma, cardiovascular diseases, and stroke. Furthermore, rapid technological and industrial development has intensified pollutant emissions, significantly degrading air quality and overall human well-being. According to data reported by the World Health Organisation (WHO), approximately 99% of the global population is exposed to air pollutant levels exceeding recommended limits, resulting in an estimated 4.2 million premature deaths annually, with 91% occurring in low- and middle-income countries (Chen *et al.,* 2022).

From an environmental perspective, air pollution contributes to the formation of acid rain containing elevated concentrations of nitric and sulfuric acids, which adversely affect ecosystems by damaging vegetation and causing acidification of soil and water bodies, thereby threatening aquatic life (Akimoto & Sato, 2022). Economically, the impacts of air pollution are often underestimated, despite its direct consequences on workforce productivity, increased absenteeism, premature mortality, and reduced agricultural output, all of which collectively impose substantial financial burdens on national economies (World Bank & IHME, 2016).

In response to deteriorating air quality, the adoption of air cleaners, commonly referred to as air purifiers (APs), has increased across residential, commercial, educational, and healthcare settings. Commercially available APs vary widely in size, design, and cost, depending on their specifications and performance capabilities. However, many existing air purifiers present maintenance challenges, particularly in relation to the removal and cleaning of High-Efficiency Particulate Air (HEPA) filters used to capture airborne contaminants such as dust, pollen, mould, bacteria, and viruses. Previous studies indicate that Portable Air Cleaners (PACs) offer a cost-effective alternative for improving indoor air filtration, especially in spaces where centralised systems are impractical (Liu *et al.,* 2021).

Conventional air cleaning systems typically employ a multi-stage filtration process, beginning with a coarse pre-filter, followed by a Rota-filter that captures fine dust particles through high-speed rotation, and concluding with a HEPA-type filter capable of removing up to 70% of particles sized 0.3 µm and 95% of particles sized 1.0 µm (Vijayan *et al.,* 2015). Nevertheless, accumulated particulate matter on clogged HEPA filters can restrict airflow and degrade overall system performance. To address this issue, the proposed air cleaner prototype is designed with a user-friendly, detachable filter mechanism that allows for convenient filter removal, cleaning, and maintenance.

Recent advancements in Internet of Things (IoT) technologies have further transformed environmental monitoring systems by enabling autonomous, real-time data acquisition and control through connected devices. IoT frameworks allow physical systems to interact seamlessly with cloud-based applications via Machine-to-Machine (M2M) communication, facilitating intelligent decision-making without continuous human intervention (Mouha, 2021). When applied to air cleaning systems, IoT enables dynamic adaptation to changing environmental conditions, thereby improving operational efficiency and responsiveness.

Motivated by these challenges and technological opportunities, this study presents the design and development of a low-cost, IoT-based smart air cleaner for HVAC applications, intended to enhance indoor air quality in enclosed environments such as bedrooms, offices, and classrooms. The proposed system aims to integrate an affordable filtration mechanism with HVAC compatibility, provide real-time monitoring of critical air quality parameters including PM2.5, CO_2, and volatile organic compounds (VOCs) using a multifunctional air quality sensing unit, and enable remote access and automated control through a mobile interface via the Blynk platform. Similar IoT-enabled indoor air quality monitoring systems have been explored in recent studies, including the work by Saini et al. (Saini *et al.,* 2020), highlighting the growing relevance of smart air purification solutions. Through the integration of sensing, automation, and connectivity, the proposed system seeks to deliver an efficient, accessible, and user-centric approach to improving indoor air quality and occupant comfort.

2.0 BACKGROUND STUDY

2.1 Literature Review

Indoor air quality (IAQ) has emerged as a critical public health and engineering concern due to rapid urbanisation, increased indoor occupancy, and heightened awareness of airborne disease transmission. Pollutants such as particulate matter (PM2.5 and PM10), volatile organic compounds (VOCs), carbon dioxide gas (CO_2), and bioaerosols have been strongly associated with respiratory, cardiovascular, and infectious diseases. In response, portable and smart air purification systems have gained prominence as flexible, cost-effective, and rapidly deployable solutions compared with centralised HVAC retrofitting.

This section presents a systematic review of prior research on air purification technologies, air quality indexing, sensor-driven control mechanisms, energy-efficient operation, and IoT-based intelligent monitoring frameworks. Emphasis is placed on experimental methodologies, system architecture, performance metrics, and reported outcomes, thereby establishing a strong theoretical and empirical foundation for the present research.

2.2 Air Quality Index (AQI) as Control and Evaluation Metric

The Air Quality Index (AQI) has been widely adopted as a standardised metric for translating complex pollutant concentrations into interpretable health-based categories. Datta *et al.* (2023) operationalised AQI as a real-time control variable, wherein sensor measurements update system indices every second, enabling rapid decision-making for purifier activation.

Their classification scheme, ranging from best (0–40) to hazardous (>200) aligns with established environmental health thresholds and demonstrates the practical role of AQI beyond passive monitoring. Importantly, the authors integrated AQI thresholds directly into system logic, such that purifier operation dynamically adapts to pollution severity. This functional coupling between AQI and actuator response represents a shift from descriptive to prescriptive air quality management.

Similarly, Kumar and Doss (2023) expanded AQI utility by embedding it within an IoT ecosystem, where locally computed AQI values are transmitted to cloud infrastructure for forecasting and visualisation. This approach positions AQI as both a real-time indicator and a predictive planning variable, reinforcing its relevance in smart city air management strategies.

2.3 Filtration Technologies and Physical System Design

2.3.1 Hepa-Based Multi-Stage Filtration

High-Efficiency Particulate Air (HEPA) filtration remains the cornerstone of modern air purification systems. Shukla *et al.* (2022) demonstrated that a multi-stage configuration combining pre-filters, activated carbon filters, and HEPA media achieved 99.99% removal efficiency for $PM_{2.5}$, validating the effectiveness of layered filtration architectures.

Lowther *et al.* (2020) provided further quantitative evidence through controlled chamber experiments, revealing that CADR scales positively with purifier size and fan speed, albeit at the expense of higher power consumption. Their findings underscore a critical design trade-off between purification performance and energy efficiency, particularly relevant for long-duration indoor deployment.

Dubey *et al.* (Dubey *et al.,* 2021), conducting real-world indoor evaluations, reported PM reductions ranging from 12% to 53%, with higher CADR models outperforming smaller units under polluted conditions. These results highlight the context-dependency of purifier performance and emphasise the importance of matching purifier capacity to room volume and pollution load.

2.3.2 Portable Purifiers in Large and Shared Spaces

The effectiveness of portable air purifiers in mitigating airborne transmission risks has been rigorously examined in public settings. Zhai *et al.* (2021) evaluated floor-standing and table top purifiers in restaurant environments, demonstrating that appropriately positioned units can significantly alter airflow patterns, drawing contaminated air toward filtration inlets.

Aldekheel *et al.* (2022) extended this investigation to university classrooms, showing that operating HEPA purifiers at high flow rates reduced particle residence time from 4–6 hours to under 40 minutes, effectively accelerating aerosol decay. These findings provide compelling evidence that portable purifiers can serve as viable engineering controls for infection mitigation when HVAC modifications are impractical.

2.4 Sensor-Driven Automation and Smart Control Mechanisms

Recent advances emphasise the integration of environmental sensors and adaptive control logic to enhance purifier responsiveness and efficiency. Datta *et al.* (2023) implemented continuous gas and particulate sensing, enabling second-by-second AQI updates and automatic system actuation.

Ukagwu *et al.* (2024) advanced this paradigm by incorporating microcontroller-based control systems that dynamically adjust fan speed based on real-time air quality measurements. Their design integrates particulate, gas, and humidity sensing with optional UV-C sterilisation, illustrating a comprehensive cyber-physical approach to indoor air management. Notably, Kocak and Bunyatova (2025) introduced occupancy-aware control, where motion sensors reduce energy consumption during periods of inactivity. Their system achieved approximately 30% energy savings without compromising filtration efficiency, highlighting the value of contextual awareness in smart purifier design.

2.5 Sterilisation Technologies and Microbial Inactivation

Beyond particulate removal, microbial sterilisation has become increasingly critical in the post-COVID-19 context. UV-C irradiation, titanium dioxide (TiO_2) photocatalysis, and hydrogen peroxide-assisted disinfection have been widely explored. Kocak and Bunyatova (2025) reported 99.99% microbial filtration efficiency, with an average log reduction of 4.11 within 60 minutes, achieved through UV-C and TiO_2-based sterilisation. These findings align with earlier observations by Shukla *et al.* (2022), who emphasised the synergistic role of filtration and sterilisation in comprehensive air purification systems.

However, while sterilisation technologies enhance pathogen control, their integration introduces additional considerations related to energy consumption, material degradation, and user safety, necessitating careful system-level optimisation.

2.6 IoT-Enabled Air Quality Monitoring and Predictive Analytics

The convergence of air purification with IoT and artificial intelligence has enabled a transition from reactive to predictive air quality management. Kumar and Doss (2023) developed an IoT-based AQI monitoring framework (AIRO) that leverages CNN-BiLSTM models to forecast pollution trends, offering users actionable insights via mobile applications.

This approach demonstrates how distributed sensor networks can democratise access to environmental data while supporting municipal-scale deployment. When integrated with smart purifiers, such systems hold potential for anticipatory control, where purification intensity is adjusted in advance of predicted pollution events.

2.7 Comparative Synthesis of Methodologies and Results

Across the reviewed studies, several methodological patterns emerge:

1. Experimental rigor ranges from controlled chamber studies (Lowther *et al.,* 2020) to real-world residential and public-space evaluations (Lu *et al.,* 2024), (Aldekheel *et al.,* 2022), (Dubey *et al.,* 2021).
2. Performance metrics consistently emphasise PM2.5 reduction, CADR, energy efficiency, and microbial inactivation rates.
3. System intelligence increasingly relies on sensor fusion, occupancy detection, and cloud-based analytics.

Collectively, these findings indicate that smart, adaptive, and energy-aware air purification systems outperform static designs, particularly in heterogeneous and dynamic indoor environments.

2.8 Research Gaps and Motivation for the Present Study

Despite significant progress, several gaps remain evident in the literature:

- Limited integration of AQI-driven logic with occupancy-aware energy optimisation in a unified framework.
- Insufficient longitudinal evaluation of smart purifiers under variable real-world pollution dynamics.
- Lack of standardised benchmarks linking AQI thresholds, purification response, and health-based outcomes.
- These limitations motivate the present research, which seeks to develop and evaluate a holistic smart air purification system that synergistically combines real-time AQI sensing, adaptive control, energy efficiency, and IoT-enabled intelligence.

The following session contemporary research on air purification technologies, AQI-based control, smart sensing, sterilisation mechanisms, and IoT integration. The reviewed evidence confirms the effectiveness of HEPA-based purification while highlighting the transformative role of intelligent control and predictive analytics. These insights directly inform the conceptual design and methodological choices of the present study, which are detailed in the subsequent chapter.

1. Health Risks from Poor Air Quality

The air cleaner addresses health and well-being concerns by employing a multi-stage filtration system capable of removing a wide range of airborne contaminants, including dust, pollen, carbon dioxide (CO_2), and fine particulate matter such as PM2.5 and PM10. It combines a True High Efficiency Particulate Air (HEPA) filter with an activated carbon layer, which effectively captures volatile organic compounds (VOCs) and unpleasant odours. To further enhance indoor air quality, the system integrates ultraviolet C (UV-C) light technology, which targets and eliminates airborne pathogens and bacteria. Additionally, the system is equipped with IoT-enabled smart sensors that monitor air pollutants in real time, including PM2.5, PM10, CO_2, and VOCs. Based on detected pollutant levels, the fan speed is automatically adjusted to maintain optimal air quality without requiring user intervention.

2. Dust, Pollen, and Indoor Allergens

To combat common household allergens, the air cleaner includes a washable pre-filter designed to trap larger particles such as dust, pet dander, and debris. This feature helps to extend the operational lifespan of the main HEPA filter by reducing its load, thereby maintaining airflow efficiency and protecting the internal components. The filtration system meets True HEPA standards, ensuring the capture of 99.97 per cent of particles sized 0.3 microns or larger, which includes most common allergens, thereby improving respiratory comfort and reducing allergy triggers.

3. Maintenance Challenges with Non-Cleanable HEPA Filters

Recognising the inconvenience of traditional, non-replaceable HEPA filters, the air cleaner uses a user-friendly cartridge system that allows for quick and hassle-free replacement. Each HEPA cartridge is equipped with a colour-changing sensor that provides a visual cue when replacement is needed, either due to saturation or damage. To encourage timely maintenance and minimise environmental waste, a filter subscription service is offered, ensuring users consistently maintain peak air cleaner performance without the hassle of sourcing new filters.

2.9 Problem Statement

Poor indoor air quality caused by airborne pollutants such as dust, pollen, VOCs, CO_2, PM2.5 and PM10 continues to pose significant health risks. Existing air purification systems often lack real-time monitoring, automatic pollutant-responsive operation, and multi-stage filtration capable of addressing both particulate and gaseous contaminants. Therefore, there is a need for a smart air quality parameter that automatically adjusts purification performance to maintain safe and healthy indoor environments.

Besides, indoor environments frequently accumulate allergens, which lead to worsening allergic symptoms, reduced air cleanliness and discomfort for users. Traditional air purifiers struggle to effectively trap both large and microscopic particles while maintaining airflow efficiency. As a result, there is a need for a smart, multi-stage air cleaning system capable of continuously detecting a filtration system that incorporates a pre-filter and True HEPA technology to ensure efficient removal of allergens and particulates while sustaining optimal airflow and prolonging filter lifespan.

In addition, many existing air purifiers rely on non-cleanable or difficult-to-replace HEPA filters, which have become one of the challenges for users in maintaining optimal device performance. Without clear indicators for filter damage, users neglect timely filter replacement, resulting in reduced purification efficiency and increased environmental waste. This highlights the need for a user-friendly filter cartridge system and accessible maintenance solutions to ensure consistent, efficient, and sustainable air cleaning performance.

3.0 METHODOLOGY

3.1 Overview Project Flow

Figure 1 presents the overall project workflow. The project began with a briefing by the coordinator to outline the development process. Students conducted preliminary research based on their proposed Final Year Project (FYP) titles to identify relevant studies and research gaps. A literature review was carried out concurrently to examine current technologies, designs, and related projects. The finalised project title was submitted to the supervisor via the Title Approval Form in Week 4; unapproved titles required further research and revision. In parallel with the literature review, a systematic survey of required materials and equipment was conducted from Week 2 to Week 11. A pricing survey using Shopee and Lazada was also performed to ensure the total cost remained within the university's RM 400 budget and to support effective budget control.

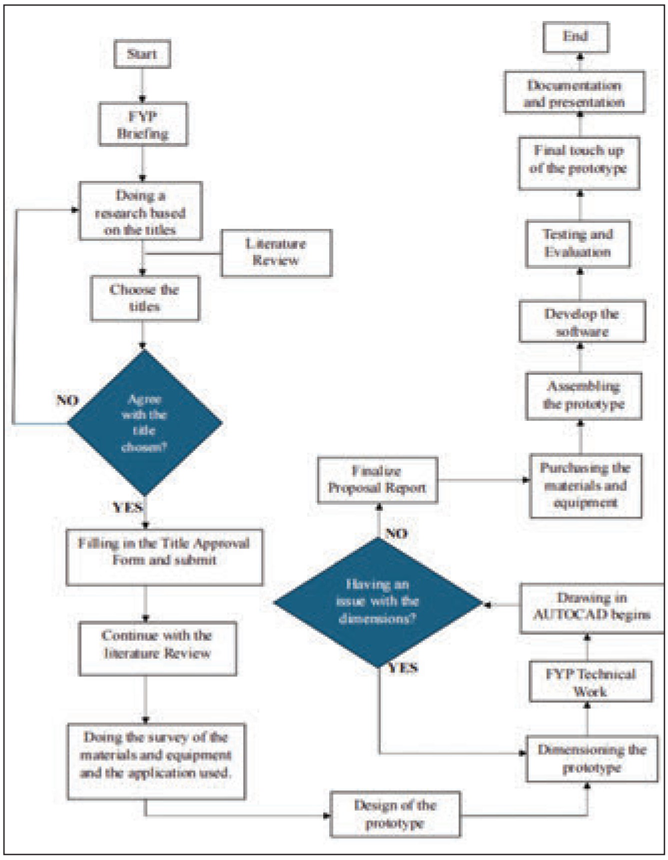

Figure 1: The overview project flow

Designing and dimensioning of the prototype were done, which will guide a drawing in CREO. The designation of the prototype was done by conducting a survey and observing some of the designs available on the market, and the reasons behind their designs, sizes, and specifications. After that, dimensioning of the prototype was done by doing a rough sketching and dimensioning of the prototype for different kinds of views, such as a 3D-view, as shown in Figure 2, and a 2D-view, which is the internal view of the prototype, as shown in Figure 3.

The Final Year Project (FYP) Technical Work was completed in accordance with university requirements and included key components such as the project introduction, prototype sketches, materials and equipment specifications, identification of research gaps, research objectives, detailed methodology, expected outcomes, and referenced literature. The Technical Work was completed with continuous guidance from the supervisor, particularly in areas such as citation methods, critical review of research articles, and clarification of expected outcomes. The completed Technical Work was submitted for assessment in Week 9. Based on the finalised design sketches and prototype dimensions, computer-aided design (CAD) modelling was performed using Creo for each internal component of the prototype. The complete assembly model is shown in the corresponding figure. Iterative redesign, re-sketching, and dimensional reanalysis were carried out throughout the modelling process to accommodate design modifications.

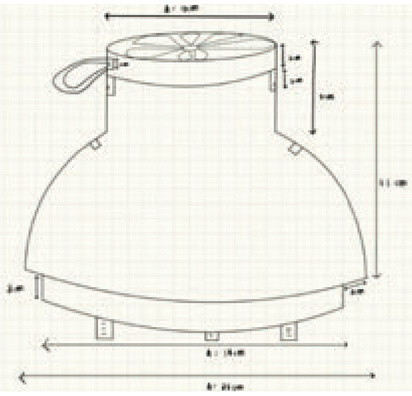

Figure 2: The 3D view of the prototype

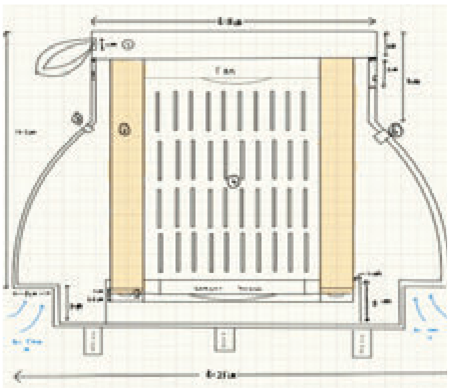

Figure 3: The internal view of the prototype

A project proposal report was prepared to provide an overview of the project, including the research gap, objectives, selected literature reviews, and a detailed list of required components and materials to ensure compliance with the allocated budget. The proposal also included a project flowchart to monitor both documentation progress and prototype development. Procurement of materials and equipment was conducted through the submission of the Material Purchase Form to the designated officer responsible for reimbursement. All purchase receipts were submitted upon receipt of the materials. Once all components were verified to be sufficient and in good condition, prototype assembly was initiated. The prototype enclosure and internal components were fabricated using 3D printing and assembled according to the finalised design specifications.

Software development was implemented using the Blynk platform to enable real-time monitoring of the Air Quality Index (AQI) and remote control of the Air Purifier (AP). System integration testing and performance evaluation were conducted to verify synchronisation between hardware and software, ensure functional reliability, and prevent component damage. Final refinements were performed to improve the prototype presentation. The project concluded with final documentation and presentation, supported by concise slides featuring clear diagrams, system flow, and technical explanations.

3.2 Designation and Dimensioning

The designation and dimensioning of the prototype began with a survey made by observing and identifying issues regarding the size and storage to place the AC. Based on the survey through observation of the AP available on the market, it is found that most of the shapes and designs available are huge and tall. The customers purchased their AP based on their choice and the requirement for the size of their house or office. Based on the research made by Iskandriawan *et al.* (2025), the airflow pattern surrounding an air purifier is greatly influenced by the product design of its constituent components, especially the blow air diffuser and the return air components. With that, the design of the AC is done precisely by comparing it with the AP available on the market.

Therefore, the invention of a small and portable AC is made to allow future users to store it even in a small storage area, and it can be brought everywhere with ease. In addition, a study has proven the effectiveness of a portable AC, where it is much quieter, less drafty, and more energy efficient (Ebrahimifakhar *et al.,* 2024). Hence, the way of designing the prototype was initiated by sketching, which includes the dimensions for each part of the prototype in detail. This includes the dimensioning of each of the small parts found on the prototype, as well as the internal components of the prototype. Figures (4 – 7) are rough sketches of each part of the components in the prototype.

3.3 Structure of the Prototype

The discussion of the structure of the prototype was made to identify what kind of materials were needed for the prototype. Through the discussion, an idea of inventing the prototype by using 3D printing for the body, top lid, filter vent, filter clip stand, and filter clip to fulfill the criteria of a portable AC and be easier to move by the user. For the 3D printing filaments, Polyethylene terephthalate Glycol (PETG) Pro type printing filaments are chosen. This is because during printing, as the temperature increases, the mechanical properties of PETG materials increase (Hsueh *et al.,* 2021).

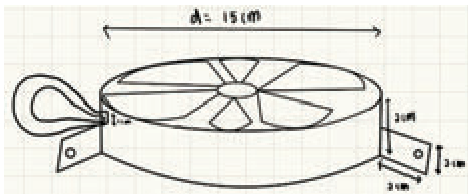

Figure 4: Sketching of the top lid

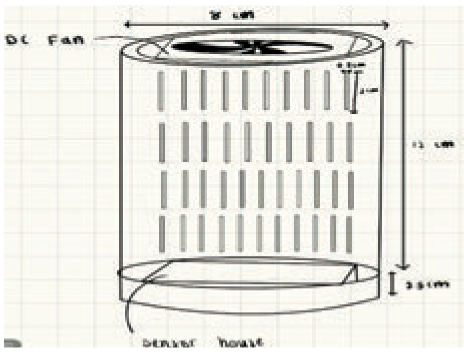

Figure 5: Sketching of the filter vent

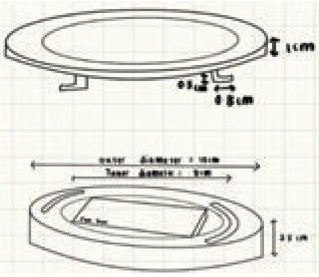

Figure 6: Sketching of the filter clip (top) and filter clip stand (bottom)

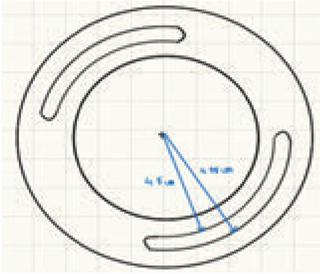

Figure 7: Sketching of the dimensions of the filter clip stand

Also, PETG Pro offers enhanced durability and impact strength, rendering it suitable for a wide array of applications (Marsavina *et al.,* 2024). Table 1 shows the list of materials and components used for the 3D printing process

Table 1: The details of the list of materials and components used and their functions

Materials and Components	Functions
3D Printer Model: CreatBot 3600 Pro Temperature used: 220°C / 80°C	To print out the body, top lid, filter vent, filter clip stand, filter clip, and openers of the prototype.
3D Printing Filament Type: PETG Pro	To create the structure of the prototype so that it is strong and durable.
Sandpaper	To remove the excess layer found on the surface of the printed prototype and to smooth the surface.
Cutting Pliers	To cut the excess filament found on the printed prototype.

However, before the printing of each part of the prototype was made, the realistic design of the prototype model was made by using Creo Parametric 8.0.4.0. The use of Creo Parametric combines two approaches, which are parametric and direct modelling. Furthermore, it is convenient to work with small applications and supports the import of formats from computer-aided design (CAD) systems from other manufacturers (Nariman *et al.,* 2025). The design was made thoroughly to ensure each part of the prototype meets the desired sketches that were prepared initially. As for the dimension, the dimension used in Creo Parametric 8.0.4.0 is millimetres (mm), although the sketches use centimetres (cm) to enlarge the drawings. Figures (8 – 12), shown below are the results of the drawings drawn in Creo Parametric 8.0.4.0.

3.4 System Overview

Figure 13 shows the flowchart of the system overview. Based on the research made, a study uses sensors to detect the condition of the surrounding air, a microcontroller, and fuzzy-logic control to adjust the DC fan speed in response to detected pollution levels (Chen *et al.,* 2022). Hence, the prototype made will use

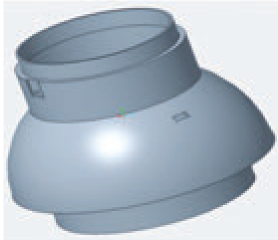

Figure 8: 3D view of body in CREO

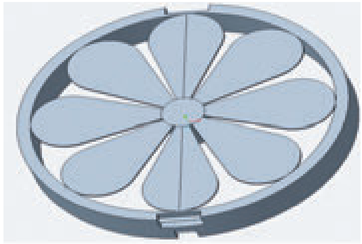

Figure 9: 3D View of top lid in CREO

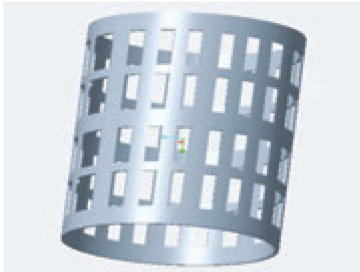

Figure 10: 3D View of filter vent in CREO

Figure 11: 3D View of filter clip in CREO

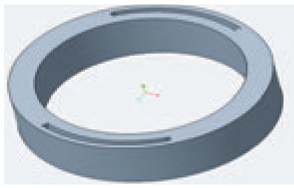

Figure 12: 3D View of filter clip stand in CREO

the same method, which is using sensors, a microcontroller, and fuzzy logic to control the DC fan speed (high speed, medium speed, or low speed) and the UVC LED light. Also, research on the usage of the Blynk platform for the user to monitor the condition of AQI is applied in this prototype to support the monitoring, alert the user, and send a predictive logic part of the system (Irdayanti & Robbani, 2022).

When the power is switched on manually or as scheduled by the user through the Blynk application, the value of the air quality index and humidity is identified and sent to the Blynk. The movement of surrounding conditions, whether caused by humans or animals, is also detected. When the AQI, temperature, and humidity of the surroundings are high, and the movement of a human is detected, the Air Cleaner (AC) will

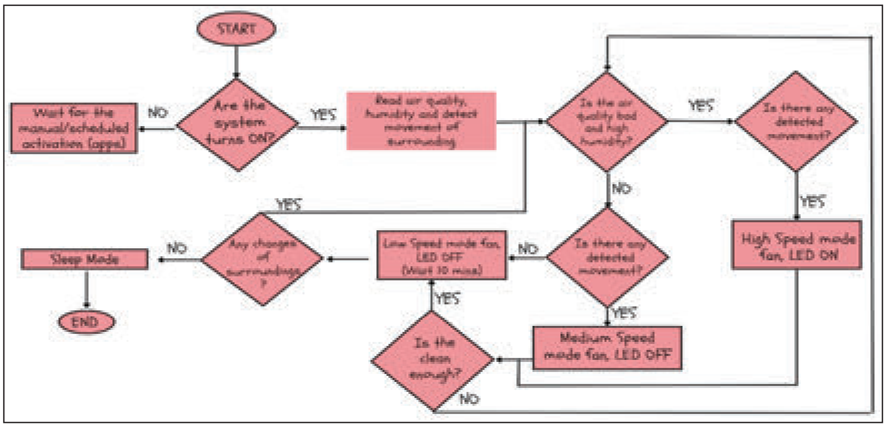

Figure 13: The flowchart of system overview

Table 2: The pin configuration and functional description of components and sensors

Pin	Sensor or Components Used	Functions
-	Arduino UNO R4 WiFi	To control and process the inputs of the sensors such as PIR Sensor 1 and 2, MQ135, and MQ2, by reading the AQI, temperature and humidity of the surroundings and send the data to Blynk so that the user can monitor it on their own and to control the speed of the Fan and the UVC LED Light through a 2 Channel Relay Module based on the commands received through programming.
D2	PIR Sensor 1	To detect the motion of humans and animals and trigger the other sensors to activate. It will be placed on the left side of the AC.
D3	PIR Sensor 2	To detect the motion of humans and animals and trigger the other sensors to activate. It will be placed on the right side of the AC.
D4	DHT11	To capture and identify the temperature and humidity of the surroundings and send the data to Blynk through the Arduino Uno R4 WiFi board.
D5	Fan that is connected to a 2 Channel Relay Module	It sucks air into the AC, which will pass through the filters, and it turns into low-speed mode, high-speed mode, and sleep mode based on the command in the Arduino.
D6	UVC LED Light that is connected to the 2 Channel Relay Module	It kills germs that cannot be seen in the air sucked into the AC and makes it clean before leaving and turns either OFF or ON based on the command in the Arduino.
A0	MQ135	To detect air quality and harmful gases available in the surroundings and help to get the AQI and send it to Blynk through Arduino.
A1	MQ2	To detect flammable gases and smoke available in the surroundings and help to get the AQI and send it to Blynk through Arduino.

put its fan into high-speed mode, and the UVC light is on. In contrast to that situation, if the AQI, temperature and humidity of the surroundings are low, but a human is detected, the AC will put its fan into a medium speed mode and the UVC light is off. For both conditions, if the air surroundings are clean enough, the AC will put its fan into a low-speed mode and the LED will turn off for 10 minutes, but if it is not, it will be processed again. The condition of the surroundings' AQI, temperature, and humidity will be ready again and will be processed until they are clean enough.

Within these 10 minutes, if there are no changes detected by the sensors of the AC, it will be put into sleep mode, unless there is a change in terms of the AQI, temperature, and humidity, and a human is detected around the AC. The AC will be put into sleep mode until the user switches it off through Blynk. Also, the data of the AQI, temperature, and humidity of the surroundings will be sent to Blynk so that it can be accessed and monitored by the user through their smartphones.

3.5 Circuit Connection

Figure 14 shows the circuit connection inside the AC. The Arduino Board used is Arduino UNO R4 WiFi, which will control all the sensors, such as MQ135, MQ2, DHT11, PIR Sensor 1, and PIR Sensor 2. It also controls the fan and UVC LED light through a 2 Channel Relay Module. Table 2 shows the configuration of the connection of the sensors and components used in this AC, as well as their functions.

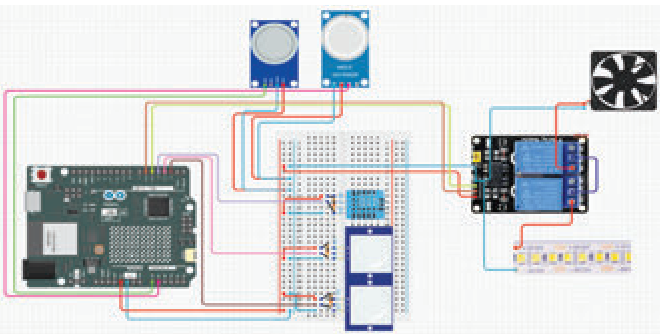

Figure 14: The circuit connection inside the air cleaner

Table 3: Data type used and their functions

Data Type	Functions
bool	For Binary Flags, such as motion detected
int	For counters and compact numeric storage where fractional precision is not required.
float	Fractional values are necessary, such as temperature, if high precision is not required
char	For short textual or Status Codes
const	For threshold constants to avoid accidental mutation
void	For functions that do not return values
loop	For continuous monitoring
string	For small, controlled textual messages, with caution due to heap usage on constrained MCUs

3.6 Arduino IDE Setup

The idea of implementing the Arduino IDE as a hardware component of the prototype is to enhance a person's lifestyle. Based on the research made by Yusop *et al.* (2024), the development of software is important to produce a good quality product to be received by the end user and fulfil stakeholder needs. In addition to that, it was mentioned that the Arduino IDE uses a variant of C/C++ to write, compile, and upload embedded code sketches for microcontrollers, which makes it a flexible and widely adopted platform for IoT and hardware prototyping (Mumtaz *et al.,* 2021).

For the prototype of AC, the C++ programming language is chosen for the prototype. With that, the Arduino IDE Software is used as it can check the commands of the code for errors and translate it into machine-readable instructions so that the microcontroller, which is Arduino UNO R4 WiFi, can understand (Yusop *et al.,* 2024).

To begin with this, the coding commands are prepared and arranged accordingly so that each block is testable, and errors are easier to locate during debugging. In coding, there are several data types used in this programming, such as bool, loop, int, char, const, float, void, and string. Table 3 below shows the functions of each of the data types used in this programming. These choices are guided by embedded systems literature showing trade-offs between integer, fixed point and floating-point arithmetic, and by coding conventions that reduce bugs and resource misuse on constrained hardware (D'Ausilio, 2012).

Also, the board manager and libraries are installed, and the Arduino Board is connected via USB cable. The right COM port is selected in the software so that it can connect easily, and it will be verified once the board detection is successful. The external libraries for Blynk, DHT, and MQ sensors are added so that they can read the data from the sensors on the Arduino UNO R4 WiFi board and transfer it to Blynk.

Before verifying, debugging, and uploading the data, WiFi and Blynk credentials are important to connect the Blynk to the sensors. This also includes the Blynk Auth Token, Blynk Template ID, and Blynk Template Name so that data can be transferred to Blynk. Figure 15 is the sample of the Blynk template ID, template name and auth token used to synchronise Blynk with the Arduino IDE.

```
#define BLYNK_TEMPLATE_ID "TMPL6FM3yqW3Q"
#define BLYNK_TEMPLATE_NAME "Vnessa Portable Air Cleaner"
#define BLYNK_AUTH_TOKEN "MGc9GK-I-twuu3PBZyH-26lLWIqlcGqV"
```

Figure 15: The sample of BLYNK template id, template name

In addition, a calculation to calculate the air quality index is employed in the coding to command the system to automatically calculate the AQI, which will be sent to Blynk. Figure 16 shows the method of inserting and applying the formula to calculate AQI in the coding system. The formula of the calculation used is shown below [27].

$$I_p = \frac{I_{HI} - I_{LO}}{BP_{HI} - BP_{LO}} \, x \, (Cp - BP_{LO}) + I_{LO} \quad [1]$$

Where,
I_p= Index of pollutants
I_{HI}= AQI value corresponding to BP_{HI}
I_{LO} = AQI value corresponding to BP_{LO}
BP_{HI} = Breakpoint that is greater than or equal to C_p
BP_{LO} = Breakpoint that is less than or equal to C_p
C_p = Rounded concentration of pollutants

```
loat calculateAQI(float C, float Clow, float Chigh, float Ilow, float Ihigh) {
  float aqi = ((Ihigh - Ilow) / (Chigh - Clow)) * (C - Clow) + Ilow;
  return aqi;
}
```

Figure 16: The method of inserting and applying the AQI formula

3.7 BLYNK Setup

Blynk is an application used to modify and widget in a system. It integrates with Arduino UNO R4 WiFi to receive a command for the control of the AC. Zain *et al.* demonstrate how the Blynk mobile application integrates with microcontroller-based sensing to deliver real-time air quality data to the user's smartphones (Dinčić *et al.,* 2023). Besides, Pramana *et al.* demonstrated how the Blynk platform can be integrated with a microcontroller-based system to remotely monitor and control smart home devices, including sensors for temperature, humidity, and appliance actuation. The study highlights the use of widgets and real time data visualisation to enhance user interaction with IoT devices (Zain *et al.,* 2024). In this situation, proper coding is needed to enable Blynk to execute commands and send signals between the mobile application and the Arduino hardware.

Table 4: The proposed widget design and functional description for air cleaner

Function	Widget	Description
Air Quality Index (AQI)	Gauge	Real-time display of AQI value from MQ135 and MQ2
Temperature	Label	DHT11 temperature in °C
Humidity	Label	DHT11 humidity in %
System Power (ON/OFF)	Switch	Turn the whole system ON/OFF
Air Quality Index Graph Analysis	Custom Chart	Graph trends for analysis

Also, some codes are needed to set up the widgets used in the Blynk, such as the widgets for the AQI, temperature, humidity, a switch to toggle the AC into 'ON' and 'OFF' modes, and the graph analysis of the AQI. The graph analysis of the AQI is used to visualise real-time AQI data trends and provide immediate insights of the indoor air quality for the user. Table 4 shows the data used for the setup of the widgets in Blynk.

Blynk provides real-time notifications that inform users of the AC system status and environmental conditions. It notifies and alerts its users when the AC system is ON', OFF, the temperature is high or low, and the AQI is too high, by sending notifications. Figure 17 shows the list of notifications received by the apps.

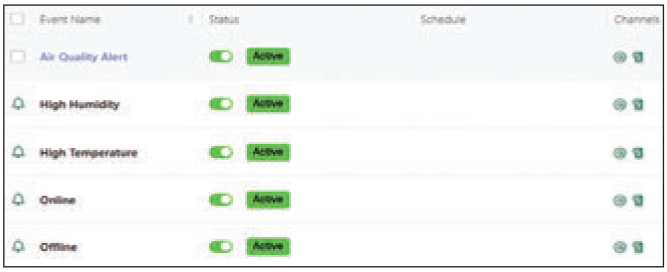

Figure 17: The event and notifications configurations of the air cleaner system

3.8 3D Printing Finishing

The final step for finishing the 3D printed prototype is important to ensure a smooth, neat, and proper surface finish. Based on the research made, it is essential to remove residuals and supports of the 3D printed prototype, clean and polish the 3D printed prototype, as it is the best practice in the workflow (Pramana *et al.,* 2025). With that, the final steps, which is removing residual and supports of the 3D printed prototypes, cleaning and polishing, are done to improve the AC's look and to smooth its surface.

Firstly, when the body of the prototype has been printed out by the 3D printing machine, the supports are removed slowly so that the structure of the prototype does not crack or damage by using cutter pliers. After that, the sanding process is done so that the surface of the body is smoothed by using sandpaper to improve its appearance. Kantharos *et al.* (2024) studied the essentials of cleaning, surface finishing, and support structure removal of 3D printed products to refine their qualities. Then, the sanded surface is cleaned by using water to remove the residue of the removed parts. These steps are repeated for other components of the prototype as well. Once cleaning and polishing are done, the components of the prototype are assembled using glue. Let the glue dry, and make sure the assembled components are strong enough.

3.9 Filters Development

The filter development process involved designing a multilayer filtration system to enhance particulate and gas absorption efficiency. The steps of developing a filter involve the selection of suitable filter media, cutting, joining, and assembling them.

As for the filter media, the first internal layer is an activated carbon filter. This is because the activated carbon filter has a high absorption capacity for gaseous pollutants and volatile organic compounds (VOC). Recent studies have demonstrated that activated carbon integrated into filter membranes significantly improves the removal of toxic gases and enhances overall air purification performance (Ryu *et al.,* 2023). Also, it can remove the odour of the surroundings. This activated carbon filter layer is measured and cut according to the required dimensions. As for the second internal layer, thick interlining fabric is used. It provides mechanical support for the thin interlining fabric outside of it so that it does not collapse. It could enhance the filtration of larger particulates and stabilise the arrangement of inner layers. S. Jung *et al.* (2020) conducted research that explains that coarser, thicker textile layers capture larger particles and support finer layers. As for the layer, which is outside of the 2 other layers, thin interlining fabric is used. It serves as a particulate filter, capturing small dust particles while maintaining airflow into the AC. It also has a low-thick surface that allows air to pass through it with minimal pressure drop. Based on the study made, thin fabrics can improve the efficiency of the particulate filtration, while keeping the pressure drop low, and preserving airflow through the system (Jung & Kim, 2020).

Figure 18: The combined filters which consists of thin and thick interlining fabrics (most outer side) and activated carbon filter (internal side)

Before assembling these layers of filter, each filter was measured along the line drawn, based on the required dimension. Then, the thin and thick interlining fabrics were joined together by using a sewing machine. Studies on multilayer textile filters emphasise that combining different fabric densities significantly enhances particulate matter removal compared to single-layer filters (Ma *et al.,* 2023). After that, they were cut accordingly so that they looked tidy. Once it is done, the joined filters are folded in 'zigzag' form. This is because the 'zigzag' form can increase the total surface area of the filters so that more particles and air can be absorbed at the same time, although the internal area of the filter vent is small.

To stick the joined thin and thick interlining fabric on the filter vent, they were glued using a hot glue gun. This method of sticking on the filter vent is repeated for the activated carbon filter. Once it is done, the excess glue around the filters is cleaned. Figure 18 shows the combined filters that will be attached to the AC.

4.0 RESULTS AND DISCUSSION

4.1 Hardware Overview

The hardware setup consists of several key components integrated to achieve air quality monitoring and purification functions. Figure 19 above is the outcome of the circuit for the AC prototype. The main control unit is the Arduino Uno R4 WiFi microcontroller, which coordinates all sensor readings and actuator responses. The MQ135 and MQ2 sensors are used to detect carbon dioxide, volatile organic compounds, and smoke levels in the surrounding air. A DHT11 sensor monitors temperature and humidity, ensuring environmental conditions are accurately recorded. The use of sections to divide the text of the paper is optional and left as a decision for the author. Where the author wishes to divide the paper into sections the formatting shown in Table 1 should be used.

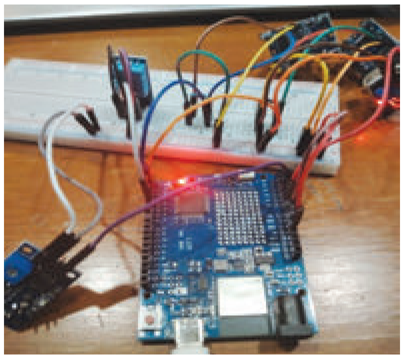

Figure 19: The circuit connection of the prototype

Two PIR sensors are employed to detect human presence, allowing the system to activate only when motion is detected, thereby improving energy efficiency. The 2-2-channel relay module serves as a switching interface, controlling the DC Fan and UV-C light based on signals from the microcontroller. Power is supplied via a regulated 12V DC adapter, ensuring stable operation of all components. Additionally, all components are mounted in a custom-designed 3D-printed enclosure, designed in Creo and sliced in Cura. The final assembly provides both protection and functionality, allowing for efficient airflow and accurate sensor readings. Figures 20 (a – f) are the product of the 3D printed prototypes of the AC.

4.2 BLYNK Overview

Blynk is an application used to monitor the condition of the AC. Figure 21(a) above is the overview of the Blynk for the AC, which includes the essential widgets to monitor the humidity, temperature and AQI and control the AC. As for the Blynk platform used by the prototype, it enables real-time monitoring and remote control of the hardware system. Sensor data from the MQ135, MQ2 and DHT11 modules are transmitted via the Arduino microcontroller to the Blynk mobile application. This allows users to view AQI, temperature, and humidity, as well as the graphs of the condition of the AQI based on time, on their smartphones.

In addition, a notification from Blynk regarding the surrounding conditions is sent automatically when the AQI drops below the threshold, demonstrating the system's ability to respond dynamically to environmental changes. Here, the user can turn the prototype into 'ON' and 'OFF' modes. This can help the user to control their AC from a distance to ease their work and save their time since they can control it anywhere and anytime. When the AC is turned ON and OFF, a notification will be sent to the user through the app, as shown in the figure below. Figures 21(b) and 21(c) are examples of the notification received by the user when their AC is turned 'ON' and 'OFF'.

(a) The 3D-printed body

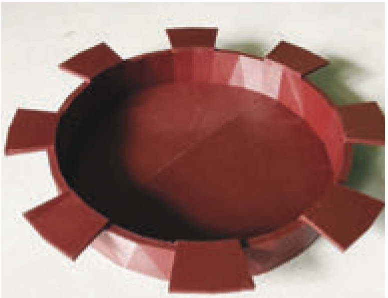

(b) The bottom part of the body

(c) The top lid

(d) The filter vent

(e) The filter stand

(f) The filter clip

Figure 20: Individual mechanical parts developed for the air cleaner prototype

4.3 Testing of the Air Cleaner

4.3.1 Case 1

The prototype is tested in a living room, 6.02 m x 2.95 m x 3.22 m, with ceiling fan speed 1, and the window is wide open. Testing is done to ensure the sensors used, such as MQ135, MQ2, PIR sensors, and DHT11, are functioning well and can provide accurate readings. Based on Figure 22 above, the readings obtained from Blynk, which is a platform used to detect the surrounding condition of the air as well as the AQI, it was found that the readings obtained are near to the accepted range. For instance, the temperature obtained from the DHT11 sensor is 28 °C and the humidity is 81%.

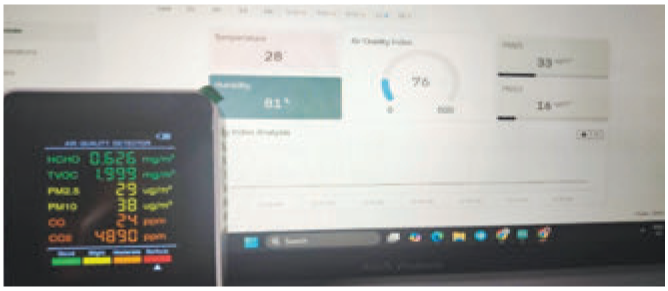

Figure 22: The testing of the accuracy of the sensors

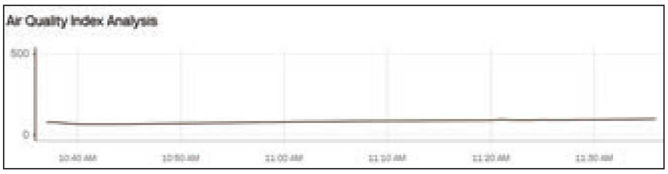

Figure 23: Graph of the AQI increment as the time increases

To test the overall functionality of the prototype, the prototype is tested in a living room (6.02 m x 2.95 m x 3.22 m), and the speed of the ceiling fan is in 'Speed 1' for 1 hour and 15 minutes. The AC is switched ON to let it fully balance for the first 15 minutes. After 15 minutes, a small increase of AQI, PM2.5 and PM10 is detected. This continued for another 30 minutes to observe a gradual increment in the value of the AQI, PM2.5 and PM10. Graph shown in Figure 23 proves the small increment value of the AQI as time increases.

After 45 minutes, a sudden spike of the AQI reaches 99, which means the value starts to get balanced based on the US AQI Standard Guideline as shown in Figure 24. After 1 hour, the AQI reached 101 while its PM2.5 is 37 μg/m³ and PM10 is 20 μg/m³. In order to check the accuracy of the AQI value obtained and measured by the prototype, the AQI formula is used to compare it with theoretical value. Figure 24 shown below is the US AQI

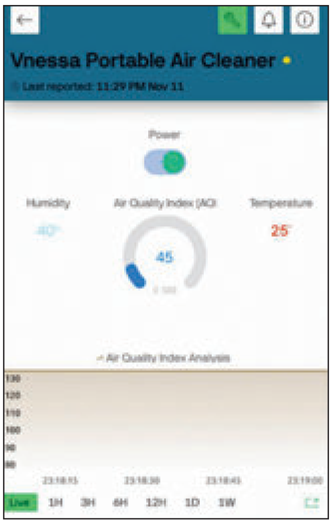

(a) The overview of the Blynk

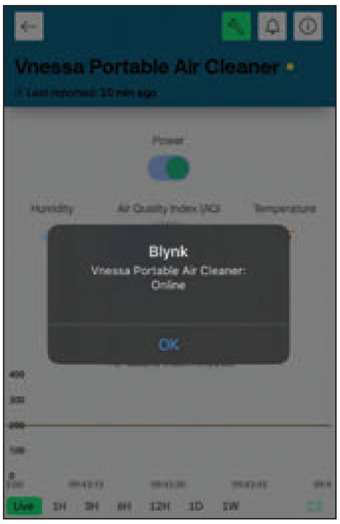

(b) The notification received when the AC is turned on

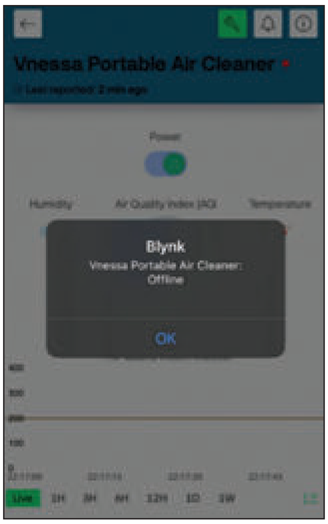

(c) The notification received when the AC is turned off

Figure 21: IoT mobile application interface for system status monitoring

Standard Guideline for PM2.5 which is used to get the range of the accuracy of the AQI.

Based on the formula of the AQI (Zahedi *et al.,* 2024),, the theoretical value of the AQI is obtained based on the step-by-step formula:

$$IP\ (Theoretical\ Value) = [(150-101)/(55.4-35.5)]\ (37-35.5) + 101 = 104.69 \quad [2]$$

$$Percentage\ Error = [(104.69 - 101) / 101] \times 100\% = 3.65\%$$

Where,
I_{HI} = 150
I_{LO} = 101
BP_{HI} = 55.4 μg/m³
BP_{LO} = 35.5 μg/m³
C_p = 37 μg/m³

After calculating the theoretical value of the AQI, the calculated value, 104.69, is compared with the measured value obtained by the prototype, 101. The percentage error, 3.65%, is found based on the calculation made above. This occurred due to the environmental issue where strong wind came from the open window and entered the MQ sensors' chamber continuously and disrupted the readings. Based on the percentage error obtained, it is found that the value is much smaller than the research made by Afrial *et al.* (2025), where the percentage error is 5% and Santoso *et al.* (2025) where the percentage error is 23.59%.

4.3.2 Case 2

As for case 2, the prototype is tested in a larger room, 12.09 m x 6.2 m x 3.22 m, with no fan from 5:17 PM to 6:35 PM. Also, this case is done continuously, where initially, the door is closed, and then it is opened to obtain the readings throughout the testing process. For almost an hour. For the first 10 to 15 minutes (5:17 PM to 5:32 PM), the system is switched ON to let it balance. After 15 minutes, the data of the AQI, PM2.5 and PM10 measured by the prototype are collected as shown in Table 5 below. In this case, when the doors are both closed and opened, to calculate the theoretical value of the AQI, the range value of the PM2.5 is chosen. Besides, starting from 5:32 PM to 6:30 PM, it is found that the range value of PM2.5 lies within the range of 55.4 to 35.5. Figures from 33 to 45 show the condition of the AQI graph, and the readings of AQI, PM2.5 and PM10 in Blynk throughout the experiment time.

Figure 25: The overview of the large size of the room

Figure 26: The overview of the large size of the room when the three doors are open

Initially, after the system is left to balance for 15 minutes, from 5:32 PM to 6:03 PM, which is 31 minutes, it is found that the values of the AQI start to increase rapidly from 109 to 132 as the time increases. This influences the increase in PM2.5 values from 43 μg/m³ to 51 μg/m³, while PM10 values range from 22 μg/m³ to 28 μg/m³. Based on the results obtained, this shows that in a closed room, with no air flow entering or leaving, the air ventilation is very low, and the air particles and dust are trapped in the room, which leads to the rapid increase of the AQI, PM2.5, and PM10 values. Besides, the Percentage error of the AQI obtained is very large, which ranges from 9.61% to 5.43%. This is due to the imbalance condition of the closed room, which affects the value of the AQI.

However, at 6:03 PM, when the three doors are open as shown in Figure 26, a sudden spike of the AQI is from 132 to 134 while the value of the PM2.5 and PM10 is maintained at 51 μg/m³ and 28 μg/m³, each. As time increases, it is found that the value of the

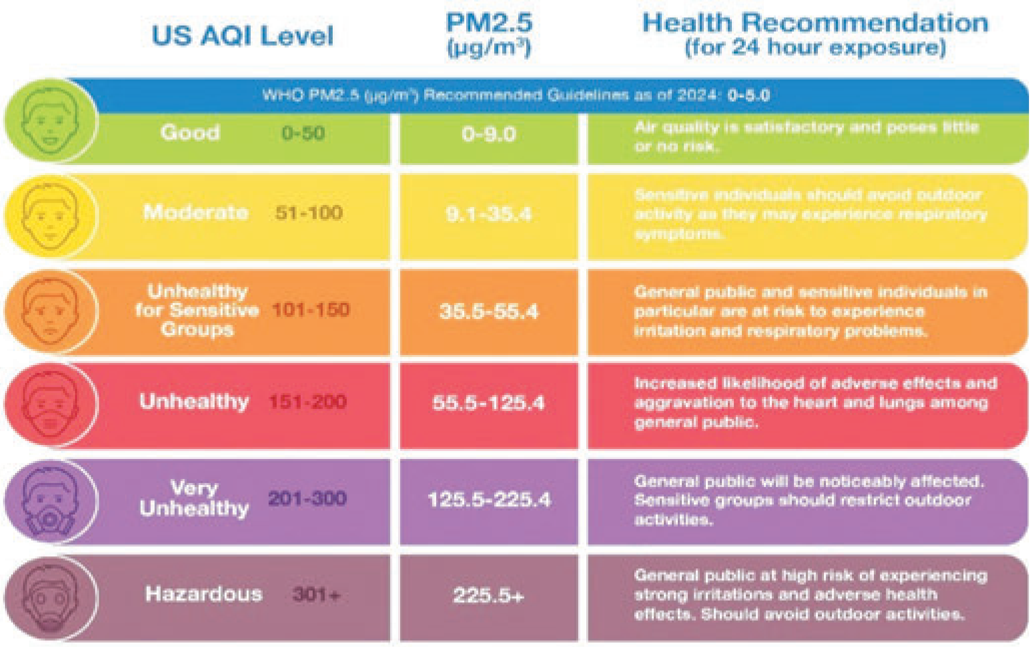

WHO PM2.5 (μg/m³) Recommended Guidelines as of 2024: 0-5.0

US AQI Level		PM2.5 (μg/m³)	Health Recommendation (for 24 hour exposure)
Good	0-50	0-9.0	Air quality is satisfactory and poses little or no risk.
Moderate	51-100	9.1-35.4	Sensitive individuals should avoid outdoor activity as they may experience respiratory symptoms.
Unhealthy for Sensitive Groups	101-150	35.5-55.4	General public and sensitive individuals in particular are at risk to experience irritation and respiratory problems.
Unhealthy	151-200	55.5-125.4	Increased likelihood of adverse effects and aggravation to the heart and lungs among general public.
Very Unhealthy	201-300	125.5-225.4	General public will be noticeably affected. Sensitive groups should restrict outdoor activities.
Hazardous	301+	225.5+	General public at high risk of experiencing strong irritations and adverse health effects. Should avoid outdoor activities.

Figure 24: The US AQI standard guideline for PM2.5

AQI maintains its value over time, and it increases slowly as the time increases. For instance, from 6:03 PM to 6:06 PM, the value of the AQI is 134, while from 6:06 PM to 6:12 PM, the AQI becomes 136, but the value of the PM2.5 and PM10 for these 2 situations is maintained at 51 μg/m³ and 28 μg/m³, each, which is around 6 minutes. In this case, the uncertainty value of the AQI is 2.

From 6:12 PM to 6:16 PM, the AQI becomes 137, and from 6:16 PM to 6:25 PM is 139, while maintaining their PM2.5 and PM10 values at 52 μg/m³ and 29 μg/m³, each. Also, the AQI spikes to 141 at 6:25 PM, and the PM2.5 and PM10 values increase to 53 μg/m³ and 30 μg/m³, each. Here, the percentage error of the AQI obtained starts to decrease from 3.38% to 2.19%.

At 6:30 PM, the AQI spikes again to 143 while maintaining its PM2.5 at 53 μg/m³ and PM10 at 30 μg/m³, while at 6:33 PM, the AQI is 144, PM2.5 is 54 μg/m³ and the PM10 stays at 30 μg/m³. This second and last case shows a much smaller percentage error, which is 0.76% and 1.77% each. This means that it is near to the accuracy of the theoretical value of the AQI. The decreasing percentage error, closer to the accuracy shows that the prototype can get a much smaller percentage error compared to the research made by Afrial *et al.* (2025)., where the percentage error is 5% and Santoso *et al.* (2025), where the percentage error is 23.59%.

With that, when the doors are open, there is air flow entering and leaving the room, and the air ventilation is much better. Therefore, it is obvious that the AQI is unable to increase rapidly during this time, but it still increases slowly. Also, at the same time, the value of the PM2.5 and PM10 increases within the range of 51 μg/m³ to 54 μg/m³, and 28 μg/m³ to 30 μg/m³, each. With that, this shows that the prototype is unable to fully help decrease the AQI of the surroundings as well as the PM2.5 and PM10 content in the air, but it can help to control it so that it does not cause the AQI to be worse.

Table 5 shows a compiled AQI, PM2.5, and PM10 in both situations, with doors closed and open from 5:17 PM to 6:35 PM. Table 6 shows the results of the theoretical value of the AQI when calculated by using the AQI formula, together with the percentage error when comparing the theoretical value with the value obtained by the prototype.

4.4 Assumptions and System Limitations

The development and evaluation of the proposed IoT-based smart air cleaner were conducted under several technical and environmental assumptions. The system is intended for indoor residential environments with moderate pollution levels and limited air exchange. AQI computation is based on the US AQI standard for PM2.5, assuming particulate matter is the dominant pollutant in the tested conditions. The

Table 5: The data obtained for AQI, PM2.5, and PM10 based on time in two different situations

Time	AQI	PM2.5 (ug/m³)	PM10 (ug/m³)	Refer to Appendix	Situation
5:32 PM to 5:34 PM	109	43	22	A1	All doors are closed
5:34 PM to 5:47 PM	122	48	25	A2	
5:47 PM to 5:52 PM	126	49	26	A3	
5:52 PM to 5:57 PM	129	50	27	A4	
5:57 PM to 6:03 PM	132	51	28	A5	
6:03 PM to 6:06 PM	134	51	28	A6	3 doors are open
6:06 PM to 6:12 PM	136	51	28	A7	
6:12 PM to 6:16 PM	137	52	29	A8	
6:16 PM to 6:25 PM	139	52	29	A9	
6:25 PM to 6:30 PM	141	53	30	A10	
6:30 PM to 6:33 PM	143	53	30	A11	
6:33 PM to 6:35 PM	144	54	30	A12	

Table 6: The theoretical value of AQI and percentage error when comparing the theoretical value of AQI with the value obtained by the prototype

Theoretical Value of AQI	Percentage Error (%)
[(150-101)/ (55.4-35.5)] (43-35.5) + 101 = 119.47	[(119.47 – 109) / 109] x 100% = 9.61
[(150-101)/ (55.4-35.5)] (48-35.5) + 101 = 131.78	[(131.78 – 122) / 122] x 100% = 8.02
[(150-101)/ (55.4-35.5)] (49-35.5) + 101 = 134.24	[(134.24 – 126) / 126] x 100% = 6.54
[(150-101)/ (55.4-35.5)] (50-35.5) + 101 = 136.70	[(136.70 – 129) / 129] x 100% = 5.97
[(150-101)/ (55.4-35.5)] (51-35.5) + 101 = 139.17	[(139.17 – 132) / 132] x 100% = 5.43
[(150-101)/ (55.4-35.5)] (51-35.5) + 101 = 139.17	[(139.17 – 134) / 134] x 100% = 3.86
[(150-101)/ (55.4-35.5)] (51-35.5) + 101 = 139.17	[(139.17 – 136) / 136] x 100% = 2.33
[(150-101)/ (55.4-35.5)] (52-35.5) + 101 = 141.63	[(141.63 – 137) / 137] x 100% = 3.38
[(150-101)/ (55.4-35.5)] (52-35.5) + 101 = 141.63	[(141.63 – 139) / 139] x 100% = 1.89
[(150-101)/ (55.4-35.5)] (53-35.5) + 101 = 144.09	[(144.09 – 141) / 141] x 100% = 2.19
[(150-101)/ (55.4-35.5)] (53-35.5) + 101 = 144.09	[(144.09 – 143) / 143] x 100% = 0.76
[(150-101)/ (55.4-35.5)] (54-35.5) + 101 = 146.55	[(146.55 – 144) / 144] x 100% = 1.77

MQ135 and MQ2 sensors are assumed to operate within their specified ranges and to be sufficiently calibrated during short-term testing, while the DHT11 sensor is assumed to provide acceptable accuracy despite its known tolerance limits. The filtration layers are assumed to be clean and unsaturated during experiments. Stable power supply and uninterrupted WiFi connectivity are also assumed for proper system operation and real-time monitoring through the Blynk platform. Several limitations should be acknowledged. The MQ-series sensors are low-cost semiconductor sensors and do not perform direct particle counting like laser-based PM sensors, which may affect AQI precision. The Clean Air Delivery Rate (CADR), airflow distribution, and pressure drop across filters were not experimentally characterised.

The prototype is optimised for small to medium-sized rooms, and performance in larger or heavily polluted environments may be reduced. Testing was conducted over limited durations; long-term sensor drift, filter lifespan, and durability were not evaluated. Although UV-C integration is included, microbial inactivation efficiency was not experimentally validated. In addition, detailed energy consumption analysis and system performance under network disruption were not assessed. Future work should incorporate higher-precision particulate sensors, long-term validation studies, airflow and CADR measurements, UV-C effectiveness testing, and energy optimisation analysis to improve system reliability and scalability.

Table 7: The total price of the materials and equipment used

Materials & Equipment	Price (RM)
PETG Pro Filament	108.46
2 Channel Relay Module	4.74
12V DC Adaptor	5.90
DHT11 Sensor	3.90
Transistor	0.50
Mosfet IRLZ44N	3.95
Male to Male Wire	3.20
Male to Female Wire	3.20
UVC LED Light Strip	12.25
Red & Black Wire	6.60
DC Jack Converter	1.65
Arduino UNO R4 WiFi	69.95
Activated Carbon Filter	6.50
Kain Gam Keras	2.80
Kain Gam Nipis	2.15
Resistor	1.20
PIR Motion Sensor	4.00
DC Fan	7.50
MQ135 Sensor	5.40
MQ2 Sensor	5.40
Breadboard	3.75
Small Tyres	5.20
Glue	12.40
TOTAL	280.60

5.0 CONCLUSION

The progress made so far in developing the AC prototype lays a strong foundation for achieving the project's intended outcomes. This AC is being developed successfully with low-cost materials and equipment. It also consists of a low-cost multistage filtration system, which includes an HEPA and an activated carbon filter. The overall total cost for this AC is RM280.60 as shown in Table 7, which consists of the price of each of the materials used.

Besides, this AC can provide a real-time value of the AQI, PM2.5 and PM10 values that are measured by the multifunctional indoor air quality meter. The results shown by the AC are close to the agreement to the expected values. When calculating the theoretical values, it is found that the results provided by the AC have a small difference and uncertainties from the theoretical values. This also leads to much smaller values of the percentage error. Therefore, as the time increases, the system of the AC will be more balanced and will eventually produce a small percentage error of the AQI. In addition, the usage of Blynk as a platform to control and monitor the AQI, PM2.5 and PM10 successfully provides remote access and control to the AC. For instance, the user can control the switch, either to switch it ON or OFF, of the AC through Blynk. They can also monitor the history of the AQI measured by the system. With that, this AC has proven that the usage of the mobile interface applied in this AC is user-friendly. ■

ACKNOWLEDGEMENT

This research was funded by Universiti Tenaga Nasional, Malaysia.

AUTHORS' CONTRIBUTIONS

Vanessa Anastacia Bong	Conceptualisation, methodology, investigation, data curation, formal analysis, visualisation, writing original draft.
Lay Sheng Ewe	Conceptualisation, supervision, project administration, resources, writing.
Emadaddin Abdo Mohammed Alazzani	Supervision, writing, review & editing.
Sara Kit Yee Lee	Writing, review & editing.
Chee Fui Wong	Writing, review & editing.

REFERENCES

[1] Akimoto, H., & Sato, K. (2022). Development of science and policy related to acid deposition in East Asia over 30 years. *Atmospheric Environment: X.* https://doi.org/10.1186/s42834-022-00120-5

[2] Aldekheel, M., Altuwayjiri, A., Tohidi, R., Jalali Farahani, V., & Sioutas, C. (2022). The role of portable air purifiers and effective ventilation in improving indoor air quality in university classrooms. *International Journal of Environmental Research and Public Health, 19*(21), 14558. https://doi.org/10.3390/ijerph192114558

[3] Afrial, M., Rauf, M., Nouman, M., Khan, M. T., Rizwan, M. A., & Ahmad, N. (2025). Multi-sensor indoor air quality monitoring with real-time logging and air purifier

integration. *Materials Proceedings, 23*(1), 12. https://doi.org/10.3390/materproc2025023012

[4] Chen, H., Oliver, B. G., Pant, A., Olivera, A., Poronnik, P., Pollock, C. A., & Saad, S. (2022). Effects of air pollution on human health: Mechanistic evidence suggested by in vitro and in vivo modelling. *Environmental Research, 212*(Part C), 113378. https://doi.org/10.1016/j.envres.2022.113378

[5] Datta, P., Singh, J., Kumar, N., Sharma, K., & Yadav, R. (2023). Smart air purifier. In *Proceedings of the 2023 International Conference on Disruptive Technologies (ICDT)* (pp. 794–797). IEEE. https://doi.org/10.1109/ICDT57929.2023.10150554

[6] Dinčić, M. R., Perić, Z. H., Denić, D. B., & Denić, B. D. (2023). Optimization of the fixed-point representation of measurement data for intelligent measurement systems. *Measurement, 217,* 113037. https://doi.org/10.1016/j.measurement.2023.113037

[7] Dubey, S., Rohra, H., & Taneja, A. (2021). Assessing effectiveness of air purifiers (HEPA) for controlling indoor particulate pollution. *Heliyon, 7*(9), e07976. https://doi.org/10.1016/j.heliyon.2021.e07976

[8] D'Ausilio, A. (2012). Arduino: A low-cost multipurpose lab equipment. *Behavior Research Methods, 44*(2), 305–313. https://doi.org/10.3758/s13428-011-0163-z

[9] Ebrahimifakhar, A., Poursadegh, M., Hu, Y., Yuill, D. P., & Luo, Y. (2024). A systematic review and meta-analysis of field studies of portable air cleaners: Performance, user behavior, and by-product emissions. *Science of the Total Environment, 912,* 168786. https://doi.org/10.1016/j.scitotenv.2023.168786

[10] Hsueh, M. H., Lai, C. J., Wang, S. H., Zeng, Y. S., Hsieh, C. H., Pan, C. Y., & Huang, W. C. (2021). Effect of printing parameters on the thermal and mechanical properties of 3D-printed PLA and PETG using fused deposition modeling. *Polymers, 13*(11), 1758. https://doi.org/10.3390/polym13111758

[11] Irdayanti, Y., & Robbani, M. I. (2022). Design of a fuzzy logic-based intelligent hybrid air purifier using pollutant-absorbing plants. *Jurnal Elektronika dan Otomasi Industri.* https://doi.org/10.33795/elkolind.v12i2.7896

[12] Iskandriawan, B., Safaat, A., & Tristiyono, B. (2025). Air velocity and pressure measurements of portable air purifiers using numerical simulations based on product component design variation. *Journal of Applied Engineering Science, 23*(1), 141–150. https://doi.org/10.5937/jaes0-54527

[13] Jung, S., & Kim, J. (2020). Advanced design of fiber-based particulate filters. *Polymers*. https://doi.org/10.3390/polym12081714

[14] Kantaros, A., Ganetsos, T., Petrescu, F. I. T., Ungureanu, L. M., & Munteanu, I. S. (2024). Post-production finishing processes utilized in 3D printing technologies. *Processes, 12*(3), 595. https://doi.org/10.3390/pr12030595

[15] Kocak, O., & Bunyatova, U. (2025). Integrating smart air purifiers in building controls: A conceptual approach to infection and energy management. *Energy Reports, 13,* 2545–2554. https://doi.org/10.1016/j.egyr.2025.01.072

[16] Kumar, T., & Doss, A. (2023). AIRO: Development of an intelligent IoT-based air quality monitoring solution for urban areas. *Procedia Computer Science, 218*, 262–273. https://doi.org/10.1016/j.procs.2023.01.008

[17] Liu, D. T., Phillips, K. M., Speth, M. M., Besser, G., Mueller, C. A., & Sedaghat, A. R. (2021). Portable HEPA purifiers to eliminate airborne SARS-CoV-2: A systematic review. *Otolaryngology–Head and Neck Surgery, 166*(4), 615–622. https://doi.org/10.1177/01945998211022636

[18] Lowther, S. D., Deng, W., Fang, Z., Whyatt, J. D., Wild, O., Wang, X., & Jones, K. C. (2020). How efficiently can HEPA purifiers remove priority fine and ultrafine particles from indoor air? *Environment International, 144,* 106001. https://doi.org/10.1016/j.envint.2020.106001

[19] Lu, F. T., Laumbach, R. J., Legard, A., Myers, N. T., Black, K. G., Ohman-Strickland, P., Alimokhtari, S., de Resende, A., Calderón, L., Mainelis, G., & Kipen, H. M. (2024). Real-world effectiveness of portable air cleaners in reducing home particulate matter concentrations. *Aerosol and Air Quality Research, 24,* 230202. https://doi.org/10.4209/aaqr.230202

[20] Ma, W., *et al.* (2023). Efficient, breathable, and compostable multilayer air filter material prepared from plant-derived biopolymers. *Membranes*. https://doi.org/10.3390/membranes13040380

[21] Marsavina, L., Dohan, V., & Galatanu, S. V. (2024). Mechanical evaluation of recycled PETG filament for 3D printing. *Fracture and Structural Integrity, 18*(70), 310–321. https://doi.org/10.3221/IGF-ESIS.70.18

[22] Mouha, R. A. (2021). Internet of Things (IoT). *Journal of Data Analysis and Information Processing, 9,* 77–101. https://doi.org/10.4236/jdaip.2021.92006

[23] Mumtaz, R., Zaidi, S. M. H., Shakir, M. Z., Shafi, U., Malik, M. M., Haque, A., Mumtaz, S., & Zaidi, S. A. R. (2021). Internet of Things (IoT) based indoor air quality sensing and predictive analytic—A COVID-19 perspective. *Electronics, 10*(2), 184. https://doi.org/10.3390/electronics10020184

[24] Nariman, S., Rakhmetov, M., Nurbekova, G., Issakova, G., & Orazbayeva, B. (2025). Teaching 3D engineering modeling and prototyping in Creo parametric in

educational institutions. *International Journal of Innovative Research and Scientific Studies, 8*(4), 460–467. https://doi.org/10.53894/ijirss.v8i4.7872

[25] Pramana, I. G. B. A., Akbar, L. A. S. I., & Ramadhani, C. (2025). Development of an IoT-based smart home prototype using the Blynk application. *Motivection: Journal of Mechanical, Electrical and Industrial Engineering, 7*(1), 25–36. https://doi.org/10.46574/motivection.v7i1.424

[26] Santoso, D., Santosa, S., & Sekaranom, A. (2025). Low-cost sensor based on Internet of Things for $PM_{2.5}$ air quality monitoring. *Indonesian Journal of Geography, 57*(2), 408–422. https://doi.org/10.22146/ijg.104159

[27] Saini, J., Dutta, M., & Marques, G. (2020). Indoor air quality monitoring systems based on Internet of Things: A systematic review. *International Journal of Environmental Research and Public Health, 17,* 4942. https://doi.org/10.3390/ijerph17144942

[28] Shukla, A. K., Koul, K., & Babu, B. (2022). Study of modern air purification and sterilization techniques. *Environmental and Earth Sciences Research Journal, 9*(3), 79–89. https://doi.org/10.18280/eesrj.090301

[29] Ukagwu, K. J., Enzoionzi, A. I., Eze, V. H. U., Uche, C. K. A., & Ukagwu, F. (2024). Innovative design and implementation of portable and rechargeable air purifier and humidifier. *International Journal of Recent Technology and Applied Science, 6*(1), 14–24. https://doi.org/10.36079/lamintang.ijortas-0601.618

[30] Vijayan, V. K., Paramesh, H., Salvi, S. S., & Dalal, A. A. (2015). Enhancing indoor air quality: The air filter advantage. *Lung India, 32*(5), 473–479. https://doi.org/10.4103/0970-2113.164174

[31] World Bank & Institute for Health Metrics and Evaluation. (2016). *The cost of air pollution: Strengthening the economic case for action.* World Bank. https://doi.org/10.1596/978-1-4648-0850-5

[32] Yusop, N., Moketar, N. A., & Sadikan, S. F. N. (2024). Development of Arduino applications for IoT applications in software engineering education: A systematic literature review. *Bulletin of Electrical Engineering and Informatics, 13*(3). https://doi.org/10.11591/eei.v13i3.4506

[33] Zahedi, A., Jaafarzadeh, N., Mirr, I., & Tahmasebi, Y. (2024). Forecasting air quality index (AQI) and air quality health index (AQHI) by time series models in Ahvaz, Iran. *Environmental Health Engineering and Management Journal, 11*(4), 469–476. https://doi.org/10.34172/EHEM.2024.46

[34] Zain, N. M., Othman, M., Mohd Rozi, M. A. R., & Paidi, Z. (2024). The development of an IoT-based air quality monitoring system using the Blynk application. *Journal of Computing Research and Innovation, 9*(1), 157–166. https://doi.org/10.24191/jcrinn.v9i1.426

[35] Zhai, Z., Li, H., Bahl, R., & Trace, K. (2021). Application of portable air purifiers for mitigating COVID-19 in large public spaces. *Buildings, 11*(8), 329. https://doi.org/10.3390/buildings11080329

APPENDICES

Figure A: The AQI, PM2.5 and PM10 Value at 5:32pm to 5:34pm.

Figure B: The AQI, PM2.5 and PM10 Value at 5:34pm to 5:47pm.

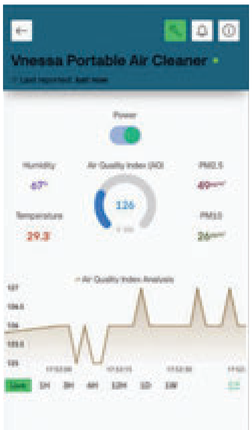

Figure C:
The AQI, PM2.5 and PM10 Value at 5:47pm to 5:52pm.

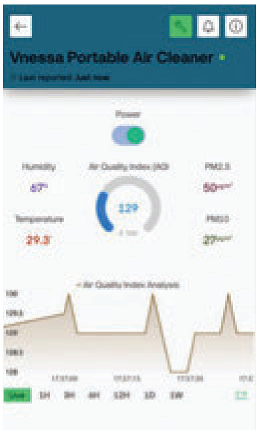

Figure D:
The AQI, PM2.5 and PM10 Value at 5:52pm to 5:57pm.

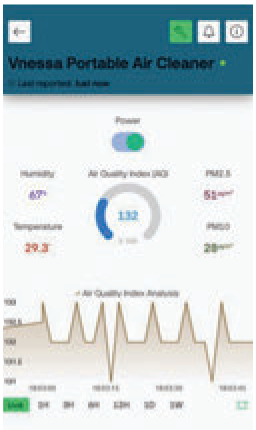

Figure E:
The AQI, PM2.5 and PM10 Value at 5:57pm to 6:03pm.

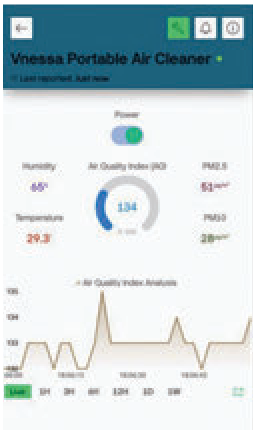

Figure F:
The AQI, PM2.5 and PM10 value at 6:03pm to 6:06pm.

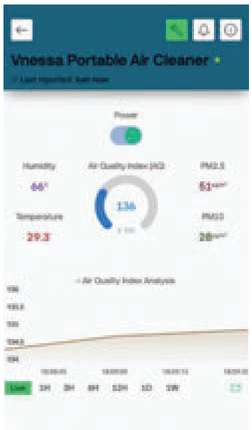

Figure G:
The AQI, PM2.5 and PM10 value at 6:06pm to 6:12pm.

Figure H:
The AQI, PM2.5 and PM10 value at 6:12pm to 6:16pm.

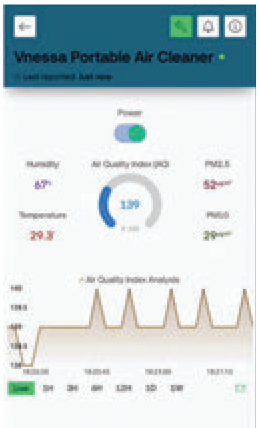

Figure I:
The AQI, PM2.5 and PM10 value at 6:16pm to 6:25pm.

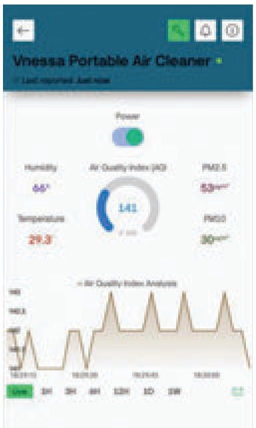

Figure J:
The AQI, PM2.5 and PM10 value at 6:25pm to 6:30pm.

Figure K:
The AQI, PM2.5 and PM10 value at 6:30pm to 6:33pm.

Figure L:
The AQI, PM2.5 and PM10 value at 6:33pm to 6:35pm.

PROFILES

VANESSA ANASTACIA BONG is a final-year Diploma in Mechanical Engineering student at Universiti Tenaga Nasional (UNITEN), Malaysia, currently undergoing industrial training at Sarawak Energy Berhad. Her interests lie in mechanical innovation and the design of practical, efficient engineering solutions that address everyday challenges.
Email Address: vnessabong36@gmail.com

LAY SHENG EWE was born in Penang, Malaysia. She received her Ph.D. in Pure Physics from the National University of Malaysia (UKM). She is currently an Associate Professor at Universiti Tenaga Nasional (UNITEN), Putrajaya Campus, Malaysia. Her research interests include material science, superconductivity, and magnetoresistance (MR). In 2020, she was awarded the Professional Technologist certification by the Malaysia Board of Technologists (MBOT). She also serves as an active committee member of the Malaysia Association of STEM Olympiads (MASO).
Email address: laysheng@uniten.edu.my

EMADADDIN ABDO ALAZZANI is a Master's candidate in Mechanical Engineering at Universiti Tenaga Nasional (UNITEN), Malaysia. He holds a Bachelor's degree in Mechanical Engineering from Universiti Malaysia Pahang (UMP). With over four years of research experience, he has contributed to postgraduate research projects and peer-reviewed publications in renewable energy and sustainable engineering. His technical expertise spans experimental design, statistical analysis (SPSS, R, Python), MATLAB, and data-driven engineering optimisation. His research interests include renewable energy systems, mechanical performance enhancement, and sustainable engineering technologies.
Email address: Emadalezany14@email.com

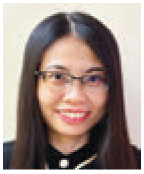

SARA KIT YEE LEE holds a Bachelor's degree in Mechanical gineering from Universiti Tenaga Nasional (UNITEN), and both her Master's and Ph.D. degrees from Universiti Malaya (UM). She is a registered Professional Engineer and ASEAN Chartered Professional Engineer (ACPE) with the Board of Engineers Malaysia (BEM), a Professional Technologist with the Malaysian Board of Technologists (MBOT), and a Chartered Engineer with the Engineering Council. She is a member of the Institution of Engineers, Malaysia (IEM) and the Institution of Mechanical Engineers (IMechE).
Email address: leeky@tarc.edu.my

CHEE FUI WONG is an Assistant Professor at the Centre of Climate Change and Disaster Risk Reduction, Department of Civil Engineering, Lee Kong Chian Faculty of Engineering and Science, Universiti Tunku Abdul Rahman (UTAR), Malaysia. He holds a Ph.D. in Engineering from UTAR, an M.Sc. in Highway and Transport Engineering, and a B.Eng. in Civil Engineering from Universiti Putra Malaysia (UPM). A registered Professional Engineer (P.Eng) and Professional Technologist (P.Tech), he is also a Fellow of the Institution of Engineers, Malaysia (FIEM), F.TAM, F.AAET, and F.AETDEW. His expertise spans highway infrastructure design, water supply and resources management, dam construction, sewerage systems, and waste management, supported by extensive experience in both local and international construction projects.
Email address: cfwong@utar.edu.my

DIGITAL TRANSFORMATION AND SUSTAINABILITY READINESS IN BRUNEI'S CONSTRUCTION INDUSTRY: AN ASSESSMENT USING THE TOE FRAMEWORK

Lee Tuck Chin[1*], Sai Keong Chan[2]

Abstract

This study examines the digital transformation and sustainability readiness of Brunei's construction industry through the lens of the Technology-Organisation-Environment (TOE) framework. As digital transformation emerges as a vital driver of productivity and sustainability within the global construction sector, the research underscores that effective adoption extends beyond mere technology integration to encompass value creation and organisational alignment. Utilising a quantitative research design, the study investigates the technological, organisational, and environmental dimensions that affect the digital readiness of construction firms in Brunei. Key findings highlight the interplay of managerial capabilities, strategic focus, and regulatory influences, revealing critical barriers and facilitators to digital adoption. The results aim to provide actionable insights for stakeholders in Brunei’s construction industry, contributing to the broader discourse on integrating digital technologies and fostering sustainable development in the context of Industry 4.0. This assessment serves as a foundation for future research and policy formulation, emphasising the importance of a holistic approach to digital transformation in enhancing operational efficiency and sustainability in construction practices.

Received: *3 February, 2026*
Revised: *28 February, 2026*
Accepted: *10 March, 2026*

[1,2]Kuala Lumpur University of Science and Technology (KLUST), Malaysia.

****Corresponding author:***
engineerltchin@gmail.com

DOI: *https://doi.org/10.54552/v87i2.346*

Keywords:
Digital transformation, Sustainability, Construction industry, Technology-Organisation-Environment (TOE) framework, Industry 4.0

1.0 INTRODUCTION

Digital transformation has become a critical driver of productivity, sustainability, and competitiveness within the global construction industry. Recent studies emphasis that successful digital transformation in construction is not merely about technology adoption, but about value creation, systems integration, and organisational alignment (Hatoum & Nassereddine, 2024). For example, Zhong *et al.* identify value-oriented strategies and integrated digital systems as key success factors in construction digitalisation.

Similarly, Asif *et al.* (2024) highlight how digitalisation in the built environment reshapes sustainability outcomes while improving operational efficiency and lifecycle performance. From a regional perspective, Le *et al.* provide evidence that Industry 4.0 adoption across Southeast Asia is strongly influenced by managerial capability, strategic focus, and institutional readiness. Their comparative analysis demonstrates that digital technologies are fundamentally reshaping value chains, redefining work coordination, and transforming traditional construction practices, indicating that digital transformation is not an incremental improvement but a structural shift in how construction value is conceived, delivered, and sustained (Gheda *et al.,* 2025; Perera *et al.,* 2023).

In the context of Industry 4.0, technologies such as Building Information Modelling, the Internet of Things, artificial intelligence, and digital twins are increasingly revolutionising construction practices (Gheda *et al.,* 2025; Olanipekun & Sutrisna, 2021). These technologies enable enhanced project coordination, data-driven decision-making, and improved performance across the entire building lifecycle, giving rise to the concept of “smart construction” characterised by interconnected digital systems and real-time data exchange (Gheda *et al.,* 2025; Rinchen *et al.,* 2024).

Within the ASEAN region, digital transformation widely recognised as a key enabler of sustainable development, with governments across Southeast Asia embedding digital mandates into national infrastructure and urban development policies to accelerate progress. Singapore, for instance, has made BIM compulsory for public-sector construction projects, with enforcement led by the Building and Construction Authority and supported by comprehensive regulatory frameworks and industry training programmes (Sabri & Kurnia, 2025).

2.0 LITERATURE REVIEW

The literature on digital transformation distinguishes between digitisation, digitalisation, and full digital transformation, where the latter represents a structural shift in business models and decision-making cultures rather than merely the adoption of isolated tools (Owais *et al.,* 2025; Zulu *et al.,* 2023).

This perspective aligns with the concept of Construction 4.0, which integrates advanced technologies such as Building Information Modelling, robotics, automation, the Internet of Things, artificial intelligence, and digital twin technologies to enhance productivity, efficiency, and sustainability in construction workflows (Jelodar, 2025).

Despite the potential of these tools to redefine traditional project management practices, the actual integration of digital technologies into day-to-day project workflows remains inconsistent across contexts (Qadir *et al.,* 2025). Scholarly investigations suggest that this inconsistency is often attributed to a complex interplay of organisational, technological, and environmental barriers that impede the seamless adoption of innovations such as building information modelling, augmented and virtual reality, laser scanning, robotics, and 3D printing throughout the built asset lifecycle (Olanipekun & Sutrisna, 2021). Consequently, understanding the specific dynamics of these barriers requires a robust theoretical framework that can systematically evaluate the technological, organisational, and environmental dimensions influencing adoption outcomes (Olanipekun & Sutrisna, 2021; Qadir *et al.,* 2025).

The Technology–Organisation–Environment framework, or TOE originally developed by Tornatzky and Fleischer, provides a comprehensive structure for analysing the technological, organisational, and environmental contexts that shape the innovation adoption process within enterprises. This model is particularly relevant for the construction sector, as it allows researchers to assess how technological readiness, organisational capability, and environmental regulation collectively influence efficiency, safety, and sustainability outcomes (Qadir *et al.,* 2025). Specifically, the technological dimension examines the characteristics and compatibility of digital tools, the organisational dimension assesses internal resources, management support, and workforce readiness, whilst the environmental dimension considers regulatory pressures, industry standards, and external stakeholder expectations (Gong *et al.,* 2024; Qadir *et al.,* 2025).

By adopting this multidimensional perspective, the study extends the application of the TOE framework to evaluate the specific drivers and barriers influencing digital adoption within Brunei's construction sector, drawing on established decision-making factors identified in contemporary construction research (Hatoum & Nassereddine, 2024; Qadir *et al.,* 2025).

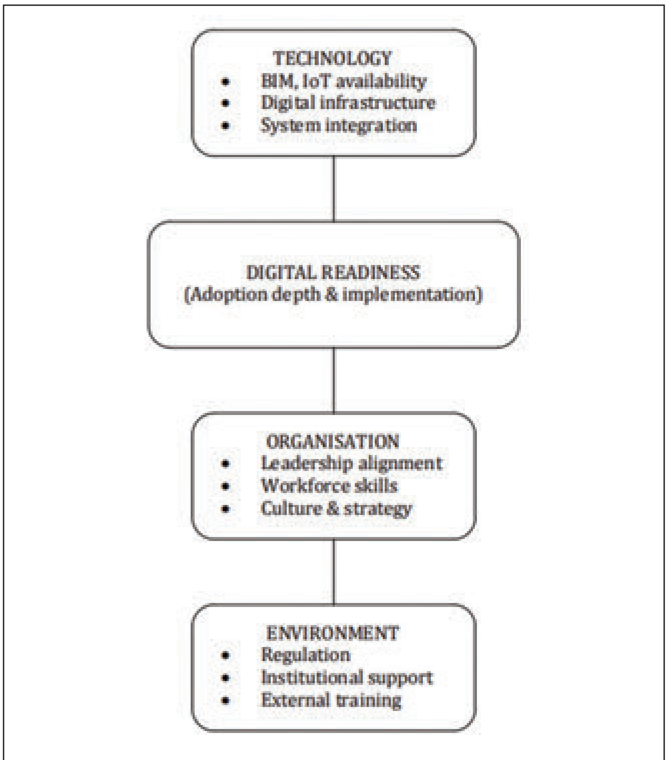

Figure 1: TOE framework to assess digital transformation readiness in Brunei's construction industry

3.0 METHODOLOGY

This study adopts a conceptual and policy-focused research methodology to assess Brunei's readiness for digital transformation in the construction sector. Instead of collecting primary empirical data, the research synthesises existing academic literature, government policy documents, and regional case studies to develop a structured readiness assessment. This approach is appropriate given the exploratory and strategic nature of the study, which focuses on institutional alignment, policy context, and sectoral transformation rather than operational-level data.

Tornatzky and Fleischer's Technology–Organisation–Environment framework serves as the core theoretical foundation. It enables a systematic assessment of digital readiness by examining technological capabilities, organisational preparedness, and the external policy and regulatory environment. This framework is particularly suited to construction-sector evaluations in emerging and small-scale economies such as Brunei. Figure 1 presents the TOE framework adopted in this study to assess digital transformation readiness in Brunei's construction industry. The framework illustrates how technological capabilities, organisational readiness, and environmental conditions jointly influence firms' digital adoption and implementation outcomes.

Table 1: Operationalisation of the TOE framework and evidence sources

TOE Dimension	Indicators Assessed	Evidence Sources Used
Technology	Availability of digital infrastructure (e.g., BIM platforms, IoT readiness); system integration capability; maturity of digital tools across the project lifecycle	Academic literature on Construction 4.0; national policy documents; ASEAN digital construction benchmarks
Organisation	Leadership commitment to digitalisation; existence of digital strategy; workforce digital skills; organisational learning culture; SME capability constraints	Peer-reviewed studies; industry reports; comparative evidence from ASEAN construction sectors
Environment	Regulatory alignment; enforcement mechanisms; institutional coordination; availability of external support (training, advisory services, incentives)	Government policy documents; regional best-practice cases (e.g., Singapore, Malaysia, Vietnam); international construction studies

Table 1 outlines the indicators used to assess digital transformation readiness under the TOE framework and the corresponding evidence sources employed in this study.

Its methodological relevance aligns with previous TOE-based studies that use regional comparisons to contextualise national performance and identify transferable best practices (Amade, 2022; Hatoum & Nassereddine, 2024; Addy *et al.,* 2023; Qadir *et al.,* 2025). Such comparative analysis highlights structural gaps and strategic enablers that may not be visible when examining Brunei in isolation, offering a more nuanced understanding of digital adoption dynamics in similar institutional settings (Maaz *et al.,* 2025; Tjandra *et al.,* 2022).

This approach recognises that digital transformation readiness is shaped by a complex interplay of technological, organisational, and environmental factors, which the TOE framework systematically categorises (Alkhamery *et al.,* 2021; Hatoum & Nassereddine, 2024). Table 1 summarises the key empirical findings across the technological, organisational, and environmental dimensions of the TOE framework, highlighting dominant patterns, constraints, and moderating factors influencing digital readiness among construction firms.

4.0 RESEARCH DESIGN

A secondary-data research design underpins this study. There are no primary data collection such as surveys, interviews, or field observations was conducted. Instead, the analysis draws on a structured review of peer-reviewed publications, national development plans, policy reports, ASEAN documents, and official government portals. This approach ensures a comprehensive evidence base that is both credible and aligned with the study's conceptual objectives.

Key national references include Wawasan Brunei 2035 and the Twelfth National Development Plan, which articulate the country's long-term development priorities and digital ambitions (Jelodar, 2025). These were evaluated alongside scholarly and industry literature (Hatoum & Nassereddine, 2024; Olanipekun & Sutrisna, 2021; Qadir *et al.,* 2025) to determine the extent to which national digitalisation objectives are reflected in construction-sector practices.

Benchmarking against regional counterparts particularly Singapore, Malaysia, and Vietnam provides comparative insights into more advanced digital construction ecosystems. This mirrors methods in previous TOE-informed studies that emphasise systematic qualitative analysis (Addy *et al.,* 2023; Hatoum & Nassereddine, 2024). The research process followed three sequential phases:

1. literature and policy review,
2. regional benchmarking, and
3. synthesis and development of a tailored digital transformation roadmap.

4.1 Selection of Literature and Policy Sources

Sources were obtained from Google Scholar, Scopus-indexed journals, regional repositories, and government portals. Inclusion criteria required publications focused on digital transformation in construction, smart technologies, sustainable infrastructure, or ASEAN development initiatives. Documents were limited to the period 2015–2025.Core policy materials included Wawasan Brunei 2035 and the Twelfth National Development Plan (Jelodar, 2025). Regional benchmarking used Vietnam's BIM implementation roadmap, construction guidelines from the Philippine Department of Public Works and Highways, and digital construction strategies from Singapore and Malaysia. Scholarly works by Olanipekun & Sutrisna (2021), Hatoum & Nassereddine (2024), and Qadir *et al.* (2025) substantiated the theoretical grounding of the TOE framework.

4.2 Regional Benchmarking Framework

Benchmarking was performed across six ASEAN countries—Singapore, Malaysia, Vietnam, Thailand, Indonesia, and the Philippines—selected for their documented digital construction initiatives and institutional relevance to Brunei (Tjandra *et al.,* 2022). Selection criteria included:

1. publicly available national digital construction policies,
2. differing institutional maturity levels, and
3. alignment with ASEAN digital priorities, such as the ASEAN Smart Cities Network.

This comparative framework positions Brunei's digital readiness against regional peers, identifies transferable best practices, and highlights strategic gaps requiring policy and organisational attention.

4.3 Operationalisation of the TOE Framework

The TOE framework was operationalised across its three foundational dimensions (Gong *et al.,* 2024; Hatoum & Nassereddine, 2024):

Technology: Evaluation of digital infrastructure preparedness, availability of platforms such as BIM and IoT, and system integration extents within construction.

Organisation: Assessment of workforce digital proficiencies, leadership commitment, SME engagement, and training/professional development provisions.

Environment: Scrutiny of regulatory architectures, institutional coordination, policy mechanisms, and industry participation structures for digital transformation.

Indicators per dimension were adapted from ASEAN benchmarks and attuned to Brunei's contextual specificities. This operationalisation coheres with Vision 2035's aspiration for a technology-enabled society and RKN12's prioritisation of innovation-led, sustainable infrastructure. Predominantly qualitative, this methodology furnishes a robust scaffold for prospective empirical inquiries. Its outputs are designed to apprise policymakers, institutions like PUJA, and construction stakeholders with a cogent roadmap integrating academic rigour and regional exemplars (Hatoum & Nassereddine, 2024; Olanipekun & Sutrisna, 2021). The subsequent section presents the findings derived from this systematic analysis, structured according to the technological, organisational, and environmental dimensions of the TOE framework to elucidate the current state of digital readiness in Brunei's construction sector.

From the technological perspective, the study indicates that although foundational digital infrastructure is established, the adoption of advanced tools such as Building Information Modelling and Internet of Things solutions remains nascent and uneven (Qadir *et al.,* 2025; Sajat *et al.,* 2025). Basic software is commonly used for administrative purposes, but more complex, interoperable systems—capable of supporting data-driven decision-making and lifecycle performance management—are not yet widely integrated. This disparity stems from the technological context wherein perceived disruption, implementation risks, and uncertainty regarding benefits inhibit widespread adoption (Tjandra *et al.,* 2022).

Organisational constraints further exacerbate these limitations. Many firms lack top management support, a digitally competent workforce, and the information-sharing cultures needed to sustain complex transformation initiatives (Maaz *et al.,* 2025). The absence of comprehensive training programmes and strategic leadership commitment creates a capability gap that prevents firms from leveraging digital technologies for productivity and sustainability gains (Gheda *et al.,* 2025). Autocratic and hierarchical organisational cultures contribute to slow adoption, stifling the collaborative innovation necessary for digital integration (Abdulqader *et al.,* 2025). Resistance is especially pronounced among long-tenured employees whose experiential expertise conflicts with new digital systems, following traditional change-cycle patterns where manual proficiency reinforces opposition (Bidhendi *et al.,* 2025). Such resistance arises not from technological naivety but from deeply ingrained institutional norms (Oti-Sarpong *et al.,* 2021).

The environmental dimension further reveals that regulatory frameworks and institutional mechanisms remain critical yet underdeveloped. Although policies encourage digitalisation, current regulations lack enforcement strength and strategic alignment, resulting in fragmented, voluntary adoption that fails to produce systemic transformation (Onososen & Innocent, 2025; Gheda *et al.,* 2025; Hatoum & Nassereddine, 2024). Traditional business models and conservative organisational mindsets reinforce a short-term approach in which firms prioritise immediate project delivery over long-term capability building (Gardner, 2022).

Addressing these entrenched barriers requires interventions that align technological capability with organisational culture and institutional mandates (Naji *et al.,* 2024; Oti-Sarpong *et al.,* 2021). This includes establishing supportive learning environments, valuing the institutional knowledge of older employees, and adopting process-centric approaches that reduce perceptions of displacement (Olanipekun & Sutrisna, 2021; Xames & Topcu, 2025). Effective change management—built on informing, guiding, and involving employees is necessary to mitigate fears of job loss, competence concerns, and perceived loss of control (Valtonen & Holopainen, 2025; Cieslak & Valor, 2024; Noroozi, 2024).

Tailored interventions must also consider demographic differences, as older individuals may struggle to keep pace with rapid technological advancement (Nkomo & Kalisz, 2024). Successful transformation ultimately depends on leadership that supports data-driven decision-making, collaborative problem-solving, and adaptive management (Seppänen *et al.,* 2025). Resistance often stems from directors reluctant to change established practices, even when employees are ready to innovate (Zulu *et al.,* 2023). Establishing urgency and forming strong guiding coalitions are therefore critical for overcoming managerial inertia and driving sector-wide transformation (Nesindande *et al.,* 2024).

5.0 RESULTS

The findings derived from the structured synthesis and regional benchmarking analysis reveal distinct patterns across the technological, organisational, and environmental dimensions of the TOE framework. Overall, organisational factors demonstrate comparatively stronger associations with digital readiness outcomes than technological or environmental conditions. Table 2 synthesises the empirical findings reported in the Results section, highlighting dominant patterns, constraints, and moderating factors influencing digital readiness across Brunei's construction firms.

Table 2: Summary of results by TOE dimension

TOE Dimension	Key Findings	Evidence from Results
Technology	High awareness but uneven implementation of digital tools	BIM and digital systems adoption concentrated among large firms; SMEs face cost barriers
	Financial constraints limit adoption	Software, hardware, and integration costs cited as major barriers
	Digital literacy affects effective usage	Firms with lower workforce digital skills show weaker implementation
Organisation	Strong association between leadership alignment and adoption	Firms with clear digital strategies demonstrate higher uptake
	Firm size moderates readiness	SMEs lack financial, managerial, and time resources
	Workforce skills moderate adoption outcomes	Digital skills strengthen link between technology access and implementation
	Organisational culture influences diffusion	Learning-oriented cultures show higher acceptance of digital tools
Environment	Regulatory pressure alone insufficient	Policy mandates weakly associated with implementation levels
	External support positively influences adoption	Firms with access to training/advisory services report higher uptake
	Environmental effects strongest for SMEs	SMEs depend more on external institutional support

Table 3: Summary of results by TOE dimension

Dimension	Current level	Gap Severity
Technology	Moderate	Medium
Organisation	Low-Moderate	High
Enviroment	Moderate	Medium

To further illustrate the relative strengths and constraints identified across the TOE dimensions, Table 3 presents a consolidated digital readiness profile of Brunei's construction sector. The visual representation highlights the comparative positioning of technological capability, organisational preparedness, and environmental support mechanisms, thereby clarifying areas where capability gaps are most pronounced.

5.1 Technologica Dimension

Within the technological dimension, the results show that while awareness of digital tools such as Building Information Modelling (BIM) and digital permitting system is relatively high, actual implementation remains uneven and is predominantly observed among larger firms. Small and medium-sized enterprises (SMEs) report significantly lower adoption levels, citing financial constraints related to the cost of software, hardware, and system integration as major barriers. These findings are consistent with prior studies that identify cost-related barriers as a key determinant of limited digital uptake among smaller firms (Santos, 2023).

The analysis further indicates that access to digital tools does not necessarily translate into effective usage. Firms reporting lower levels of workforce digital literacy also demonstrate lower levels of implementation, suggesting that technological readiness is associated not only with access to digital infrastructure but also with employees' ability to utilise these tools effectively (Syah *et al.,* 2025; Saka *et al.,* 2021). This pattern is particularly evident among SMEs, where limited technical capability constrains the operationalisation of available technologies.

5.2 Organisational Dimension

The organisational dimension exhibits the strongest association with digital readiness outcomes. The results indicate that leadership competency and strategic alignment are positively associated with higher levels of digital adoption. Firms with clearly articulated digital strategies and leadership commitment to digital initiatives demonstrate significantly greater uptake of digital technologies than firms without such alignment (Johari *et al.,* 2024).

Firm size further moderates organisational readiness, with smaller firms reporting limited access to financial resources, time, and dedicated managerial capacity to support digital initiatives. These constraints are associated with lower adoption levels and reduced implementation scope (Zulu *et al.,* 2023). The findings also show that organisations reporting higher levels of workforce digital skills exhibit stronger relationships between technology availability and actual implementation, indicating that employee capability moderates organisational digital readiness outcomes (Bilal *et al.,* 2024).

In addition, the results suggest that organisational culture is associated with digital adoption levels. Firms characterised by internal support for learning and experimentation report higher levels of acceptance and use of digital tools, whereas firms lacking such support demonstrate slower diffusion of digital practices (Shojaei & Burgess, 2022; Zulu *et al.,* 2023). Organisations without a coherent digital strategy also report difficulties aligning technology investments with business objectives, which is associated with fragmented and limited adoption (Johari *et al.,* 2024).

5.3 Environmental Dimension

Within the environmental dimension, regulatory pressure and institutional support exhibit a weaker direct association with digital adoption than anticipated. The results indicate that policy mandates alone are not significantly associated with higher implementation levels, particularly where enforcement mechanisms and targeted support are limited (Gheda *et al.,* 2025).

However, the study shows that firms with access to external support mechanisms such as industry training programmes and technical advisory services report higher levels of digital implementation than firms without such access. Where external requirements and incentives are unclear or absent, environmental factors are negatively associated with the extent of digital technology use (Masry & Chronéer, 2025). This pattern is most pronounced among SMEs, which rely more heavily on external support to compensate for internal resource limitations.

Overall, the finding indicate that digital readiness in Brunei's construction sector is associated with organisational preparedness, with technological infrastructure and environmental support exercising conditional influence. While awareness of digital tools is widespread, effective implementation is uneven and strongly associated with organisational readiness factors particularly leadership alignment, workforce capability, and firm size. Environmental factors exhibit a conditional influence, with external support mechanisms playing a more significant role than regulatory pressure alone in shaping adoption outcomes.

6.0 DISCUSSION

The findings reinforce the view that digital transformation is fundamentally an organisational change process shaped as much by human and strategic factors as by technological capability. Consistent with prior research, technology alone does not determine transformation success; organisational culture, leadership alignment, and workforce competence play equally critical roles in building digital advantage (Cyfert *et al.,* 2025; Lu, 2024; Mladenova *et al.,* 2025). A supportive and innovation-oriented business culture enables firms to move beyond superficial tool adoption towards meaningful integration of digital practices (Fahmi *et al.,* 2023; Zulu *et al.,* 2023). This cultural alignment is particularly important for SMEs, where resource constraints necessitate strategic clarity and internal cohesion (Tonder *et al.,* 2023).

From a Resource-Based View perspective, internal capabilities especially human capital constitute a central source of competitive advantage in digital transformation (Silva *et al.,* 2025). The digital self-efficacy of leaders and the digital literacy of employees significantly influence transformation outcomes (Costa *et al.,* 2023; Inga-Ávila *et al.,* 2023). Managerial attitude, competence, and the ability to reconfigure resources are decisive in translating digital opportunities into operational performance (Minh *et al.,* 2024; Hu *et al.,* 2024; Mou *et al.,* 2022). Firms that embed digitalisation within organisational strategy and align it with clearly defined roles and objectives are more likely to achieve sustainable outcomes than those treating digital tools as optional add-ons (Mladenova *et al.,* 2025; Colapinto *et al.,* 2021).

Human capital development emerges as a critical enabling mechanism. Employee digital knowledge and platform proficiency directly affect transformation capability and indirectly shape performance outcomes (Thi & Thu, 2025). However, SMEs often encounter skill gaps, resistance to change, and legacy-system dependence, which constrain progress (Seppänen *et al.,* 2025). Addressing these barriers requires targeted skill enhancement, leadership development, and structured change management processes (Bozkuş, 2023; Agustian *et al.,* 2023; Krajčík *et al.,* 2023). Evidence further suggests that employee skills positively moderate the relationship between organisational capabilities and digital transformation outcomes (Hu *et al.,* 2024).

At the ecosystem level, coordinated institutional support is essential. Partnerships with educational institutions and industry associations, along with structured training initiatives, can reduce capability gaps and strengthen relational capital within the sector (Awonuga *et al.,* 2024; Bhuiyan *et al.,* 2024). Policymakers play a pivotal role by promoting lifelong learning frameworks, incentivising workforce reskilling, and supporting affordable digital infrastructure (Azigi & Baffour, 2024; OECD, 2023; Oikawa *et al.,* 2024). Educational reform and targeted literacy initiatives are particularly important for enhancing SME competitiveness and bridging digital divides (Raji *et al.,* 2024; Přívara *et al.,* 2025; Syah *et al.,* 2025). Regulatory clarity, cybersecurity assurance, and data protection mechanisms further enhance trust and participation in digital systems (Ewim *et al.,* 2024; Tóth *et al.,* 2025).

Regional benchmarking was conducted across six ASEAN construction ecosystems—Singapore, Malaysia, Vietnam, Thailand, Indonesia, and the Philippines—to contextualise Brunei's digital transformation readiness within comparable institutional environments. The comparison focused on key structural dimensions aligned with the TOE framework, including the presence and enforcement of BIM mandates, SME enablement mechanisms, digital skills ecosystems, and overall sectoral maturity.

Singapore represents the most advanced benchmark, characterised by mandatory BIM implementation, strong regulatory enforcement, and institutionalised training infrastructure. Malaysia and Thailand demonstrate structured yet evolving approaches, with sectoral mandates and expanding digital skills initiatives. Vietnam and Indonesia exhibit roadmap-based or policy-driven frameworks with moderate enforcement and developing institutional support. The Philippines reflects an emerging digital construction ecosystem with framework-level policies and comparatively limited SME support structures.

On the other hand, Brunei's positioning reflects policy encouragement rather than enforcement-backed mandates, with developing training ecosystems and emerging SME support mechanisms. The comparative assessment highlights that the primary gap lies not in policy intent but in the institutional depth, enforcement consistency, and capability-building infrastructure required to translate strategic objectives into widespread sectoral adoption.

To contextualise the findings within the broader regional landscape, Table 3 compares Brunei's digital readiness positioning with selected ASEAN construction ecosystems. This benchmarking exercise highlights differences in policy enforcement, SME support structures, and institutional maturity, providing a reference point for identifying transferable practices and strategic gaps.

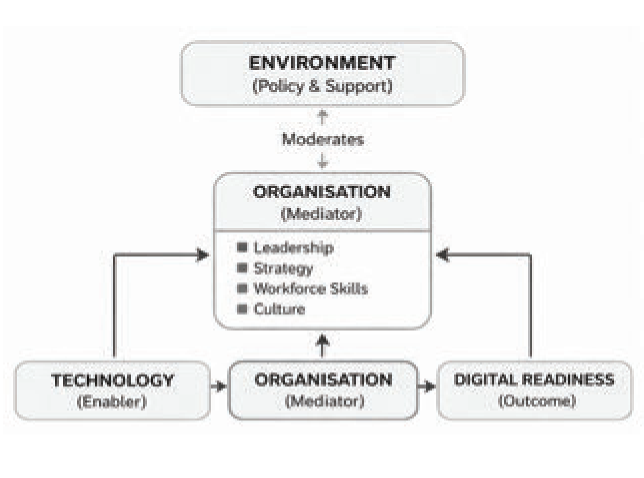

Figure 2: Interaction of TOE dimensions influencing digital transformation outcomes

Building on the empirical patterns and regional comparison, Figure 2 conceptualises the interaction among technological capability, organisational readiness, and environmental conditions, illustrating the mediating role of organisational preparedness in translating digital infrastructure into effective transformation outcomes. The model illustrates the mediating role of organisational readiness in translating digital infrastructure and policy conditions into effective transformation outcomes.

Overall, the findings suggest that sustainable digital transformation in Brunei's construction sector depends not merely on technological availability, but on the strategic integration of leadership vision, organisational culture, workforce capability, and supportive institutional conditions. Aligning human capital development with long-term strategic planning is therefore central to strengthening sector-wide digital readiness and competitiveness (Awonuga *et al.,* 2024; Budiarti & Firmansyah, 2024; Utomo *et al.,* 2023).

7.0 CONCLUSION

The study assessed digital transformation and sustainability readiness in Brunei's construction sector using the Technology-Organisation-Environment framework, integrating secondary-data synthesis with regional benchmarking analysis requires the alignment of technological capacity, organisational readiness, and environmental support under the TOE framework.

Table 3: Comparative digital readiness positioning within selected ASEAN construction ecosystems

Country	BIM Mandate	Enforcement Strength	SME Support	Digital Skills Ecosystem	Overall Maturity
Singapore	Mandatory	Strong	Extensive	Institutionalised	High
Malaysia	Sectoral / Partial	Moderate	Moderate	Expanding	Moderate–High
Vietnam	Roadmap-based	Emerging	Moderate	Developing	Moderate
Thailand	Strategic roadmap	Moderate	Developing	Expanding	Moderate
Indonesia	Policy-driven	Moderate	Emerging	Developing	Moderate
Philippines	Framework-based	Emerging	Limited–Moderate	Developing	Moderate–Low
Brunei	Policy encouragement	Limited	Emerging	Developing	Moderate

While digital infrastructure provides a necessary foundation, successful adoption is driven by organisational capabilities and external enablers, particularly for SMEs facing financial and digital literacy constraints (Ammeran & Latip, 2024; Seppänen *et al.,* 2025). Strengthening skills development, leadership commitment, and industry partnerships is therefore essential to accelerate Construction 4.0 adoption and enhance competitiveness (Romero & Mammadov, 2024; Syah *et al.,* 2025).

The findings underscore the importance of stakeholder collaboration, structured training, and phased implementation to support national digital-economy aspirations (Gheda *et al.,* 2025; Supriadi *et al.,* 2023). However, the cross-sectional design limits causal inference. Future research should adopt longitudinal and mixed-method approaches to track digital maturity, assess policy impacts, and refine interventions such as skills assessments, ESG integration, and SME-oriented incentives (Bidhendi *et al.,* 2025; Ghobakhloo *et al.,* 2024; Silva *et al.,* 2025). Synthesising these findings, the analysis demonstrates that digital transformation readiness in Brunei's construction sector is shaped by the interaction of technological capability, organisational preparedness, and environmental support structures. ■

AUTHORS' CONTRIBUTIONS

Lee Tuck Chin	Conceptualisation, research design, methodology development, secondary-data synthesis and regional benchmarking analysis, framework operationalisation, visualisation, drafting of the original manuscript, and revision of the final version.
Sai Keong Chan	Conceptual guidance, methodological supervision, critical review and intellectual revision of the manuscript, and overall academic oversight of the research.

REFERENCES

[1] Abbasnejad, B., Nepal, M. P., Mirhosseini, S. A., Moud, H. I., & Ahankoob, A. (2021). Modelling the key enablers of organizational building information modelling (BIM) implementation: An interpretive structural modelling (ISM) approach. *Journal of Information Technology in Construction, 26,* 974.

[2] Abdulqader, M., Alias, A. H. B., Alias, A. H., & Zuhri, M. Y. M. (2025). DT, BIM, and IoTs Contributions and Barriers in Construction PM: A PRISMA. *Civil and Environmental Engineering.*

[3] Addy, M. N., Kwofie, T. E., Agbonani, D. M., & Essegbey, A. E. (2023). Using the TOE theoretical framework to study the adoption of BIM-AR in a developing country: the case of Ghana. *Journal of Engineering Design and Technology, 22*(6), 1913.

[4] Ademci, E., & Gündeş, S. (2021). Individual and Organisational Level Drivers and Barriers to Building Information Modelling. *Journal of Construction in Developing Countries, 26*(1), 89.

[5] Agustian, K., Mubarok, E. S., Zen, A., Wiwin, W., & Malik, A. J. (2023). The Impact of Digital Transformation on Business Models and Competitive Advantage. *Technology and Society Perspectives (TACIT), 1*(2), 79.

[6] Al-Husain, R., Jasim, T. A., Mathew, V., Al-Romeedy, B. S., Khairy, H. A., Mahmoud, H. A., Liu, S., El-Meligy, M. A., & Alsetoohy, O. (2025). Optimizing sustainability performance through digital dynamic capabilities, green knowledge management, and green technology innovation. *Scientific Reports, 15*(1), 24217.

[7] Alkhamery, N., Zainol, F. A., & Al-Nashmi, M. M. (2021). The Role of Dynamic Capabilities in Reconfiguring Operational Capabilities for Digital Business Transformation. *The Journal of Management Theory and Practice (JMTP), 2*(1), 1.

[8] Amade, B. (2022). Exploring the influence of information and communication technology (ICT) on construction supply chain management: Empirical evidence from a construction project's perspective. *Journal of Project Management, 8*(1), 67.

[9] Ammeran, M. Y., & Latip, M. S. A. (2024). Influencing Factors Of Digital Transformation In Developing Economies A Case Study Of Malaysia's SME Sector. *International Journal of Business and Society, 25*(2), 696.

[10] Asif, M., Naeem, G., & Khalid, M. (2024). Digitalization for sustainable buildings: Technologies, applications, potential, and challenges. Journal of Cleaner Production, 442, 141814.

[11] Awonuga, K. F., Nwankwo, E. E., Oladapo, J. O., Okoye, C. C., Odunaiya, O. G., & Scholastica, U. C. (2024). Driving sustainable growth in SME manufacturing: The role of digital transformation, project, and capture management. *International Journal of Science and Research Archive, 11*(1), 2012.

[12] Azigi, E., & Baffour, P. T. (2024). Digitalization and Employment among Small and Medium Enterprises in Ghana. DergiPark *(Istanbul University)*.

[13] Barragan, K. E., & Becker, F. S. R. (2024). Keeping pace with the digital transformation — exploring the digital orientation of SMEs. *Small Business Economics*.

[14] Belyamani, I., Mfarrej, M. F. B., Ahmad, S. Z., & Bakar, A. R. A. (2025). Pathways linking green digital transformation to sustainable development through knowledge sharing and dynamic capabilities. *Discover Sustainability, 6*(1).

[15] Bhuiyan, M. R. I., Faraji, M. R., Rashid, M., Bhuyan, M. K., Hossain, R., & Ghose, P. (2024). Digital Transformation in SMEs Emerging Technological Tools and Technologies for Enhancing the SME's Strategies and Outcomes. *Journal of Ecohumanism, 3*(4), 211.

[16] Bidhendi, A., Poshdar, M., Jelodar, M. B., & Hamzeh, F. (2025). Enabling Lean Construction 4.0 through human-centric digital transformation: organisational leadership insights. *Engineering Construction & Architectural Management, 1*.

[17] Bilal, M., Zhao, X., Wu, J., Sohu, J. M., Akhtar, S., & Hassan, M. I. U. (2024). Digital Transformation and SME Innovation: A Comprehensive Analysis of Mediating and Moderating Effects. *Journal of the Knowledge Economy, 16*(1), 1153.

[18] Bozkuş, K. (2023). Organizational Culture Change and Technology: Navigating the Digital Transformation. In *IntechOpen eBooks*. IntechOpen.

[19] Budiarti, I., & Firmansyah, D. (2024). Innovatoion capability: Digital transformation of human resources and digital talent in SMEs. *Journal of Eastern European and Central Asian Research (JEECAR), 11*(3), 621.

[20] Celary, O., & Piwowarczyk, Z. (2025). The role of digital initiatives in advancing esg in polish industrial companies. *Scientific Papers of Silesian University of Technology Organization and Management Series, 2025*(225), 55.

[21] Chen, D., & Wang, S. (2024). Digital transformation, innovation capabilities, and servitization as drivers of ESG performance in manufacturing SMEs. *Scientific Reports, 14*(1).

[22] Chen, H., Popaitoon, S., & Mumi, A. (2025). Investigating corporate entrepreneurship strategy through digital transformation: a dynamic capabilities perspective. *Journal of Innovation and Entrepreneurship, 14*(1).

[23] Chen, X., Chang-Richards, A., Ling, F. Y. Y., Yiu, T. W., Pelosi, A., & Yang, N. (2024). Effects of digital readiness on digital competence of AEC companies: a dual-stage PLS-SEM-ANN analysis. *Building Research & Information, 52*(8), 905.

[24] Cieslak, V., & Valor, C. (2024). Moving beyond conventional resistance and resistors: an integrative review of employee resistance to digital transformation. *Cogent Business & Management, 12*(1).

[25] Colapinto, C., Finotto, V., & Coco, N. (2021). Supporting pervasive digitization in Italian SMEs through an open innovation process. In *Routledge eBooks* (p. 259). Informa.

[26] Costa, A., Presenza, A., & Abbate, T. (2023). Digital transformation in family-owned winery SMEs: an exploratory analysis in the South-Italian context. *European Journal of Innovation Management, 26*(7), 527.

[27] Cyfert, S., Dyduch, W., Szumowski, W., & Prause, G. (2025). Are we ready for digital transformation? The role of organizational culture, leadership and competence in building digital advantage. *Central European Management Journal, 33*(2), 219.

[28] Dahlan, A., Shafia, M. H. M., Tatung, T., & Basrowi, B. (2025). Digital transformation: The role of AI, social dynamics, and political support on the quality of strategic decisions and their implications for the progress of Islamic banking in Malaysia and Indonesia. *International Journal of Data and Network Science, 9*(3), 701.

[29] Daoud, A. O., Oke, A. E., Singh, A. K., Famakin, I. O., Aziz, K. F., & Olayemi, T. M. (2025). Exploring the building information modelling benefits for sustainable construction using PLS-SEM. *Scientific Reports, 15*(1).

[30] Dauda, J. A., Chavan, N. N., Saka, A. B., Ajayi, S., & Oyegoke, A. S. (2024). An appraisal of barriers to digitalisation of construction industry in developing countries: perspective from India. *International Journal of Construction Management, 25*(7), 770.

[31] Dolla, T., Jain, K., & Delhi, V. S. K. (2023). Strategies for digital transformation in construction projects: stakeholders' perceptions and actor dynamics for Industry 4.0. *Journal of Information Technology in Construction, 28,* 151.

[32] Drydakis, N. (2022). Improving Entrepreneurs' Digital Skills and Firms' Digital Competencies through Business Apps Training: A Study of Small Firms. *Sustainability, 14*(8), 4417.

[33] Elete, T. Y., Nwulu, E. O., Erhueh, O. V., Akano, O. A., & Aderamo, A. T. (2024). Digital transformation in the oil and gas industry: A comprehensive review of operational efficiencies and case studies. *International Journal of Applied Research in Social Sciences, 6*(11), 2611. Fair East Publishers.

[34] Ewim, C. P.-M., Okeke, N. I., Alabi, O. A., Igwe, A. N., & Ofodile, O. C. (2024). Customer-Centric digital transformation framework: Enhancing service delivery in SMES for underserved populations. *International Journal of Management & Entrepreneurship Research, 6*(10), 3493.

[35] Fahmi, T. A., Tjakraatmadja, J. H., & Ginting, H. (2023). An empirical study of emerging digital culture and digital attitudes in an established company. *Journal of Industrial Engineering and Management, 16*(2), 342.

[36] Gadzali, S. S., Gazalin, J., Sutrisno, S., Prasetya, Y. B., & Ausat, A. M. A. (2023). Human Resource Management Strategy in Organisational Digital Transformation. *Jurnal Minfo Polgan, 12*(1), 760.

[37] Gardner, N. (2022). Digital Transformation and Organizational Learning: Situated Perspectives on Becoming Digital in Architectural Design Practice. *Frontiers in Built Environment, 8.*

[38] Gheda, M. L. M., Chung, H. M., Aziz, M. F., & Nusran, N. F. M. (2025). Bridging the Digital Divide: Overcoming Challenges in Technology Adoption in Malaysia's Construction Industry. Malaysian *Journal of Social Sciences and Humanities (MJSSH), 10*(1).

[39] Ghobakhloo, M., Mahdiraji, H. A., Iranmanesh, M., & Jafari-Sadeghi, V. (2024). From Industry 4.0 Digital Manufacturing to Industry 5.0 Digital Society: a Roadmap Toward Human-Centric, Sustainable, and Resilient Production. *Information Systems Frontiers.*

[40] Gong, Z., Dacre, N., & Dong, H. (2024). Fostering Digital Transformation through Project Integration Management. *SSRN Electronic Journal.*

[41] Hatoum, M. B., & Nassereddine, H. (2024). Determining Decision-Making Factors for Technology Adoption in the Construction Industry. In *Artificial intelligence.* IntechOpen.

[42] Hu, Y., Pan, Y., Miao, Y., & Chen, P. (2024). Navigating Digital Transformation and Knowledge Structures: Insights for Small and Medium-Sized Enterprises. *Journal of the Knowledge Economy.*

[43] Hui, S. (2024). Leveraging digital tools for enhanced green building cost analysis: A sustainable approach to construction economics. *E3S Web of Conferences, 546,* 2002.

[44] Inga-Ávila, M. F., Churampi-Cangalaya, R. L., Ulloa-Ninahuamán, J., Inga-Ávila, J. L., Uribe-Hinostroza, M., Inga-Aliaga, M. Á., & Huamán-Pérez, F. (2023). Digital transformation and competitiveness in Peruvian small business. *International Journal of Data and Network Science, 7*(4), 1797.

[45] Jelodar, M. B. (2025). Generative AI, Large Language Models, and ChatGPT in Construction Education, Training, and Practice. *Buildings, 15*(6), 933.

[46] Jian, Z., Xu, G., & Li, X. (2025). Intersection of ESG performance and corporate innovation: a perspective of vertical linkages within the industrial chain. *Frontiers in Sustainability, 6*.

[47] Johari, M. S., Mahmud, S. H., Mohamed, S. F., Misnan, M. S., Kamarudin, T., & Dzahir, M. A. M. (2024). A SWOT Analysis of Digitalization in the Construction Firm: Challenges and Barriers to Managers Level in Malaysia. *International Journal of Research and Innovation in Social Science,* 1520.

[48] Kapogiannis, G., Palaios, P., & Sawhney, A. (2024). Digital Construction led Growth Asymmetries in Europe: The need for Collaborative Culture. *Construction Economics and Building, 24.*

[49] Karawya, H. (2024). Impact of Digital Transformation on Organizational Culture within Saudi Enterprises: The Mediating Roles of Leadership Styles. *Research Square (Research Square).*

[50] Khakwani, M. S., Zafar, A., Mahmood, G., & Khan, Q. (2024). Impact of Digital Transformation and Green Manufacturing Practices on Firm Performance with Mediating Role of Green Product Innovation: An Empirical Investigation with PLS-SEM Modeling. *Sustainable Business and Society in Emerging Economies, 6*(1).

[51] Krajčík, V., Novotný, O., Civelek, M., & Zvolánková, S. S. (2023). Digital Literacy and Digital Transformation Activities of Service and Manufacturing SMEs. *Journal of Tourism and Services, 14*(26), 242.

[52] Lemoun, A. A., Dellagi, H., Al-Daoud, K. I., & Abusalma, A. (2024). The nexus between digital supply chain and sustainability: An empirical study in pharmaceutical companies in Jordan. *Uncertain Supply Chain Management, 12*(3), 1461.

[53] Leogrande, A., Drago, C., & Arnone, M. (2024). Analyzing Regional Disparities in E-Commerce Adoption Among Italian SMEs: Integrating Machine Learning Clustering and Predictive Models with Econometric Analysis. *Research Square (Research Square).*

[54] Lerman, L. V., Benitez, G. B., Müller, J. M., Sousa, P. R. de, & Frank, A. G. (2022). Smart green supply chain management: a configurational approach to enhance green performance through digital transformation. *Supply Chain Management An International Journal, 27*(7), 147.

[55] Liu, W., Ahmad, M. N. N., & Mazlan, N. S. (2024). Research on the impact of digital economy on green total factor productivity: theoretical mechanism and multidimensional empirical analysis. *Frontiers in Environmental Science, 12.*

[56] Liu, Y. C., Cao, Y., Fang, J., & Li, J. (2025). How Digital Transformation Enhances Corporate Green Performance. *Journal of Global Information Management, 33*(1), 1.

[57] Liu, Y., & Li, W. (2025). From technological empowerment to green performance: empirical evidence on Digitalization-driven energy conservation and emission reduction in logistics enterprises — a case study of SF holding. *Energy Informatics, 8*(1).

[58] Lu, Y. (2024). Impact of Digital Technologies on Organizational Change Strategies: A Review. *Research Journal in Business and Economics, 2*(1), 1. Geological Society of London.

[59] Maaz, Z. N., Bandi, S., & Mahdzir, M. (2025). Developing a Big Data Analytics Adoption Framework for the Construction Industry: A Grounded Theory Approach. *Journal of Construction in Developing Countries, 30*(1), 247.

[60] Mahmutaj, L. R., & Jusufi, N. (2023). The importance of digital skills in firms' innovation: the case of Western Balkans. *Journal of Technology Management & Innovation, 18*(3), 98.

[61] Mapping ESG risks in the polish logistics: a causal layered analysis and foresight perspective. (2025). *Scientific Papers of Silesian University of Technology Organization and Management Series, 2025*(223).

[62] Masry, A. E., & Chronéer, D. (2025). Obstacles to BIM Adoption in Construction Production: A Study of Swedish Construction Contractors' Experiences. *Buildings, 15*(18), 3288.

[63] Miao, Z., & Zhao, G. (2023). Configurational paths to the green transformation of Chinese manufacturing enterprises: a TOE framework based on the fsQCA and NCA approaches. *Scientific Reports, 13*(1).

[64] Mihu, C., Pitic, A. G., & Bayraktar, D. (2023). Drivers of Digital Transformation and their Impact on Organizational

Management. *Studies in Business and Economics, 18*(1), 149.

[65] Minh, L., Nguyen, N. T., Toan, D. V., Thao, T. D., Huyen, N. T., & Hoài, N. T. (2024). Digital transformation in Vietnam: A case study of Hanoi SMEs. *International Journal of advanced and applied sciences, 11*(4), 207.

[66] Mladenova, I., Vladimirov, Z., & Harizanova, O. (2025). Digital transformation, organisational capabilities, and SME performance - size matters. *Eastern Journal of European Studies, 16*(1), 216.

[67] Mou, A. J., Hossain, Md. S., & Siddiqui, N. A. (2022). Digital transformation in marketing: evaluating the impact of web analytics and SEO on SME growth. *American Journal of Interdisciplinary Studies, 3*(4), 61.

[68] Mushattat, M. A. J. A., Al-Sulaiti, K. I., Halbusi, H. A., Alhitmi, H. K., & Al-Sulaiti, I. (2025). Investigating innovative tourism and hospitality sustainability modeling the moderating roles of mobile information technology and green human resource management. *Discover Sustainability, 6*(1).

[69] Naji, K. K., Gündüz, M., Alhenzab, F. H., Al-Hababi, H., & Al-Qahtani, A. (2024). A Systematic Review of the Digital Transformation of the Building Construction Industry. *IEEE Access, 12*, 31461. Institute of Electrical and Electronics Engineers.

[70] Nesindande, A. R.-M., Saurombe, M. D., & Joseph, R. M. (2024). Exploring changes in banking workplaces because of digital technology implementation. *SA Journal of Human Resource Management, 22.*

[71] Nguyen, N. D., Mac, T.-T., & Hoang, H.-H. (2025). Supply chain collaboration and green supply chain management: A bibliometric review, 2000–2023. *Journal of Transport and Supply Chain Management, 19.*

[72] Nkomo, L. I., & Kalisz, D. (2024). Digital Transformation and Employee Wellbeing: Investigating the Intersection of Technology and Wellness. In *Studies in systems, decision and control* (p. 163). Springer International Publishing.

[73] Noroozi, M. (2024). Navigating Resistance to Technological Change in Organizations: A Holistic Approach. *Proceedings of the ... European Conference on Management, Leadership and Governance, 20*(1), 425.

[74] OECD. (2023). *OECD SME and Entrepreneurship Outlook 2023.*

[75] Oikawa, K., Iwasaki, F., Sawada, Y., & Shinozaki, S. (2024). Unintended Consequences of Business Digitalization among MSMEs during the COVID-19 Pandemic: The Case of Indonesia. *SSRN Electronic Journal.*

[76] Olanipekun, A. O., & Sutrisna, M. (2021). Facilitating Digital Transformation in Construction—A Systematic Review of the Current State of the Art. *Frontiers in Built Environment, 7.*

[77] Onososen, A., & Innocent, M. (2025). Unpacking Impediments to Digital Transitioning in the Built Environment: An Institutional Analysis Approach, 1(1).

[78] Oostveen, A., Eimontaite, I., & Fletcher, S. (2025). Human factors in digital manufacturing technology adoption: a workforce perspective. *The International Journal of Advanced Manufacturing Technology.*

[79] Oti-Sarpong, K., Pärn, E., Burgess, G., & Zaki, M. (2021). Transforming the construction sector: an institutional complexity perspective. *Construction Innovation, 22*(2), 361.

[80] Owais, O. A., Poshdar, M., GhaffarianHoseini, A., Ying, F., Jaafar, K., Sarhan, S., & Sheikhkhoshkar, M. (2025). From Competency Mapping to Digital Twin Integration: Developing a Next-Gen Digital Project Manager Model for Smart Construction. *Journal of Information Technology in Construction, 30*(1), 1431.

[81] Perera, S., Jin, X., Samaratunga, M., & Gunasekara, K. (2023). Drivers and barriers to digitalisation: a cross-analysis of the views of designers and builders in the construction industry. *Journal of Information Technology in Construction, 28*, 87.

[82] Pfister, P., & Lehmann, C. (2023). Measuring the Success of Digital Transformation in German SMEs. *Journal of Small Business Strategy, 33*(1).

[83] Pricopoaia, O., Cristache, N., Lupașc, A., & Iancu, D. (2025). The implications of digital transformation and environmental innovation for sustainability. *Journal of Innovation & Knowledge, 10*(3), 100713.

[84] Přívara, A., Rahman, A., Ognjanović, I., Hasnaoui, A., & Hachard, V. (2025). From Survival to Growth: Digital Strategies for Micro and Small Enterprises. *Strategic Change.*

[85] Qadir, S., Alawag, A. M., Baarimah, A. O., Zia, N., Alajmi, M., Almujibah, H., & Alyami, H. (2025). The role of digital technologies in enhancing construction project management. *Scientific Reports, 16*(1), 1486.

[86] Raji, M. A., Olodo, H. B., Oke, T. T., Addy, W. A., Ofodile, O. C., & Oyewole, A. T. (2024). The digital transformation of SMEs: a comparative review between the USA and Africa. *International Journal of Management & Entrepreneurship Research, 6*(3), 737. Fair East Publishers.

[87] Rinchen, S., Banihashemi, S., & Alkilani, S. (2024). Driving digital transformation in construction: Strategic insights into building information modelling adoption in developing countries. *Project Leadership and Society, 5,* 100138.

[88] Romero, I., & Mammadov, H. (2024). Digital Transformation of Small and Medium-Sized Enterprises as an Innovation Process: A Holistic Study of its Determinants. *Journal of the Knowledge Economy, 16*(2), 8496.

[89] Sabri, S., & Kurnia, S. (2025). Digital Transformation of Urban Planning in Australia: Influencing Factors and Key Challenges. *arXiv (Cornell University).*

[90] Sajat, C. J. A., Baharuddin, H. E. A., & Ghazali, F. A. (2025). Digitalisation Adoption Toward National Construction Policy 2030 in the Malaysian Construction Industry. *Built Environment Journal, 21.*

[91] Saka, A. B., Chan, D. W. M., & Mahamadu, A. (2021). Rethinking the Digital Divide of BIM Adoption in the AEC Industry. *Journal of Management in Engineering, 38*(2).

[92] Sangosanya, T. A., Salleh, S. S. M. M., & Saraih, U. N. (2025). Pathways to digital entrepreneurship adoption among Malaysian SMEs: Analysing the determinants and technology readiness dynamics. *Journal of International Entrepreneurship.*

[93] Santos, E. (2023). Tech-driven transformation: Investigating digitalization dynamics across varying firm sizes. *Journal of Information Economics, 1*(3).

[94] Seppänen, S., Ukko, J., & Saunila, M. (2025). Understanding determinants of digital transformation and digitizing management functions in incumbent SMEs. *Digital Business, 5*(1), 100106.

[95] Setyadi, A., Pawirosumarto, S., Damaris, A., & Syarif, D. (2025). Integrating green HRM and sustainable operations: the moderating role of digital transformation in the Indonesian energy sector. *Discover Sustainability, 6*(1).

[96] Shojaei, R. S., & Burgess, G. (2022). Non-technical inhibitors: Exploring the adoption of digital innovation in the UK construction industry. *Technological Forecasting and Social Change, 185*, 122036.

[97] Silva, A. da, Almeida, I. D. de, Dionísio, A., Rabadão, C., & Capela, C. (2025). How digital technologies enhance competitiveness in manufacturing SMEs. *Journal of Innovation and Entrepreneurship, 14*(1).

[98] Silva, P. iacute cia C. de S. e, Gunarathne, N., & Kumar, S. (2024). Exploring the impact of digital knowledge, integration and performance on sustainable accounting, reporting and assurance. *Meditari Accountancy Research.*

[99] Supriadi, I., Maghfiroh, R. U., & Abadi, R. (2023). Transforming MSMEs through Innovation and Technology: Driving Growth and Sustainability in the Digital Age. In *Advances in economics, business and management research/Advances in Economics, Business and Management Research* (p. 241). Atlantis Press.

[100] Surahman, S., Shee, H., Fitrian, Z., Adi, A. S., & Yudaruddin, R. (2023). The effect of digital transformation and innovation on SMEs' performance in times of COVID-19. *Problems and Perspectives in Management, 21*(4), 84.

[101] Syah, H., Suhud, U., & Rizan, M. (2025). Empowering MSMEs in The Digital Era: A Systematic Literature Review on The Role of Digital Literacy. *Greenation International Journal of Economics and Accounting, 3*(2), 185.

[102] Thi, M. L. N., & Thu, T. D. (2025). How internal factors determine digital transformation: The moderating role of leader's project management competence. *Journal of Project Management, 10*(2), 271.

[103] Tjandra, K. D., Irawan, F. G., Nugraha, P., & Sunindijo, R. Y. (2022). Drone Readiness in the Indonesian Construction Industry. *Construction Economics and Building, 22*(4).

[104] Tonder, C. van, Hasanefendic, S., Bossink, B., Schachtebeck, C., & Nieuwenhuizen, C. (2023). Internal organizational factors driving digital transformation for business model innovation in SMEs. *Journal of Business Models, 11*(2).

[105] Tran, T. A., & Khoa, B. T. (2025). Integrating leadership, identity, and knowledge systems for sustainable performance in the era of digital transformation. *Discover Sustainability, 6*(1).

[106] Trang, T. T., Likhitruangsilp, V., & Yabuki, N. (2025). A Fuzzy Cognitive Map for Identifying the Interrelationship of Critical Success Factors for Digital Transformation Implementation by Construction Contractors. *Engineering Journal, 29*(7), 45.

[107] Utomo, A. A., Maulida, M., & Musa, S. (2023). Organizational Inertia, Digital Capabilities, Digital Transformation, and Firm Competencies. *The South East Asian Journal of Management, 17*(1), 130.

[108] Valtonen, A., & Holopainen, M. (2025). Mitigating employee resistance and achieving well-being in digital transformation. *Information Technology and People, 38*(8), 42.

[109] Vararean-Cochisa, D., & Crisan, E.-L. (2024). The digital transformation of the construction industry: a review. *IIM Ranchi Journal of Management Studies.*

[110] Wang, T., & Shen, Y. (2025). Unlocking the potential of supply chain digitalization for enhancing enterprise green transformation performance: evidence from China. *Humanities and Social Sciences Communications, 12*(1).

[111] Wu, X., Li, L. Zhen., Liu, D., & Li, Q. (2024). Technology empowerment: Digital transformation and enterprise ESG performance—Evidence from China's manufacturing sector. *PLoS ONE, 19*(4).

[112] Xames, M. D., & Topcu, T. G. (2025). Digital Engineering Transformation as a Sociotechnical Challenge: Categorization of Barriers and Their Mapping to DoD's Policy Goals. *arXiv (Cornell University).*

[113] Xia, J., Wu, Z., & Chen, B. (2022). How digital transformation improves corporate environmental management: A review and research agenda. *Frontiers in Environmental Science, 10.* Frontiers Media.

[114] Xie, X., & Qi, Y. (2024). Exploring the relationships between different dimensions of digital transformation and corporate greenization: evidence from listed companies in China. *Frontiers in Environmental Science, 12.*

[115] Zulu, S. L., Saad, A. M., Ajayi, S., Dulaimi, M., & Unuigbe, M. (2023). Digital leadership enactment in the construction industry: barriers undermining effective transformation. *Engineering Construction & Architectural Management, 31*(10), 4062.

[116] Zulu, S. L., Saad, A. M., Ajayi, S., & Unuigbe, M. (2023). Determinants of an effective digital transformation in construction organisations: a qualitative investigation. *Built Environment Project and Asset Management, 13*(6), 896.

[117] Zulu, S. L., Saad, A. M., Ajayi, S., Unuigbe, M., & Dulaimi, M. (2023). A thematic analysis of the organisational influences on digitalisation in construction firms. *Journal of Engineering Design and Technology, 22*(6), 1755.

PROFILES

LEE TUCK CHIN is a Professional Engineer with extensive experience in mechanical and electrical engineering, infrastructure development, and digital transformation in construction. He holds several international fellowships, including Fellow AAET, Fellow AETDEW, Honorary Fellow AFEO, Fellow PUJA Brunei, Fellow IMechE (UK), Fellow IET (UK), and Fellow IMQ. He is an ASEAN Engineer, a Chartered Engineer with the UK Engineering Council, and a practising Professional Engineer registered with BAPEQS, Brunei Darussalam. He serves as President of the Institute of Engineers of PUJA (Brunei) for 2024–2025 and Chairman of the Institution of Mechanical Engineers (Brunei Group) for 2024. He is also an Adjunct Associate Professor at Universiti Teknologi Brunei. His current PhD research focuses on digital transformation in construction, particularly organisational readiness and technology adoption. He has presented and published papers at CAFEO, contributing to regional discussions on digitalisation and engineering innovation, and remains committed to advancing professional practice and supporting Brunei's long-term development goals.
Email address: engineerltchin@gmail.com

SAI KEONG CHAN is a Professor at the Faculty of Business, Information and Human Sciences, Kuala Lumpur University of Science and Technology (KLUST), Malaysia. He holds a Bachelor of Arts in Media Studies from Universiti Malaya, a Master of Business Administration in Marketing from Universiti Putra Malaysia, and a Doctorate in Marketing from Universiti Teknologi Malaysia. He has over 25 years of professional experience, including eight years in the marketing industry and more than 20 years in higher education. His research interests include ecological behaviour and beliefs, technology acceptance, e-commerce, influencer marketing, digital marketing, and consumer behaviour in technology-driven environments. He has presented his research at numerous national and international conferences and has published widely in peer-reviewed journals indexed in reputable international databases. His work contributes to advancing both theoretical and practical understanding of contemporary marketing, digital transformation, and technology-enabled business strategies.
Email address: csk@iukl.edu.my

INFLUENCE OF SONICATION AMPLITUDE ON SURFACE PERFORATION OF CHITOSAN MACROBEADS AND DYE ADSORPTION

Kabilarasan Thanasegaran[1], Swee Pin Yeap[2*], Li Sze Lai[3], Jing Lin Ng[4], Chaomeng Dai[5], Kah Hon Leong[6], Pey Yi Toh[7]

Abstract

Due to industrialisation and globalisation, water sources are increasingly contaminated with dyes. Among the various available methods, adsorption using chitosan macrobeads is a feasible technique for dye removal. However, despite existing studies on the use of chitosan macrobeads for dye adsorption, the influence of controlled surface perforation induced by ultrasonication on their structural integrity and dye adsorption performance has been scarcely reported. Hence, this project aimed to develop chitosan macrobeads with a surface-perforated structure and to investigate how these surface alterations influence their dye adsorption efficiency. Here, chitosan macrobeads were formed using the gelation method and subsequently subjected to high-intensity sonication at various amplitudes (20 %, 40 %, 60 %, 80 %, and 100 %) for 5 minutes to induce surface perforation. As anticipated, significant changes in the surface structure were observed via electron microscopic analysis. In particular, the bead surfaces exhibited wavy and corrugated layers, with the presence of cracks and pores following sonication. Nevertheless, macrobeads treated at higher sonication amplitudes (≥ 60 %) experienced surface rupture, resulting in flake-like layers. Subsequently, dye adsorption studies showed a slight improvement in adsorption efficiency when chitosan macrobeads were sonicated at 40 % amplitude compared to non-sonicated samples. However, a detrimental effect was observed at higher sonication amplitudes (≥ 60 %), where a significant reduction in adsorption efficiency occurred. This study provides insight into the possibility of modifying chitosan macrobeads by imposing intense sonication to generate surface perforations, which subsequently alter their water treatment efficiency.

Received: *29 October, 2025*
Revised: *14 January, 2026*
Accepted: *10 March, 2026*

[1,2,3]Department of Chemical & Petroleum Engineering, Faculty of Engineering, Technology & Built Environment, UCSI University, 56000, Cheras, Kuala Lumpur, Malaysia.

[4]Faculty of Civil Engineering, Universiti Teknologi MARA (UiTM), 40450 Shah Alam, Selangor, Malaysia

[5]College of Civil Engineering, State Key Laboratory of Disaster Reduction in Civil Engineering, Tongji University, 1239 Siping Road, Shanghai 200092, P. R. China.

[6]Department of Civil Engineering, Lee Kong Chian Faculty of Engineering and Science, Universiti Tunku Abdul Rahman 43000, Kajang, Selangor, Malaysia.

[7]Department of Petrochemical Engineering, Faculty of Engineering and Green Technology, Universiti Tunku Abdul Rahman 31900, Kampar, Perak, Malaysia.

Corresponding author:
yeapsw@ucsiuniversity.edu.my

DOI: *https://doi.org/10.54552/v87i2.324*

Keywords:
Chitosan bead, Dye pollution, Water treatment, Sonication, Surface perforation

1.0 INTRODUCTION

Adsorption is one of the most widely used approaches for industrial effluent treatment, surpassing other processes such as advanced oxidation and membrane filtration due to its simplicity, technical maturity, high efficiency, and cost-effectiveness (Al-Ghouti *et al.,* 2023; Fouda-Mbanga, Onotu, & Tywabi-Ngeva, 2024). A variety of adsorbents are available for this approach, including activated carbon, zeolites, metal organic frameworks (MOFs), resins, nanomaterials, and biopolymers. Among all adsorbents, activated carbon is well known for its ability to separate a wide range of organic and chemical compounds. Nevertheless, despite its widespread use, the production of activated carbon is costly due to the requirement for high-temperature carbonization (Aulia, Aprilianda, Arsyad, & Johan, 2019; Y. Li *et al.,* 2025) and various chemicals for activation (such as NaOH, H_3PO_4, and Z_nCl_2) (Aulia *et al.,* 2019; Gao, Yue, Gao, & Li, 2020; Muttil, Jagadeesan, Chanda, Duke, & Singh, 2023). These requirements increase the operational costs and environmental burden especially when it comes to large-scale usage. On the other hand, nanoparticles represent a cutting-edge technology with high adsorption efficiency; however, their large-scale application is limited due to recent concerns regarding nano (toxicity) (Frazier *et al.,* 2023; Thu, Haider, Khan, Sohail, & Hussain, 2023). In contrast, biopolymers such as chitosan have gained increasing attention, as they are derived from natural resources, environmentally friendly, and biodegradable. More importantly, chitosan possesses abundant functional groups which include $–NH_2$ and $–OH$ that making it suitable to adsorb pollutants (Gamage *et al.,* 2023; Hashem & Farag, 2025). In fact, it was recently reported that chitosan has lower carbon footprint (1.5–2.5 kg CO_2-eq/kg) compared to activated carbon (8–12 kg CO_2-eq/kg) (Hashem & Farag, 2025), making it a potential low environmental impact adsorbent.

Chitosan is a linear polysaccharide consists of random copolymer of β-(1→4)-linked D-glucosamine and N-acetyl-D-glucosamine (Qiu, Hamilton, & Temenoff, 2011). This biopolymer is normally produced through the deacetylation of chitin (Aranaz *et al.,* 2021), which is extracted from natural sources such as the exoskeletons of crustaceans and insects (Ngasotter *et al.,* 2023), the gladius of squid (Kim, Song, Kim, Kim, & Jin, 2024), the cuttlebone of cuttlefish (Hazeena *et al.,* 2022), and the cell walls of fungi (Huq *et al.,* 2022). Despite its common use as a flocculant in water treatment, chitosan is also a promising adsorbent due to its unique functional groups, namely, amino and hydroxyl groups, which facilitate interactions or chelation with both organic and inorganic pollutants (Dago-Serry, Maroulas, Tolkou, Kokkinos, & Kyzas, 2024; Rostami & Khodaei, 2024). For instance, it was recently reported that both chitosan powder and chitosan bead are effective at adsorbing Direct Blue 78 dye from aqueous solution, with maximum adsorption capacities of 10.5 mg/g and 26.3 mg/g, respectively (Elzahar & Bassyouni, 2023). The adsorption was governed by electrostatic attraction between the positively charged chitosan molecules and the negatively charged dye molecules. Meanwhile, chitosan also able to form complexes (via chelate) with various transition metal ions and heavy metal ions include Cu^{2+}, Ni^{2+} and Hg^{2+} (Firnanelty, Chadijah, Ratna, Nurhuda, & Sittiama, 2021). In fact, chitosan can be manufactured into different structural forms include hydrogels, beads, membranes, fibres, films, and aerogels, which give more rooms to improve its adsorption capacity (Dago-Serry *et al.,* 2024; Kuang *et al.,* 2023; Rostami & Khodaei, 2023).

While the use of dissolved chitosan as a flocculant for water treatment has been reported for decades, it often results in the formation of sludge (Guibal & Roussy, 2007; Guibal, Touraud, & Roussy, 2005; Sanghi & Bhattacharya, 2005). In contrast, employing chitosan in solid forms as an adsorbent (e.g., beads) enables pollutant removal through adsorption without producing sludge. The solid form of chitosan is typically produced through physical gelation (Li, Qin, Xue, Lin, & Jiang, 2025; Lu, Zou, Zhou, Huang, & Zhang, 2022) or through chemical crosslinking with agents such as glutaraldehyde and epichlorohydrin (Beppu, Vieira, Aimoli, & Santana, 2007; Sapuła, Bialik-Wąs, & Malarz, 2023; Xiao, Shan, & Wu, 2023). For instance, our recent work demonstrated that chitosan macrobeads were able to remove over 90% of green algae from pond water, leaving a clear solution; in contrast, flocculating the green algae with dissolved chitosan resulted in a cloudy solution, indicating the presence of sludge (Thanasegaran, Yeap, Lai, & Wong, 2023). Research has been ongoing to further modify this biopolymer in order to enhance its adsorption efficiency (Upadhyay, Alimohammadi, & Tehrani, 2024). For instance, a recent study by Rodrigues *et al.* (2025) showed that pre-treatment of chitosan films with ethanol (immersion for 24 hours) and NaOH (immersion for 2 seconds) significantly improved mechanical stability and doubled the adsorption capacity (Rodrigues, Lopes, Longhinotti, & Diógenes, 2025). Despite existing studies on the use of chitosan macrobeads for dye adsorption, the influence of controlled surface perforation induced by ultrasonication on their structural integrity and dye adsorption performance has been scarcely reported. To close this research gap, in the present work, chitosan macrobeads were produced via gelation and subsequently treated with various ultrasonication conditions to induce surface perforation. Subsequently, the ultrasonicated chitosan macrobeads were characterised to assess changes in surface structure and functionality prior to their application in dye removal. It was hypothesised that the formation of pores on the bead surface would provide additional adsorption sites, thereby improving the overall adsorption efficiency.

2.0 METHODOLOGY

2.1 Materials

The materials used in this study included chitosan with a molecular weight of 30,000–190,000 g/mol (Sigma-Aldrich), acetic acid (AcOH) with a purity of 99.8–100.5% (Sigma-Aldrich), sodium hydroxide (NaOH) (Chemiz (M) Sdn. Bhd.), and methyl orange (MO) (Chemiz (M) Sdn. Bhd.). All chemicals were used as received without further purification or modification.

2.2 Synthesis of Chitosan Macrobead

The preparation of the adsorbent was referred to the previous research works (Thanasegaran *et al.,* 2023) and (Wong, Tay, & Lim, 2020). Firstly, 2 g of chitosan powder was dissolved in 100 mL of 1% (v/v) AcOH solution to prepare a chitosan stock solution. The mixture was magnetically stirred at 400 rpm for 24 hours to ensure complete dissolution. Meanwhile, a 10 M NaOH solution was prepared by dissolving 40 g of NaOH pellets in 100 mL of distilled water. The chitosan stock solution was then carefully added dropwise into the NaOH solution using a dropper, resulting in the formation of chitosan macrobeads. To ensure uniform macrobead size, the same dropper was used throughout the synthesis, and droplets were released at approximately the same rate. During this process, the NaOH solution was gently stirred at 125 rpm to prevent the stacking of the macrobeads. The formed chitosan macrobeads were allowed to stand for 24 hours to enhance their structural rigidity. Finally, the macrobeads were thoroughly rinsed with distilled water to remove any residual reactants before being used in subsequent studies. Note that the average size of the macrobeads is around 30 mm, as reported in our previous work (Thanasegaran *et al.,* 2023).

2.3 Preparation of Sonicated Chitosan Macrobeads

Sonicated macrobeads were prepared using a similar procedure to that described in Section 2.1, with the exception that the formed chitosan macrobeads were subjected to high-intensity sonication at varying amplitudes (20%, 40%, 60%, 80%, and 100%) for 5 minutes using an ultrasonic processor (Hielscher UP200s), prior to rinsing with distilled water. The sonication amplitude was varied to induce different levels of surface perforation on the chitosan macrobeads. Figure 1

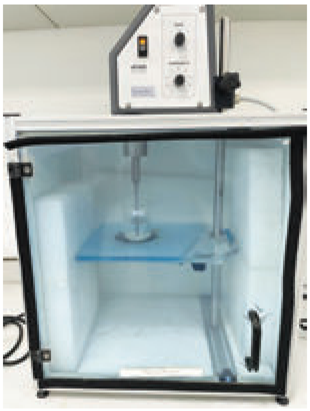

Figure 1: The setup of the probe sonicator for surface perforation of chitosan macrobeads. The probe tip was immersed in the solution up to 1 cm above the bottom of the beaker

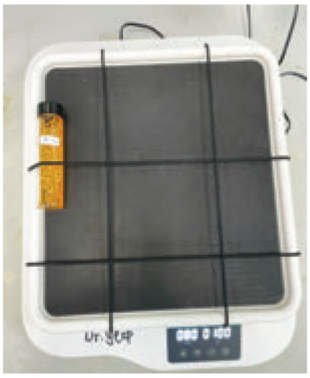

Figure 2: The conduct of MO adsorption study on an orbital shaker

shows the experiment setup for this section. The sonicated chitosan macrobeads were stored in distilled water and used for dye adsorption experiments within one month. Prior to adsorption, excess surface moisture was gently removed by carefully tapping the beads with tissue paper.

2.4 Characterise Structure Morphology and Functional Group of the Chitosan Macrobeads

The surface morphology and functional groups of the synthesized samples were analysed using a Scanning Electron Microscope (SEM, Tescan VEGA3) and Fourier Transform Infrared Spectroscopy (FTIR, PerkinElmer Spectrum Two), respectively. A series of SEM images were captured at various magnifications. Prior to analysis, all samples were sputter-coated with platinum. This characterisation was performed on six samples: chitosan macrobeads and chitosan macrobeads sonicated at amplitudes of 20% to 100%, in order to observe changes in size and surface morphology. Meanwhile, FTIR was used to identify changes in surface functional groups resulting from the sonication treatment at varying amplitudes.

2.5 Dye Adsorption Test

A stock solution of MO at a concentration of 1000 mg/L was prepared by dissolving 1000 mg of the dye in 1 L of distilled water. This stock solution was subsequently diluted to obtain the desired concentrations for experimental use. The concentration of the MO solution was determined using a UV-Vis spectrophotometer (Biobase BK-UV1800PC) operating in absorbance wavelength of 468 nm. A calibration curve was constructed at this wavelength using MO concentrations ranging from 10 to 70 mg/L, correlating absorbance values with dye concentration.

The adsorption test was conducted to investigate the effect of sonication amplitude on dye removal efficiency using 10 g of as-prepared chitosan macrobeads treated at different amplitudes (0 %, 20 %, 40 %, 60 %, 80 %, and 100 %). Each type of macrobeads was placed in a glass bottle containing 20 mL of a 50 mg/L MO dye solution to initiate the adsorption process. The bottles were then placed on an orbital shaker (Joanlab OS-20) operating at 200 rpm, as illustrated in Figure 2. After 3 hours of shaking, the adsorption process was terminated, and the final dye solution was transferred into a cuvette for absorbance measurement. The adsorption efficiency was calculated using Equation 1.

$$R\,(\%) = \frac{C_0 - C_e}{C_0} \times 100\% \qquad \text{(Eqn. 1)}$$

Where, C_o and C_e represent the initial and final concentrations of the dye solution (mg/L) respectively, while R is the removal efficiency.

3.0 RESULTS AND DISCUSSION

3.1 Changes in Surface Morphology of the Chitosan Macrobeads

The surface morphology of the as-prepared chitosan macrobeads was examined using SEM, and the results are shown in Figure 3. As illustrated in Figure 3, the incorporation of sonication altered the surface structure of the macrobeads by transforming the initially smooth surface (Figure 3a) into a rougher texture (Figure 3b-f). By taking a closer look at the surface structure of the sonicated chitosan macrobeads at higher magnification (5000×), it was found that the bead surface exhibits wavy and corrugated layers with the presence of cracks and pores. Furthermore, chitosan macrobeads treated at higher sonication amplitudes of 60 %, 80 %, and 100 % were noticed to have ruptured into flake-like layers. Apparently, the application of sonication has imposed intense physical forces that disrupting the internal bonding network (hydrogen bonds) of the chitosan macrobeads (Jamalabadi, Saremnezhad, Bahrami, & Jafari, 2019; Khoerunnisa *et al.,* 2021), leading to the rupture of the bead surface into flake-like structure.

The direct contact of the sonication probe with the beads serves as another reason leading to such a broken structure. Accordingly, the present study has successfully modified the surface morphology of the macrobeads by varying the sonication amplitude. It is envisaged that the formation of pores and cracks will increase the available active sites for pollutant adsorption (Ang *et al.,* 2024).

Figure 4 depicts digital photographs of the chitosan macrobead solutions after sonication treatment. Notably, the cloudiness of the water changes with the sonication amplitude, with samples treated at higher amplitudes (e.g., 80% and 100%) appearing cloudier. The water turns cloudy due to a higher amount of disintegrated chitosan suspended in it.

3.2 Changes in Surface Functional Groups of the Chitosan Macrobeads

Figure 5 shows the FTIR spectra of both unsonicated and sonicated chitosan macrobeads, scanned across the wavenumber range of 4000 cm^{-1} to 400 cm^{-1}, to examine differences in their functional groups. Table 1 presents the corresponding functional groups associated with each significant peak observed in the spectra. Overall, all the beads exhibit peaks at similar wavenumber ranges, including a signal at 896 cm^{-1}, which corresponds to the C–H bending out of the plane of the monosaccharide ring (Fernandes

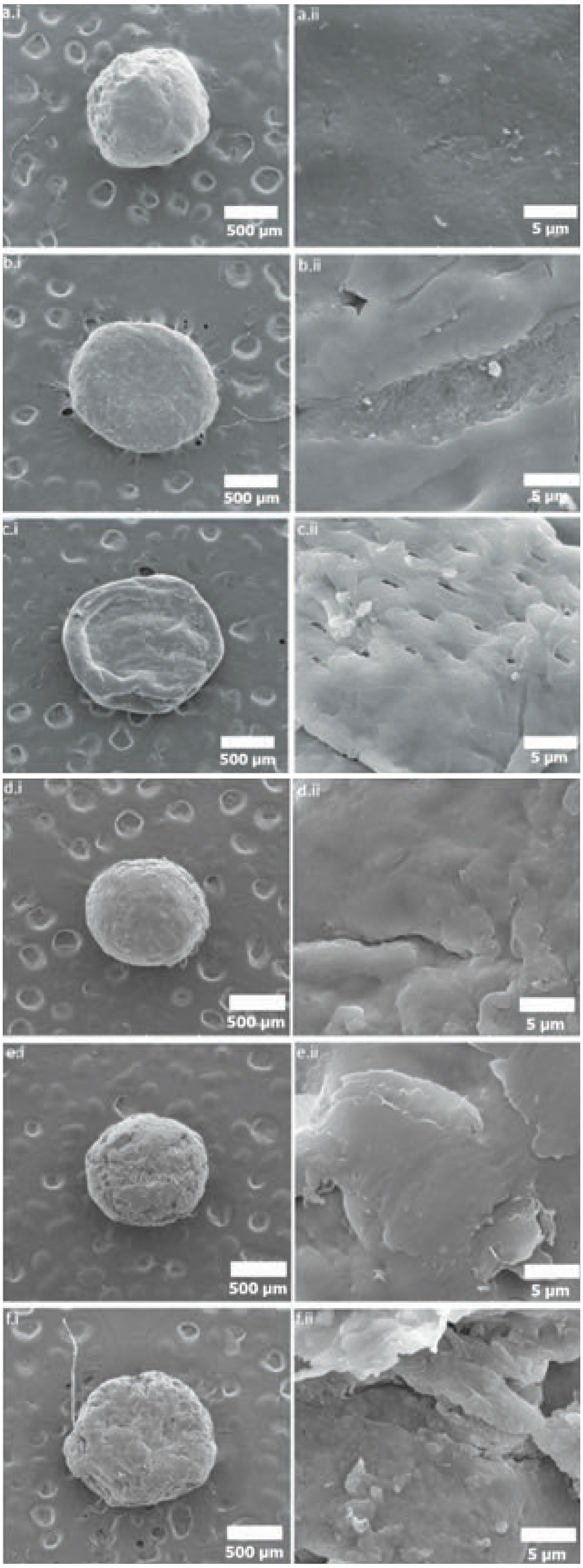

Figure 3: SEM images of chitosan macrobead obtained at 50x (left) and 5000x (right) magnifications. The chitosan macrobeads were sonicated at (a) 0 %, (b) 20 %, (c) 40 %, (d) 60 %, (e) 80 %, and (f) 100 % for 5 mins

Queiroz, Melo, Sabry, Sassaki, & Rocha, 2015). Meanwhile, the pronounced peak observed between 1029.87 cm^{-1} and 1079.79 cm^{-1} is attributed to the stretching vibrations of the C–O bonds (Dissanayake, Pathirana, Wanasekara, Mahltig, & Nandasiri, 2023). In addition, the C-O-C bridge's asymmetric stretching is responsible for the absorption band at 1149.33 cm^{-1} (Dissanayake *et al.,* 2023). The small signal around 1251.78 cm^{-1} corresponded to the bending vibrations of OH present in chitosan (Fernandes Queiroz *et al.,* 2015).

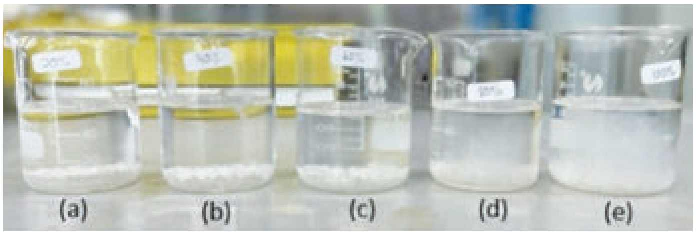

Figure 4: Digital photographs showing the changes in water cloudiness after the chitosan macrobeads being sonicated using (a) 20 %, (b) 40 %, (c) 60 %, (d) 80 %, and (e) 100 % of sonication amplitude

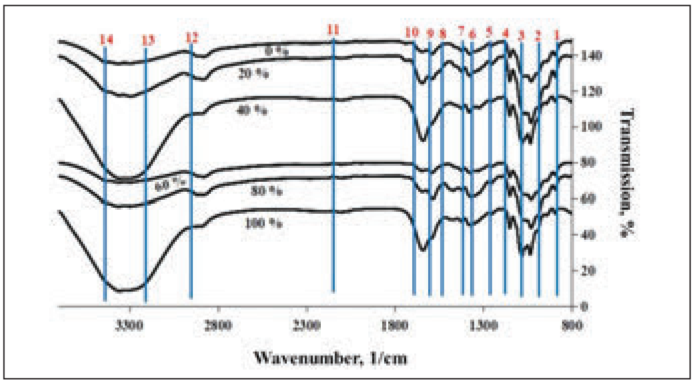

Figure 5: FTIR spectra of the unsonicated and sonicated chitosan macrobeads

Table 1: Legend for FTIR spectra shown in Figure 5

No.	Wavenumber (cm^{-1})	Functional Group	References
1	893.54	• C-H stretching	(Fernandes Queiroz *et al.,* 2015)
2-3	1029.87 - 1079.79	• C-O stretching	(Dissanayake *et al.,* 2023)
3-4	1149.33	• C-O-C	(Dissanayake *et al.,* 2023)
5	1251.78	• OH	(Fernandes Queiroz *et al.,* 2015)
6-7	1375.78 - 1420.55	• CH_2 bending and CH_3 deformation	(Moosa, Ridha, & Kadhim, 2016)
8-9	1584.08 - 1588.24	• N-H stretching	(Dissanayake *et al.,* 2023)
9-10	1645.75	• C=O in the $NHCOCH_3$ group	(Chung & Ong, 2021; Dissanayake *et al.,* 2023)
11-12	2800 - ~2900	• C-H symmetric and asymmetric stretching	(Fernandes Queiroz *et al.,* 2015)
13-14	3291.52 - 3362.48	• O-H stretching vibrations. • N-H stretching vibrations	(Chung & Ong, 2021)

The bending vibration of N-H cause the absorptions between 1584.08 cm^{-1} and 1588.24 cm^{-1} (Dissanayake *et al.,* 2023). The presence of residual acetyl groups is evidenced by the bands at approximately 1645.75 cm^{-1} (C=O stretching of amide I) (Chung & Ong, 2021; Dissanayake *et al.,* 2023). The absorption bands at ~2800 cm^{-1} and ~2900 cm^{-1} can be assigned to C-H symmetric and asymmetric stretching, correspondingly (Fernandes Queiroz *et al.,* 2015). As shown in the FTIR spectrum of chitosan macrobeads, a strong absorption band from 3291 cm^{-1} to 3362 cm^{-1} was attributed to the overlapped stretching vibration of –OH and N–H (Chung & Ong, 2021). Note that there is no clear trend on the intensity of the absorption band from 3291 cm^{-1} to 3362 cm^{-1}, which is likely due to non-uniform water retention in the beads arising in the sample drying stage prior to FTIR analysis. Despite that, regardless of the sonication amplitude, the FTIR spectra of the chitosan macrobeads appear to be the same. Such observation suggested that the application of sonication does not alter the key functional groups of the chitosan macrobeads. Notably, the band at 1645.75 cm^{-1} shows increased intensity in the sonicated beads relative to the unsonicated ones, likely due to the exposure of internal functional groups resulting from surface exfoliation.

3.3 Unsonicated and Sonicated Chitosan Macrobeads for Dye Adsorption

Next, the as-prepared chitosan macrobeads were used for adsorption of MO. In this regard, the adsorption of MO onto the chitosan macrobeads is primarily governed by electrostatic attraction, as the dye is anionic due to sulfonate groups (Wu *et al.,* 2021) and chitosan is cationic due to protonated –NH_2 groups under acidic to ~ pH 6.38 (point of zero charge) conditions (Munim, Saddique, Raza, & Majeed, 2018). The effects of varying the sonication amplitude from 0 % to 100 % on chitosan macrobeads and its subsequent impact on MO adsorption efficiency were investigated. As depicted in Figure 6, chitosan macrobeads treated with sonication amplitudes of 0 %, 20 %, 40 %, 60 %, 80 %, and 100 % exhibited adsorption removal efficiencies of 40 %, 41 %, 42 %, 31 %, 30 %, and 29 %, respectively. This result demonstrates that the sonication amplitude does have a considerable impact on the removal effectiveness. By taking a closer look at the experimental standard deviation and significance of the study, it was found that there is no significant difference in the adsorption efficiencies of chitosan macrobeads produced at 0 %, 20 %, and 40 % efficiency despite the average value showed a slight increment from 40 % to 42 %. The slight increase can be attributed to surface perforation induced by sonication, which creates additional adsorption sites (as shown in Figure 3a-c).

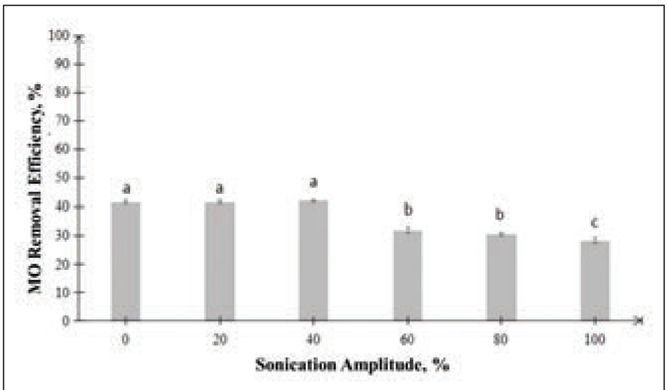

Figure 6: MO removal efficiency using the unsonicated and sonicated chitosan macrobeads. Experimental conditions: 50 mg/L MO solution, pH 5, 20 mL total dye volume, 8 g chitosan macrobeads, agitation speed of 200 rpm, and contact time of 3 hours.

**statistically significant difference determined by t-test (P < 0.05)*

Nevertheless, chitosan macrobeads treated with higher sonication amplitudes (ranging from 60 % to 100 %) exhibited a reduction in adsorption efficiency. This outcome can be attributed to the breaking of chitosan macrobeads under the intense cavitation-induced mechanical stresses exerted during sonication. As presented in Figure 3d–f, the surface of the chitosan macrobeads ruptured into small flake-like structures rather than forming pores. Furthermore, some of these small structures disintegrated from beads and remained suspended in the water, appearing as a cloudy solution as shown in Figure 4c–d. These disintegrated fragments caused the beads to be less solidified and lack surface integrity, resulting in reduced MO adsorption performance. Apparently, a stable and well-formed bead is essential for effective adsorption applications.

Figure 7: Digital images showing the appearance of the a) initial MO solution (50 mg/l), and remaining solution after adsorbed by chitosan macrobeads prepared at sonication amplitude of b) 0 %, c) 20 %, d) 40 %, e) 60 %, f) 80 %, and g) 100 %

Figure 7 shows the digital image of the leftover solution of MO molecules after the adsorption process, a darker orange colour in samples Figure 7f and Figure 7g indicated the adsorption process was less successful, rendering a higher MO concentration in the remaining solution. This result contrasts with (Low, Tan, Chin, & Tan, 2018), who reported that peanut husk powder sonicated with the same probe sonicator at 60 % amplitude exhibited more surface pores and higher adsorption efficiency than the unsonicated counterpart. Such deviation could be ascribed to the less resilience of the chitosan macrobeads towards cavitation-induced mechanical stresses as compared to peanut husk powder.

4.0 CONCLUSION

The present work revealed that modification of chitosan macrobeads can be achieved through the application of intense ultrasonication. Electron microscopic analysis showed that chitosan macrobeads sonicated at amplitudes of 20 % – 40 % exhibited wavy and corrugated surfaces, along with the formation of cracks and pores. However, increasing the sonication amplitude to 60 % – 100 % resulted in fragmentation of the bead surface into flake-like structures. In fact, under such high sonication amplitudes, some fragments of the beads have disintegrated and became suspended in the solution, causing the initially clear water to turn turbid. FTIR analysis showed that key functional groups of chitosan, including –OH, C=O and N–H bonds, were retained in the sonicated counterparts. In terms of dye adsorption efficiency, the unsonicated chitosan macrobeads were able to remove 40 % of MO after 3 hours of batch adsorption. Only a slight increase in adsorption efficiency was observed when the chitosan macrobeads were moderately sonicated; the slight increase is attributed to sonication-induced surface perforation, creating additional adsorption sites.

However, a significant reduction in adsorption efficiency was observed when the chitosan macrobeads were sonicated at amplitudes ≥ 60 %, as supported by SEM analysis showing that the bead surfaces had fragmented into flake-like structures, with portions of them have disintegrated from the beads. In overall, this study has demonstrated that controlled ultrasonication is a feasible method to tailor the surface structure of chitosan macrobeads, thereby offering insights for modifying chitosan-based adsorbents for effective water treatment applications. For future studies, further optimization of the sonication-induced surface perforation should be carried out by manipulating other sonication conditions which include sonication time and temperature. The macrobead structure can be further characterised for crystallinity via X-ray Diffraction and surface area using Brunauer–Emmett–Teller analyser. In addition, the dye desorption and reusability of the chitosan macrobeads in dye adsorption applications should be investigated. ■

ACKNOWLEDGEMENT

This authors thanks UCSI University for providing facilities and resources for completion of this project.

AUTHORS' CONTRIBUTIONS

Kabilarasan Thanasegaran	Methodology, Formal analysis, Investigation, Writing - Original Draft.
Swee Pin Yeap	Conceptualisation, Visualisation, Supervision, Resources, Funding acquisition, Validation, Writing - Review & Editing.
Li Sze Lai	Conceptualisation, Resources, Writing - Review & Editing.
Jing Lin Ng	Conceptualisation, Investigation, Visualisation.
Chaomeng Dai	Visualisation, Conceptualisation.
Kah Hon Leong	Visualisation, Conceptualisation.
Pey Yi Toh	Conceptualisation, Resources, Visualisation.

REFERENCES

[1] Al-Ghouti, M. A., Ashfaq, M. Y., Khan, M., Al Disi, Z., Da'na, D. A., & Shoshaa, R. (2023). State-of-the-art adsorption and adsorptive filtration based technologies for the removal of trace elements: A critical review. *Science of The Total Environment,* 895, 164854. doi: https://doi.org/10.1016/j.scitotenv.2023.164854

[2] Ang, Y., Kabilarasan, T., Teo, S. S., Lim, L. H., Su, S. F., Mangnomek, V., Yeap, S. P. (2024). Ultrasound treatment of chitosan macrobeads for crack formation and application in column dynamics sorption of methyl orange. *International Journal of Environmental Science and Technology*. https://doi.org/10.1007/s13762-024-06236-w

[3] Aranaz, I., Alcántara, A. R., Civera, M. C., Arias, C., Elorza, B., Heras Caballero, A., & Acosta, N. (2021). Chitosan: An overview of its properties and applications. Polymers, 13(19), 3256. https://doi.org/10.3390/polym13193256

[4] Aulia, Aprilianda, Arsyad, F. S., & Johan, A. (2019). Temperature carbonization effect on the quality of activated carbon based on rubber seed shell. *Journal of Physics: Conference Series,* 1282(1), 012043. https://doi.org/10.1088/1742-6596/1282/1/012043

[5] Beppu, M. M., Vieira, R. S., Aimoli, C. G., & Santana, C. C. (2007). Crosslinking of chitosan membranes using glutaraldehyde: Effect on ion permeability and water absorption. *Journal of Membrane Science,* 301(1), 126-130. doi: https://doi.org/10.1016/j.memsci.2007.06.015

[6] Chung, W.-Y., & Ong, S.-T. (2021). Effective removal of reactive brown 10 from aqueous solution by using chitosan beads: batch and experimental design studies. *Journal of Physical Science,* 32(1), 91-108.

[7] Dago-Serry, Y., Maroulas, K. N., Tolkou, A. K., Kokkinos, N. C., & Kyzas, G. Z. (2024). How the chitosan structure can affect the adsorption of pharmaceuticals from wastewaters: An overview. *Carbohydrate Polymer Technologies and Applications,* 7, 100466. https://doi.org/10.1016/j.carpta.2024.100466

[8] Dissanayake, N. S. L., Pathirana, M. A., Wanasekara, N. D., Mahltig, B., & Nandasiri, G. K. (2023). Removal of methylene blue and congo red using a chitosan–graphene oxide-electrosprayed functionalized polymeric nanofiber membrane. *Nanomaterials,* 13(8), 1350.

[9] Elzahar, M. M. H., & Bassyouni, M. (2023). Removal of direct dyes from wastewater using chitosan and polyacrylamide blends. *Scientific Reports,* 13(1), 15750. https://doi.org/10.1038/s41598-023-42960-y

[10] Fernandes Queiroz, M., Melo, K. R. T., Sabry, D. A., Sassaki, G. L., & Rocha, H. A. O. (2015). Does the use of chitosan contribute to oxalate kidney stone formation? *Marine Drugs,* 13(1), 141-158.https://doi.org/10.3390/md13010141

[11] Firnanelty, Chadijah, S., Ratna, Nurhuda, S., & Sittiama. (2021). Synthesis of chitosan-CuO composite and it's application as heavy metal adsorbent. *Journal of Physics: Conference Series,* 1899(1), 012029. https://doi.org/10.1088/1742- 6596/1899/1/012029

[12] Fouda-Mbanga, B. G., Onotu, O. P., & Tywabi-Ngeva, Z. (2024). Advantages of the reuse of spent adsorbents and potential applications in environmental remediation: A review. *Green Analytical Chemistry,* 11, 100156. doi: https://doi.org/10.1016/j.greeac.2024.100156

[13] Frazier, E. A., Patil, R. P., Mane, C. B., Sanaei, D., Asiri, F., Seo, S. S., & Sharifan, H. (2023). Environmental exposure and nanotoxicity of titanium dioxide nanoparticles in irrigation water with the flavonoid luteolin. RSC Advances, 13(21), 14110-14118. https://doi.org/10.1039/d3ra01712e

[14] Gamage, A., Jayasinghe, N., Thiviya, P., Wasana, M. L. D., Merah, O., Madhujith, T., & Koduru, J. R. (2023). Recent application prospects of chitosan based composites for the metal contaminated wastewater treatment. *Polymers*, 15(6), 1453.

[15] Gao, Y., Yue, Q., Gao, B., & Li, A. (2020). Insight into activated carbon from different kinds of chemical activating agents: A review. *Science of The Total Environment,* 746, 141094. https://doi.org/10.1016/j.scitotenv.2020.141094

[16] Guibal, E., & Roussy, J. (2007). Coagulation and flocculation of dye-containing solutions using a biopolymer (Chitosan). *Reactive and Functional Polymers,* 67(1), 33-42.https://doi.org/10.1016/j.reactfunctpolym.2006.08.008

[17] Guibal, E., Touraud, E., & Roussy, J. (2005). Chitosan interactions with metal ions and dyes: dissolved-state vs. solid-state application. *World Journal of Microbiology and Biotechnology,* 21(6), 913-920. https://doi.org/10.1007/s11274-004-6559-5

[18] Hashem, A., & Farag, S. (2025). Chitosan-based adsorbents for water purification: Mechanisms, performance, and sustainability. *Applied Surface Science Advances,* 30, 100804. https://doi.org/10.1016/j.apsadv.2025.100804

[19] Hazeena, S. H., Hou, C.-Y., Zeng, J.-H., Li, B.-H., Lin, T.-C., Liu, C.-S., Shih, M.-K. (2022). Extraction optimization and structural characteristics of chitosan from Cuttlefish (S. pharaonis sp.) bone. *Materials,* 15(22), 7969.

[20] Huq, T., Khan, A., Brown, D., Dhayagude, N., He, Z., & Ni, Y. (2022). Sources, production and commercial applications of fungal chitosan: A review. *Journal of Bioresources and Bioproducts,* 7(2), 85-98. https:// doi.org/10.1016/j.jobab.2022.01.002

[21] Jamalabadi, M., Saremnezhad, S., Bahrami, A., & Jafari, S. M. (2019). The influence of bath and probe sonication on the physicochemical and microstructural properties of wheat starch. *Food Science & Nutrition,* 7(7), 2427-2435. https://doi.org/10.1002/fsn3.1111

[22] Khoerunnisa, F., Yolanda, Y. D., Nurhayati, M., Zahra, F., Nasir, M., Opaprakasit, P., & Ng, E.-P. (2021). Ultrasonic synthesis of nanochitosan and its size effects on turbidity removal and dealkalization in wastewater treatment. *Inventions,* 6(4), 98.

[23] Kim, J.-K., Song, M.-O., Kim, J., Kim, S., & Jin, J. (2024). Cryomilling-assisted high purity β-chitin extraction from Uroteuthis edulis pens. *International Journal of Biological Macromolecules,* 268, 131815. https://doi. org/10.1016/j.ijbiomac.2024.131815

[24] Kuang, J., Cai, T., Dai, J., Yao, L., Liu, F., Liu, Y., Peng, H. (2023). High strength chitin/chitosan-based aerogel with 3D hierarchically macro-meso-microporous structure for high-efficiency adsorption of Cu(II) ions and Congo red. *International Journal of Biological Macromolecules,* 230, 123238. https://doi. org/10.1016/j.ijbiomac.2023.123238

[25] Li, Y., Yan, X., Cui, Z., Yuan, J., Xu, B., & Yang, G. (2025). Design and preparation of activated carbon with high specific surface area and porosity through an organic activator coupled with co2 activation. *Advanced Materials Interfaces,* 12(3), 2400450. https://doi.org/10.1002/admi.202400450

[26] Li, Z., Qin, R., Xue, J., Lin, C., & Jiang, L. (2025). Chitosan-based hydrogel beads: developments, applications, and challenges. *Polymers,* 17(7), 920.

[27] Low, S. K., Tan, M. C., Chin, N. L., & Tan, K. W. (2018). Comparative studies on ultrasound pre-treated peanut husk powder and ultrasound simultaneous process on heavy metal adsorption. *International Journal of Engineering,* 31(8), 1334-1340.

[28] Lu, Z., Zou, L., Zhou, X., Huang, D., & Zhang, Y. (2022). High strength chitosan hydrogels prepared from NaOH/urea aqueous solutions: the role of thermal gelling. *Carbohydrate Polymers,* 297, 120054. https://doi.org/10.1016/j.carbpol.2022.120054

[29] Moosa, A., Ridha, A., & Kadhim, N. (2016). Use of Biocomposite Adsorbents for the Removal of Methylene Blue Dye from Aqueous Solution. *American Journal of Materials Science,* 2016, 135-146. https://doi.org/10.5923/j. materials.20160605.03

[30] Munim, S. A., Saddique, M. T., Raza, Z. A., & Majeed, M. I. (2018). Preparation and physico-chemical characterization of β-cyclodextrin incorporated

chitosan biosorbent beads with potential environmental applications. *Materials Research Express,* 5(6), 065503. https:// doi: 10.1088/2053-1591/aac707

[31] Muttil, N., Jagadeesan, S., Chanda, A., Duke, M., & Singh, S. K. (2023). Production, types, and applications of activated carbon derived from waste tyres: an overview. *Applied Sciences,* 13(1), 257.

[32] Ngasotter, S., Xavier, K. A. M., Meitei, M. M., Waikhom, D., Madhulika, Pathak, J., & Singh, S. K. (2023). Crustacean shell waste derived chitin and chitin nanomaterials for application in agriculture, food, and health – A review. *Carbohydrate Polymer Technologies and Applications,* 6, 100349. https://doi.org/10.1016/j.carpta.2023.100349

[33] Qiu, Y., Hamilton, S. K., & Temenoff, J. (2011). Improving mechanical properties of injectable polymers and composites. In B. Vernon (Ed.), *Injectable Biomaterials* (pp. 61-91): Woodhead Publishing.

[34] Rodrigues, S. G. G., Lopes, G. S., Longhinotti, E., & Diógenes, I. Z. N. (2025). Chitosan pretreatment: evidence of enhanced mechanical stability and adsorption capacity to produce a hybrid material. *Journal of the Brazilian Chemical Society,* 36(5), 1-10.

[35] Rostami, M. S., & Khodaei, M. M. (2023). Chitosan-based composite films to remove cationic and anionic dyes simultaneously from aqueous solutions: Modeling and optimization using RSM. *International Journal of Biological Macromolecules,* 235, 123723. https://doi.org/10.1016/j.ijbiomac.2023.123723

[36] Rostami, M. S., & Khodaei, M. M. (2024). Recent advances in chitosan-based nanocomposites for adsorption and removal of heavy metal ions. *International Journal of Biological Macromolecules,* 270, 132386. https://doi.org/10.1016/j.ijbiomac.2024.132386

[37] Sanghi, R., & Bhattacharya, B. (2005). Comparative evaluation of natural polyelectrolytes psyllium and chitosan as coagulant aids for decolourization of dye solutions. *Water Quality Research Journal,* 40(1), 97- 101. https://doi.org/10.2166/wqrj.2005.009

[38] Sapuła, P., Bialik-Wąs, K., & Malarz, K. (2023). Are natural compounds a promising alternative to synthetic cross-linking agents in the preparation of hydrogels? *Pharmaceutics,* 15(1), 253.

[39] Thanasegaran, K., Yeap, S. P., Lai, L. S., & Wong, V. L. (2023). Chitosan powder vs. chitosan macrobead: feasibility test for separation of microalgae from real pond water. *Chemical Engineering Transactions,* 106, 1021-1026. https://doi.org/10.3303/CET23106171

[40] Thu, H. E., Haider, M., Khan, S., Sohail, M., & Hussain, Z. (2023). Nanotoxicity induced by nanomaterials: A review of factors affecting nanotoxicity and possible adaptations. *OpenNano,* 14, 100190. https://doi.org/10.1016/j.onano.2023.100190

[41] Upadhyay, A., Alimohammadi, F., & Tehrani, R. (2024). Engineering porosity-tuned chitosan beads: balancing porosity, kinetics, and mechanical integrity. *ACS Omega,* 9(31), 33857-33867.https://doi.org/10.1021/acsomega.4c03583

[42] Wong, V. L., Tay, S. Y., & Lim, S. S. (2020). Enhanced removal of methyl orange from aqueous solution by chitosan-CaCl2 beads. *IOP Conference Series: Materials Science and Engineering,* 736(2), 022049. https://doi.org/10.1088/1757-899x/736/2/022049

[43] Wu, L., Liu, X., Lv, G., Zhu, R., Tian, L., Liu, M., Liao, L. (2021). Study on the adsorption properties of methyl orange by natural one-dimensional nano-mineral materials with different structures. *Scientific Reports,* 11(1), 10640. https://doi.org/10.1038/s41598-021-90235-1

[44] Xiao, L., Shan, H., & Wu, Y. (2023). Chitosan cross-linked and grafted with epichlorohydrin and 2,4-dichlorobenzaldehyde as an efficient adsorbent for removal of Pb(II) ions from aqueous solution. *International Journal of Biological Macromolecules,* 247, 125503. https://doi.org/10.1016/j.ijbiomac.2023.125503

PROFILES

KABILARASAN THANASEGARAN completed his Master of Philosophy in Chemical Engineering at UCSI University in 2024. He obtained his Bachelor's degree from UCSI University, Malaysia. His research focuses on the synthesis of bio-adsorbents for applications in environmental remediation.
Email address: kabilarasan0527@gmail.com

SWEE PIN YEAP is currently an Associate Professor in the Department of Chemical and Petroleum Engineering at UCSI University. He obtained his PhD in Chemical Engineering in 2016 and has since made significant and sustained contributions to the field of nanoscience and nanotechnology. His research primarily focuses on the synthesis, functionalisation, and interfacial engineering of nanoparticles and low-dimensional nanomaterials for sustainable energy and environmental applications. He has established an independent research profile while actively contributing to postgraduate training and the broader scientific community.
Email address: yeapsw@ucsiuniversity.edu.my

LI SZE LAI is an Assistant Professor in the Department of Chemical and Petroleum Engineering, Faculty of Engineering, Technology and Built Environment, UCSI University, Malaysia. She holds a Doctor of Philosophy in Chemical Engineering and a Bachelor of Engineering (Honours) in Environmental Engineering. Her research interests focus on membrane technology for gas separation and wastewater treatment, including CO_2 capture, gas transport modelling, and the removal of heavy metals from wastewater. She also works on computational fluid dynamics (CFD) simulation, additive manufacturing, and the development of advanced membrane systems for environmental and industrial applications.
Email address: lails@ucsiuniversity.edu.my

JING LIN NG is a Senior Lecturer in the Faculty of Civil Engineering at Universiti Teknologi MARA (UiTM), Shah Alam, Selangor, Malaysia. She earned her PhD in Water Resources Engineering from Universiti Putra Malaysia (UPM) and her Bachelor of Engineering in Biological and Agricultural Engineering from the same university. Her research focuses on water resources engineering, hydrological modelling, climate change impacts, drought forecasting, artificial intelligence applications, and uncertainty assessment of hydrological models.
Email address: jinglin.ng@uitm.edu.my

CHAOMENG DAI is a Professor in College of Civil Engineering, State Key Laboratory of Disaster Reduction in Civil Engineering, Tongji University. His research focuses on groundwater security, including the migration and transformation of pollutants in groundwater, modeling and simulation of contaminant behavior, and the application of novel environmental functional materials/nanomaterials for groundwater remediation.
Email address: daichaomeng@tongji.edu.cn

KAH HON LEONG is an Associate Professor in the Department of Civil Engineering at University Tunku Abdul Rahman (UTAR). He holds a PhD in Civil and Environmental Engineering from University Malaya and professional qualifications from the Board of Engineers Malaysia and the Malaysia Board of Technologists. His research focuses on advanced material technologies for photocatalysis and environmental engineering applications. He is also an expert in ESG frameworks and green finance, specialising in sustainable investment strategies and ESG-linked industry practices.
Email address: khleong@utar.edu.my

PEY YI TOH is an Associate Professor in the Department of Petrochemical Engineering, Faculty of Engineering and Green Technology, Universiti Tunku Abdul Rahman. Dr. Toh obtained her Doctor of Philosophy in Chemical Engineering and Bachelor of Engineering (Hons) in Chemical Engineering, both from Universiti Sains Malaysia. Her research expertise focuses on magnetophoretic separation of microalgae, nanotechnology, environmental remediation, biofuel production, microalgal biosequestration, and phycoremediation, with an emphasis on developing sustainable solutions for environmental and energy applications.
Email address: tohpy@utar.edu.my

MANUSCRIPT PREPARATION GUIDELINES FOR IEM JOURNAL AUTHORS

The aim of publishing the Journal of the Institution of Engineers Malaysia (or IEM Journal) is to promote the advancement of science, engineering, and technology; disseminate new and current knowledge; share novel findings among practising engineers, researchers and other interested colleagues. Hence, the IEM Journal covers a wide range of practical and diversified engineering disciplines, including publishing papers on any subjects relevant to the engineering and technology of today. As in other journals, all paper submissions to the IEM journal will be peer-reviewed by professionals.

Submission of a contribution is taken to manifest the fact that the submission has not been submitted, accepted, published, or copyrighted elsewhere. To avoid publication delays, please send all manuscripts to the Editor (via the Online Journal Submission) and observe the following guidelines. Each paper is independently peer-reviewed.

Types of Papers

IEM Journal will accept any submissions that fall within the three types of papers shown below:

- **Research Paper**

Significant research and development or applications in any field of engineering and/or technology. Submissions should be about 8-14 pages.

- **Review Paper**

Articles which summarises the state-of-the-art of a specific area of research. Submissions should be about 10-20 pages.

- **Brief Paper**

A concise description of new technical concepts or applications within the scope of the journal. Submission should be about 4 pages

Together with the paper submission, at least four (4) reviewers complete with their contact details (official postal and email address, and telephone number) are to be proposed by authors. Reviewers should be the experts in their research areas.

Plagiarism Policy

IEM Journal strictly prohibits any form of Plagiarism.

If the manuscript has been presented, published, or submitted for publication elsewhere, please inform the Editor. Our primary objective is to publish technical materials not available elsewhere.

Format and Elements of Submitted Texts

a) Initial Submission

For initial submission and reviewing, ALL papers are accepted regardless of the formatting used.

b) Final Submission

Upon final submission of paper, authors are required to follow the manuscript instruction guidelines and paper template as presented below.

Please prepare your main text document in Microsoft Word and PDF format, text should be single line spaced, line numbered and pages should be numbered. You can download the paper template here.

Please note that the style that you submit your paper in (e.g. any additional italics or bold fonts, bullet points, etc.) may be changed on publication to accommodate our publication style.

Manuscript Style

Language:

- The language of the IEM Journal is in English. However, a paper in Bahasa Melayu is also accepted. For accepted papers, an abstract in English and Bahasa Melayu must be included.
- The manuscript should be able to be readily understood by an engineer and researchers alike and should avoid any colloquialisms.
- The terms, including nomenclature and abbreviations, and style should be consistent throughout your journal paper. If you collaborate with other writers, please communicate clearly with them.
- Avoid referring directly to the names of individuals, organisations, products, or services unless essential to the comprehension of the manuscript. Gratuitous flattery or derogatory remarks about a person or organisation should not be included.
- Symbols and Units: SI and derived units should be used, if possible.
- Abbreviations: the use of internationally recognised abbreviations is allowed in the text. The abbreviations should be defined on first use. Abbreviations should not be used in the title.

Manuscript Guide

The following is a detailed manuscript preparation guide for articles submitted to IEM Journal; however, they can, in the most part, be used as a basis for other article types amending to concur with the page limit and premise of the formats, as appropriate.

The manuscript should be typewritten using single-spacing, font of 12 Times Roman; on one side of sheet only and in a single column format.

Title

Titles are limited to 150 characters, including spaces. Please avoid the use of any abbreviations, acronyms, or formulae. Titles should clearly reflect the content of the manuscript and any search terms that readers may use should be considered and incorporated.

List of Authors Name

List down all the names of authors (who has contributed to the paper) and the respective affiliations. From the list of authors, place an asterisk (*) next to the corresponding author's name. Provide an official email address of the corresponding author. **Please DO NOT include your personal telephone number on the title page.**

Abstract

Provide an informative 100 to 250 words abstract at the head of the manuscript. This should be a concise reflection of the aims, findings, conclusions and any interesting or important results. Carefully incorporate any terms that may be used by potential interested readers to improve the article's discoverability online (search engine optimisation). The abstract should contain no reference. Abbreviations that are not commonly used should be defined (for the benefit of the non-specialist reader) at first use.

Keywords

These are used for indexing. Please include between 3-5 keywords.

List of Notations

Please provide a list of symbols and definitions used in the text. This will ease our readers.

Introduction

A concise summary of current background knowledge, with reference to relevant previous works in the field should be presented. Please also describe the objectives of and justification for the work contained in the submitted manuscript.

Main Text

The methods and processes applied to investigate and achieve the objectives should be communicated in sufficient detail that readers could repeat the work successfully. The results should be reported clearly and interpreted accurately and analysed thoroughly. Figures/tables can be used to support these results.

It is important that all research articles include a section at the end of the main text that highlights the novelty of the results to the engineering field and any potential applications.

All sections should be numbered in Arabic such as 1, 2, etc. with the title in capitals. Sub-sections should be numbered such as 1.1, 2.3, etc. Numbered all equations in round brackets ( ) flush to the right. The equation should be in the centre.

Style for Illustrations (Tables and Figures)

Try to include the illustrations in between the text. Each illustration must be numbered such as "Figure 1, Figures 2-3, etc." and have a meaningful caption at the bottom. For tables, the caption must be at the top.
On graphs, show only the coordinate axes, or at most the major grid lines, to avoid a dense hard-thread result.

All lettering should be large enough to permit legible reduction of the figure to column width. Typing on figures is not acceptable. Photographs should be glossy prints, of good contrast and gradation and any reasonable size.

Conclusions

A concise summary of the results of case studies or research project papers and the lessons learned should be discussed. If necessary, please elaborate the applicability / relevance of your article to readers in other countries.

Research journals must discuss the practical relevance and potential applications of the engineering work described. This is important to readers working in engineering related practice.

Please also include relevant references to demonstrate how previous engineering research work has been used. These references could be standards, codes or relevant past journal papers.

Appendices

Additional information, such as tables or mathematical derivations can be included. These will be included in the article.

Acknowledgements

Please provide acknowledgement details to those persons or organization that contributed to the paper. Additional details required by funding bodies can be included.

References

The references to other literature that you have cited in your main text should be based on the APA style of referencing (Author, Date) as described below. Please refer https://apastyle.apa.org/ for a detailed guide on the referencing style.

- Single author: (Author, Year) or Author (Year)
- Two authors: (Author 1 & Author 2, Year) or Author 1 and Author 2 (Year)
- Three and more authors: (Author 1 et al., Year) or Author 1 et al. (Year)

In the text, the author and year of the reference should be put in parentheses immediately after the work referred to, for example 'Controlled tests on the Millennium Bridge (Chapman et al., 2005; Murray & Geddes, 1987; Wilby et al., 2011) during which…..' or 'as mentioned by Lim et al. (2018), the NCA derived from the agricultural wastes…'

All references must be listed, in full, at the end of the paper in alphabetical order, irrespective of where they are cited in the text.

In the reference section, the references should be written in full, as follows:

Books: Author 1 surname, author 1 initials, & Author 2 surname, author 2 initials. (Year of publication). Book title. Publisher, City, Country. doi reference. For example:

Kobayashi, K., Khairuddin, A. R., Ofori, G. & Ogunlana, S. (Eds.). (2009). *Joint ventures in construction*. Thomas Telford, London, UK.

Owen, G. & Totterdill, B. (2008). *The dispute board hearing. In Dispute Boards: Procedures and Practice*. Thomas Telford, London, UK.

Journal, magazine and newspaper articles: Author 1 surname, author 1 initials, & Author 2 surname, author 2 initials. (Year of publication). Paper title. Journal title, Volume (Issue number), First page-Last page. doi reference. Unpublished papers and theses should not be cited as they are not readily available.

Lim, J. L. G., Raman, S. N., Lai, F. C., Zain, M. F. M., & Hamid, R. (2018). Synthesis of nano cementitious additives from agricultural wastes for the production of sustainable concrete. *Journal of Cleaner Production*, 171, 1150-1160. https://doi.org/10.1016/j.jclepro.2017.09.143.

Soon, F. C., Khaw, H. Y., Chuah, J. H., & Kanesan, J. (2018). Hyper-parameters optimisation of deep CNN architecture for vehicle logo recognition. *IET Intelligent Transport System*, 12(8), 939-946. https://doi.org/10.1049/iet-its.2018.5127.

Conference proceedings: Author 1 surname, author 1 initials, & Author 2 surname, author 2 initials. (Year of publication). Paper title. Proceedings title, Volume (Issue number), First page-Last page. doi reference. Unpublished conference proceedings (i.e. that were only given to delegates) should not be cited as they are not generally available.

Chuah, J. H., Khaw, H. Y., Soon, F. C., & Chow, C. (2017). Detection of Gaussian noise and its level using deep convolutional neural network. *Proceedings of the TENCON 2017 - 2017 IEEE Region 10 Conference*, 2447-2450. https://doi.org/10.1109/TENCON.2017.8228272.

Unpublished material should not be included in the Reference list.

Please refer to https://apastyle.apa.org/ for a detailed guide on the referencing style. Authors should strictly adhere to the referencing style specified herein.

Mathematical Equations

Only relevant equations should be included in the main text and should be numbered. An equation editor program can be used to type in a formula.

Figures and tables caption list: Please supply a figure caption list at the end of your journal paper. Figures and tables must be put in the text in consecutive order. All figures must have a brief title accompanied with a short description.

Brief Profile

At the end of the manuscript, each author should provide a brief profile (less than 150 words), together with recent photographs (preferable less than 3 MB).

Corresponding Authors

We only permit one corresponding author per submission.

Conflict of Interest

Conflict of interest occurs when an author (or the author's institution) has personal or financial relationships that inappropriately influence the statements in the publication. Authors should ensure that publications will be written in an unbiased, ethical and responsible manner. The authors working on any sponsored engineering work or publications should declare such work under Conflict of Interest during submission.

Submission of Paper

Authors are required to submit via the IEM Online Journal Submission (OJS) through the following link:

https://iemjournal.com.my/index.php/iem/about/submissions.

Together with the manuscript, the corresponding author should enclose a cover letter containing the significance of the paper, the postal and email address, and telephone number for correspondence. In the cover letter, kindly provide four (4) names as reviewers. The selected reviewers must have the relevant knowledge and research experience. Provide the reviewers postal and email addresses and telephone numbers (if possible).

Further Enquiries

For further enquires, please contact Secretariat at the address shown below:

The Institution of Engineers, Malaysia
Bangunan Ingenieur, Lots 60 & 62, Jalan 52/4
Peti Surat 223 (Jalan Sultan), 46720 Petaling Jaya, Selangor Darul Ehsan
Tel: 03–78900130 Fax: 03–79577678
E-mail: pub@iem.org.my or iemjournal@gmail.com

The Institution of Engineers, Malaysia

Bangunan Ingenieur, Lots 60/62, Jalan 52/4, Peti Surat 223 (Jalan Sultan), 46720 Petaling Jaya, Selangor Darul Ehsan
Tel: 03-78900130 Fax: 03-79577678 E-mail: sec@iem.org.my IEM Homepage: http://www.myiem.org.my

REFEREES FOR VETTING OF IEM PUBLICATIONS

Dear IEM Members/Readers,

The Standing Committee on Information and Publications is revising the list of referees to assist in the vetting of articles received from members and non-members. The referees should preferably be at least Corporate Members of The Institution or graduates with higher degrees.

The aim of appointing the referee is to ensure and maintain a standard in the IEM Publications namely the bulletin and the Journal.

Members who are interested to be placed in the database of referees are to return the registration form to the IEM Secretariat, providing details of their degrees and particular expertise and experience in the engineering fields.

We need your services to look into the vetting of articles received for Publications and due acknowledgement would be announced yearly in the Bulletin. Referees must be committed to return the papers within a month from date of appointment.

Chairman
Standing Committee on Information and Publications

All correspondences are to be addressed to: -

The Chief Editor
Standing Committee on Information and Publications
The Institution of Engineers, Malaysia
Bangunan Ingenieur, Lots 60 & 62, Jalan 52/4
P.O. Box 223 (Jalan Sultan)
46720 Petaling Jaya
Selangor Darul Ehsan

Email: pub@iem.org.my

AREAS OF INTEREST FOR VETTING OF PAPERS

Please tick (√) the appropriate area of interest that you are able to vet the papers.

□ Acoustics
□ Engineering Education
□ Military Vehicles
□ Room Temperature
□ Aerodynamics
□ Environmental Engineering
□ Mini Pressure Meters
□ Safety Engineering
□ Air Conditioning
□ Fine Chemical
□ Mining Engineering
□ Scaffolding Works
□ Air Pollution Control
□ Finite Element
□ Naval Architecture
□ Seepage
□ Aircraft
□ Fire Detection
□ Navigation
□ Sewerage
□ Airport Engineering
□ Fire Engineering
□ Oil & Gas Engineering
□ Shipbuilding
□ Aluminium Design
□ Floods
□ Operation Research
□ Signal Processing
□ Arbitration
□ Food Processing
□ Palm Oil Industries
□ Solar Energy Technology
□ Automation
□ Foundation Engineering
□ Petrochemicals
□ Steelworks Design
□ Automotive Engineering
□ Fuzzy Logic
□ Petroleum Engineering
□ Stream Turbine Power Plant
□ Biochemical Engineering
□ Gas Engineering
□ Pharmaceuticals
□ Sructural Analysis
□ Biotechnology
□ Geotechnical
□ Piling
□ Structural Rehabilitation
□ Boiler Engineering
□ Heat Exchanger
□ Plumbing Engineering
□ Survey Engineering
□ Bridge Engineering
□ Highway
□ Pollution Control
□ Taligates
□ Building Services
□ Hydraulics
□ Ports & Harbour Engineering
□ Telecommunication
□ Coastal Engineering
□ H.V. Electrical Distribution
□ Power Electronics
□ Thermal Engineering
□ Co-Generation
□ Industrial Engineering
□ Power Generation
□ Timber Design
□ Computer Engineering
□ Industrial Transport
□ Pressure Vessels
□ Tool Engineering
□ Concrete Design
□ Industrial Ventilation
□ Prestressed Concrete
□ Transfer Tunnels
□ Concrete Technology
□ Information Technology
□ Project Management
□ Transportation Engineering
□ Construction Management
□ Instrumentation
□ Public Administration
□ Urban Planning
□ Control Engineering
□ Lighting System
□ Public Health Engineering
□ Vehicles
□ Drainage Engineering
□ L.V. Electrical Distribution
□ Quarry Engineering
□ Vertical Transportation
□ Dynamics Design
□ Manufacturing
□ Railways
□ Waste Treatment
□ Earthworks
□ Mass Transit
□ Reclamation Works
□ Waste Water
□ Edible Oil Refining
□ Mechanical Handling Equipment
□ Refrigeration
□ Water Resources Engineering
□ Electrical Transmission
□ Management
□ Reinforced Concrete Beams
□ Water Pollution Control
□ Electrochemical
□ Metal Fabrication
□ Road Transport
□ Wind Engineering
□ Electrotechnology
□ Metallurgy
□ Robotics
□ Others (please specify)
□ Energy Technology
□ Micro Electronics
□ Roof Structures

DISCIPLINES / SUB-DISCIPLINES OF VETTER

Please tick (√) the appropriate boxes.

□ Aerospace
□ Electrical
□ Marine
□ Petroleum
□ Aeronautical
□ Electronics
□ Mechanical
□ Production
□ Agricultural
□ Environmental
□ Mining
□ Structural
□ Chemical
□ Industrial
□ Naval Architecture
□ Others (Please specify)

VETTER'S DETAILS

Name : ______________________
Membership No. : ______________________ *(if applicable)*
Grade : □ Graduate □ Member □ Fellow □ Affliate □ Others
(please specify) ______________________
Qualifications : ______________________
Addresses : *(Office)* ______________________
____
(Residence) ______________________
____
Contact No. : __________ *(Handphone)* __________ *(Office)* __________ *(Residence)*
E-mail Address : ______________________

Please mail all correspondences to the below. Please tick (√) the appropriate boxes.
Mail to : □ Office □ Residence

Brief Biodata (not longer than 50 words) (to be appended with this Reply Slip).
____
____
____
____
____

Have you ever reviewed submissions for publication in any Journal(s) before? □ Yes □ No
If YES, name the Journal(s) ______________________

Do you have papers published in any Journal(s)? □ Yes □ No
If YES, name the Journal(s) ______________________

Date: __________ Signature : __________

IEM BRANCHES

PENANG	IEM PENANG BRANCH SECRETARIAT 1-04-02 E-Gate, Lebuh Tunku Kudin 2, 11700 Gelugor, Pulau Pinang	Tel: 04-606 599 iempenangbranch@gmail.com http://iempenang.org
SOUTHERN	IEM SOUTHERN BRANCH SECRETARIAT 24-B, Jalan Abiad, Taman Tebrau Jaya, 80400 Johor Bahru, Johor Darul Takzim	Tel: 07-331 9705 Fax: 07-331 9710 iemsouthern@gmail.com www.iemsb.org.my
PERAK	IEM PERAK BRANCH SECRETARIAT No. 60B, Jalan Lapangan Siber 1, Bandar Cyber (Business Centre), 31350 Ipoh, Perak Darul Ridzuan	Tel: 05-313 8459 iemperakbranch@gmail.com
TERENGGANU	IEM TERENGGANU BRANCH SECRETARIAT 23-05, KT Business Centre, Padang Hiliran, Jalan Sultan Mohamad, 21100 Kuala Terengganu	Tel: 09-620 4500 Fax: 09-620 4502 iemterengganu@gmail.com
NEGERI SEMBILAN	IEM NEGERI SEMBILAN BRANCH SECRETARIAT No. 77-A-1, Lorong Haruan 5/3, Oakland Commerce Square, 70300 Seremban, Negeri Sembilan	Tel: 06-631 1011 Fax: 06-631 4619 iemnsembilan@gmail.com www.iemns.org.my
MELAKA	IEM MELAKA BRANCH SECRETARIAT C/O Sri Perunding Consulting Engineers, No. 2, Jalan Malinja 2, Taman Malinja Bukit Baru, 75150 Melaka	Tel: 06-284 8028 Fax: 06-283 8919 spcesb@gmail.com
SARAWAK	IEM SARAWAK BRANCH SECRETARIAT International Engineering Centre (IntEC), A2-G-19 & A2-1-19, Isthmus Raintree Square, Lot 3249, MTLD Block 7, Jalan Keruing, 93450 Kuching, Sarawak	Tel: 06-284 8028 Fax: 06-283 8919 spcesb@gmail.com
SABAH	IEM SABAH BRANCH SECRETARIAT Lot 25, 3rd Floor, Block C, Damai Point Commercial Centre, Lorong Damai Point, Off Jalan Damai, 88100 Kota Kinabalu, Sabah	Tel: 088-259 122 Fax: 088-236 749 iemsabah@gmail.com www.iemsabah.org.my
MIRI	IEM MIRI BRANCH SECRETARIAT 2nd Floor, Unit 14 (906-3-14), Soon Hup Tower Complex, (Mega Hotel), Jalan Merbau, 98000 Miri Sarawak	Tel: 085-423 718 Fax: 085-424 718 iem.miri@gmail.com www.iem-miri.org.my
KEDAH / PERLIS	IEM KEDAH / PERLIS BRANCH SECRETARIAT No. 164, Tingkat 2, Kompleks Alor Setar, Lebuhraya Darul Aman, 05100 Alor Setar, Kedah Darul Aman	Tel: 04-734 3420 Fax: 04-733 3962 iemckps@gmail.com
PAHANG	IEM PAHANG BRANCH SECRETARIAT No. 114, Block F, Lorong Seri Teruntum, Medan Warisan, 25100 Kuantan, Pahang Darul Makmur	Tel: 019-855 6509 Fax: 09-514 6493 iempahang@gmail.com
KELANTAN	IEM KELANTAN BRANCH SECRETARIAT Lot 5139, Kompleks Niaga INOtrus Kawasan Perindustrian Pengkalan Chepa II, 6100 Kota Bharu, Kelantan	Tel: 09-773 0899 Fax: 04-733 3962 iemckps@gmail.com

IEM
JOURNAL
Volume 87, No. 2
June 2026
https://iemjournal.com.my
www.myiem.org.my

THE INSTITUTION OF ENGINEERS, MALAYSIA
Bangunan Ingenieur, Lots 60 & 62, Jalan 52/4, P.O. Box 223 (Jalan Sultan),
46720 Petaling Jaya, Selangor Darul Ehsan.
Tel: 03-7890 0130 | Fax: 03-7957 7678 | E-mail: sec@iem.org.my

IEM
The Institution of Engineers, Malaysia